



OPTIMAL ENERGY MANAGEMENT OF HYBRID ENERGY SYSTEM FOR A COMMERCIAL BUILDING

By

LEBOHANG PIUS MOJI

Thesis submitted in fulfilment of the requirements for the Degree:

Doctor of Engineering in Electrical Engineering

In the Department of Electrical, Electronic and Computer Engineering
Faculty of Engineering, Built Environment, and Information Technology
Central University of Technology, Free State

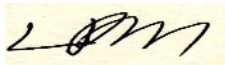
Promoter: Prof. K. Kusakana

Co-promoter: Dr B. P. Numbi

August 2022

DECLARATION

I, LEBOHANG PIUS MOJI, student number _____, hereby declare that this research project which has been submitted to the Central University of Technology, Free State, for the degree Doctor of Engineering in Electrical Engineering, is my own independent work that complies with the Code of Academic Integrity, as well as other relevant policies, procedures, rules and regulations of the Central University of Technology, Free State, and has not been submitted before by any person in fulfilment (or partial fulfilment) of the requirements for the attainment of any qualification.



L. P. MOJI

Date: August 2022

ACKNOWLEDGEMENTS

I would like to take this opportunity wholeheartedly, to thank my study supervisor, Professor Kanzumba Kusakana, for his guidance and leadership. He has been an inspirational model figure to me and has been available for matters related to this study. I wish to thank my co-supervisor, Dr Papy Numbi. I further wish to thank Dr PA Hohne, for his kind gesture of making his computer available when I required one for simulations.

Finally, I wish to thank my wife for her continuous and valuable support during this study.

ABSTRACT

High consumption of electricity in commercial buildings, is a global challenge, faced by many countries in the world. The high consumption of purchased electricity from the utility, results in high electricity bills for commercial consumers. The cost of energy consumed by the commercial buildings is high as an optimal power flow strategy to the load is not applied. The optimised on-site grid-tied hybrid renewable energy system under time of use tariff, has been found as the attractive option for solving this problem. As a result, this research work has focused on the development of an optimal energy management model, to minimise the electricity cost of a commercial building supplied by the on-site grid-tied hybrid photovoltaic-battery-diesel generator (PV-Battery-DG) hybrid renewable energy system (HRES), under time of use tariff.

The selected solution methodology has consisted of a review of related literature, selection of an appropriate case study, optimal sizing of on-site grid-tied HRES, using Hybrid Optimization Model for Electric Renewable (HOMER), development of on-site grid-tied HRES model and simulations using realistic and measured data, as well as an economic impact assessment of scheduled grid load shedding, on commercial consumers.

The optimum sizes are 18 kW for the PV, 18 kW for the DG, 6 Surrette 6CS25PS batteries and 15 kW for the bidirectional converter. The most economic NPC for the grid-tied PV-Battery-DG configuration, obtained in this study, is \$86740, while the LCOE is \$169/kWh and the operating cost is \$5212, for 25-year period. The daily economic analysis results, indicate that the optimal energy management of the hybrid system has a potential daily savings of 49.51%, based on the data provided and the assumptions made. Results have shown that the proposed grid-tied hybrid PV-Battery-DG HRES has the potential of mitigating the South African scheduled load shedding for a commercial consumer's building.

The optimal energy management of the proposed hybrid energy system under TOU has minimised both the grid consumption, as well as the consumer's bill and the diesel fuel for running the DG. The main benefit of reduced electricity purchased from the grid, is the reduced electricity bill for the commercial consumers. Daily scheduled grid load

shedding impacts differently on commercial consumers; this is due to the available renewable resources, battery SOC, as well as the amount of DG energy used.

The author anticipates that, in future, Smart grid technologies will have a positive impact on commercial demand side management. These technologies may consist of communication systems, monitoring systems, control devices and on-site HRESs. They will enable a sustainable, efficient and secure electricity supply to a commercial building.

CONTENTS

Declaration	I
Acknowledgements	II
Abstract	III
List of Figures	IX
List of Tables	XII
LIST OF SYMBOLS AND ABBREVIATIONS	XIII
CHAPTER 1: INTRODUCTION	1
1.1 Background	1
1.1.1 Demand Side Management of Commercial Buildings.....	1
1.1.2 Demand Response	2
1.1.3 Hybrid Energy Systems for Commercial Buildings.....	3
1.1.4 Smart Grid Technologies for CDSM.....	4
1.2 Problem Statement	6
1.3 Research Aim and Objectives	7
1.4 Research Scope.....	8
1.5 Research Methodology	8
1.6 Contribution to Knowledge.....	10
1.7 Publications	10
1.8 Thesis Structure.....	11
CHAPTER 2: LITERATURE REVIEW	12
2.1 Introduction	12
2.2 On-site Hybrid Renewable Energy Systems.....	12
2.2.1 Optimal Sizing of On-site Hybrid Renewable Energy Systems.....	12
2.2.2 DSM of hybrid renewable energy systems for commercial buildings	14

2.2.3	Demand side management of hybrid renewable energy systems under scheduled grid load shedding.....	15
2.3	Demand Response.....	16
2.4	DSM of hybrid energy systems for smart commercial buildings.....	18
2.5	Chapter discussions and summary	19
CHAPTER 3: OPTIMAL SIZING AND OPERATION CONTROL OF A GRID-TIED HYBRID RENEWABLE ENERGY SYSTEM FOR A COMMERCIAL BUILDING		22
3.1	Introduction	22
3.2	Case Study Description and Data Inputs	22
3.3	HRES Description and Model.....	25
3.3.1	Introduction to HOMER.....	25
3.3.2	PV System.....	26
3.3.3	Battery Storage System.....	26
3.3.4	Inverter	27
3.3.5	DG	27
3.4	Simulation Results and Discussions	29
3.5	Conclusion	32
CHAPTER 4: DEMAND SIDE MANAGEMENT OF GRID-TIED HYBRID SYSTEM FOR A COMMERCIAL BUILDING.....		34
4.1	Introduction	34
4.2	System Model Development.....	34
4.2.1	PV model.....	35
4.2.2	BSS model.....	36
4.2.3	Grid model.....	37
4.2.5	TOU tariff model.....	39
4.2.6	Aim of the optimisation model	39
4.2.7	Objective function model.....	39

4.2.8	Model constraints.....	40
4.2.9	Model solver selection.....	42
4.3	Case Study	43
4.3.1	Load description	43
4.3.2	Hybrid system sizing	44
4.3.3	Generated PV output power	45
4.3.4	Simulation parameters	46
4.4	Simulation Results and Discussions	47
4.4.1	During the first off peak period (00:00-06:00)	52
4.4.2	During the first standard period (06:00-07:00).....	52
4.4.3	During the first peak period (07:00-10:00).....	53
4.4.4	During the second standard period (10:00-18:00).....	53
4.4.5	During the second peak period (18:00-20:00).....	54
4.4.6	During the third standard period (20:00-22:00)	54
4.4.7	During the second off period (22:00-24:00)	54
4.4.8	Daily Economic Analysis	54
4.5	Conclusion	56
CHAPTER 5: OPTIMAL OPERATION OF GRID-TIED HYBRID ENERGY		
SYSTEM UNDER SCHEDULED GRID LOAD SHEDDING FOR a		
Commercial Building.....		
5.1	Introduction	57
5.2	System Model for Scheduled Grid Load shedding	58
5.2.1	Utility grid model under scheduled load shedding.....	58
5.2.2	Aim of the optimisation model	58
5.2.3	Objective function model.....	58
5.3	Case Study	59
5.4	Scheduled Load Shedding Simulation Results and Discussions.....	59
5.4.1	Area B load shedding during 00:00-04:00 schedule.....	59

5.4.2	Daily economic analysis for Area B scheduled load shedding.....	64
5.4.3	Area C scheduled load shedding: 06:00-10:00.....	65
5.4.4	Daily economic analysis for Area C scheduled load shedding.....	70
5.4.5	Area D load shedding during 12:00-16:00 schedule.....	71
5.4.6	Daily economic analysis for Area D scheduled load shedding.....	76
5.4.7	Area E scheduled load shedding: 18:00-22:00.....	77
5.4.8	Daily economic analysis for Area E scheduled load shedding.....	82
5.4.9	Economic impact of scheduled load shedding on commercial consumers.....	83
5.5	Conclusion.....	84
CHAPTER 6: CONCLUSIONS AND FUTURE RESEARCH.....		85
6.1	Conclusions.....	85
6.2	Future Work.....	86
REFERENCES.....		88

LIST OF FIGURES

Figure 1.1 Commercial Demand Side Management.....	1
Figure 1.2 Commercial Demand Response	3
Figure 3.1 Energy consumption of ETB second floor for 2018	23
Figure 3.2 Bloemfontein 2016 global horizontal irradiance data.....	24
Figure 3.3 HOMER model of grid-tied hybrid PV-Battery-DG energy system.....	29
Figure 3.4 The share of various costs of optimum PV-Battery system during the project life	30
Figure 3.5 Power generated by the PV-Battery optimally sized system.....	31
Figure 3.6 Power generated by the optimally sized PV (PV-Battery HRES) during the year	32
Figure 3.7 Converter (PV-Battery HRES) optimal power flow to the AC bus	32
Figure 4.1 Proposed grid-tied hybrid PV-battery-DG energy system.....	35
Figure 4.2 Load profile of the second floor CUT ETB building on 31 July 2018.	44
Figure 4.3 Generated PV output power for 31 July 2018.....	45
Figure 4.4 Optimal power flow from the PV to the grid.....	48
Figure 4.5 Optimal power flow from the grid to load.....	48
Figure 4.6 Optimal SOC.....	49
Figure 4.7 Optimal power flow from the grid to the BSS	49
Figure 4.8 Optimal power flow from the BSS to the grid	50
Figure 4.9 Optimal power flow from the PV to the BSS	50
Figure 4.10 Optimal power flow from the BSS to the load	51
Figure 4.11 Optimal power flow from the DG to the load.....	51
Figure 4.12 Optimal power flow from the PV to the load	52
Figure 4.13 Comparison between baseline and optimal costs.....	55
Figure 5.1 Optimal power flow from the PV to the grid for area B	60
Figure 5.2 SOC power flow for area B.....	60
Figure 5.3 Optimal power flow from the grid to the load for area B	61
Figure 5.4 Optimal power flow from the grid to the BSS for area B.....	61

Figure 5.5 Optimal power flow from the BSS to the grid for area B.....	62
Figure 5.6 Optimal power flow from the PV to the BSS for area B.....	62
Figure 5.7 Optimal power flow from the BSS to the load for area B.....	63
Figure 5.8 Optimal power flow from the DG to the load for area B.....	63
Figure 5.9 Optimal power flow from the PV to the load for area B.....	64
Figure 5.10 Area B (scheduled load shedding: 00:00-04:00) daily energy costs.....	65
Figure 5.11 Optimal power flow from the PV to the grid for area C.....	66
Figure 5.12 SOC power flow for area C.....	66
Figure 5.13 Optimal power flow from the grid to the load for area C.....	67
Figure 5.14 Optimal power flow from the grid to the BSS for area C.....	67
Figure 5.15 Optimal power flow from the BSS to the grid for area C.....	68
Figure 5.16 Optimal power flow from the PV to the BSS for area C.....	68
Figure 5.17 Optimal power flow from the BSS to the load for area C.....	69
Figure 5.18 Optimal power flow from the DG to the load for area C.....	69
Figure 5.19 Optimal power flow from the PV to the load for area C.....	70
Figure 5.20 Area C (scheduled load shedding: 06:00-10:00) daily energy costs.....	71
Figure 5.21 Optimal power flow from the PV to the grid for area D.....	72
Figure 5.22 SOC power flow for area D.....	72
Figure 5.23 Optimal power flow from the grid to the load for area D.....	73
Figure 5.24 Optimal power flow from the grid to the BSS for area D.....	73
Figure 5.25 Optimal power flow from the BSS to the grid for area D.....	74
Figure 5.26 Optimal power flow from the PV to the BSS for area D.....	74
Figure 5.27 Optimal power flow from the BSS to the load for area D.....	75
Figure 5.28 Optimal power flow from the DG to the load for area D.....	75
Figure 5.29 Optimal power flow from the PV to the load for area D.....	76
Figure 5.30 Area D (scheduled load shedding: 12:00-16:00) daily energy costs.....	77
Figure 5.31 Optimal power flow from the PV to the grid for area E.....	78
Figure 5.32 SOC power flow for area E.....	78
Figure 5.33 Optimal power flow from the grid to the load for area E.....	79
Figure 5.34 Optimal power flow from the grid to the BSS for area E.....	79
Figure 5.35 Optimal power flow from the BSS to the grid for area E.....	80

Figure 5.36 Optimal power flow from the PV to the BSS for area E.....80

Figure 5.37 Optimal power flow from the BSS to the load for area E.....81

Figure 5.38 Optimal power flow from the DG to the load for area E.....81

Figure 5.39 Optimal power flow from the PV to the load for area E82

Figure 5.40 Area E (scheduled load shedding: 18:00-22:00) daily energy costs.....83

LIST OF TABLES

Table 2.1 Comparative summary on related studies and this study.....	19
Table 3.1 High Season TOU Tariff for Mangaung Municipality (Centlec Mangaung Tariff Approval, 2018/19).....	25
Table 3.2 Technical and economic data of the HRES parameters with assumptions	28
Table 3.3 Comparisons of the first five of sixty feasible grid-tied hybrid configurations using HOMER.....	30
Table 4.1 Simulation parameters	46
Table 5.1 Impact of scheduled load shedding on consumers on 31 July 2018.....	83

LIST OF SYMBOLS AND ABBREVIATIONS

DSM	Demand Side Management
CDSM	Commercial Demand side management
DR	Demand Response
HRES	Hybrid Renewable Energy System
HRESs	Hybrid Renewable Energy Systems
PV	Photovoltaic
DG	Diesel Generator
BSS	Battery Storage System
CDR	Commercial Demand Response
RTP	Real Time Pricing
TOU	Time of Use
CPP	Critical Peak Pricing
EDP	Extreme Day Pricing
ED-CPP	Extreme Day Critical Peak Pricing
DLC	Direct Load Control
IS	Interruptible Services
EDRP	Emergence Demand Response Pricing
CMP	Capacity Market Programs
AMS	Ancillary Market Service
PV-DG-BS	Photovoltaic-Diesel Generator-Battery Storage
GSM	Global system for Mobile Communications
GPRS	General Packet Radio Service
3G	Third Generation
4G	Fourth Generation
BAN	Business Area Network
AMI	Advanced Metering Infrastructure
EMSs	Energy Management Systems
USA	United States of America
UK	United Kingdom
SAURAN	Southern African Universities Radiometric Network
ETB	Engineering Technology Building

HOMER	Hybrid Optimization Model for Electric Renewable
MINLP	Mixed Integer Nonlinear Problem
IPOPT	Interior Point Optimizer
SCIP	Solving Constraint Integer Programs
HPWH	Heat Pump Water Heaters
IoT	Internet of Things
NPC	Net Present Cost
LCOE	Levelized Cost of Energy
TNPC	Total Net Present Cost
CRF	Capital Recovery Factor
C_A	Total Annualised Cost
i	the annual rate of interest for the project life
E_{AC}	Annualised AC load
O & M	Operating and Maintenance
P_{Pv}	Output power from a PV system
I_{Pv}	Solar irradiation (kW/m^2)
η_{Pv}	Efficiency of PV generator
A_{Pv}	Total PV surface area (m^2)
η_R	PV efficiency measured at reference cell temperature
T_R	Reference cell temperature
$I_{Pv,NT}$	Solar irradiation at normal temperature
β	Temperature coefficient
NT	Normal temperature
$T_{A,NT}$	Ambient temperature at NT
$T_{C,NT}$	Cell temperature at NT
I_B	Global irradiation (kWh/m^2)
I_D	Diffuse irradiation (kWh/m^2)
R_B	Geometric factor
η_c	BSS charging efficiency
η_d	BSS discharging efficiency
σ	Self-discharged factor
SOC	State of Charge

$\Delta t = t_s$	Sampling time
C_b	BSS capacity
j	Sampling interval
N	Horizon period
SOC^{min}	Minimum SOC
SOC^{max}	Maximum SOC
$\$$	United States of America dollar (USD)
P_{grid}	Grid power
$P_{disp-grid}$	Dispatched power from grid
P_{DG}^{min}	Lower bound DG power output
P_{DG}^{rated}	Rated DG power output
F_c	DG fuel consumption
C_f	Diesel fuel cost (\$/L)
Q	DG coefficient (L/(kW) ² h)
R	DG coefficient (L/(kWh))
S	DG coefficient (L/h)
DR	Demand Response
ρ	TOU tariff feed-in tariff (\$/kWh)
p_o	TOU off-peak price (\$/kWh)
p_p	TOU peak price (\$/kWh)
ρ_s	TOU standard price feed-in tariff (\$/kWh)
ρ_{fi}	Feed-in tariff (\$/kWh)
$\alpha_{grid}(t)$	The grid availability parameter at time t
$P_{grid(max)}$	The maximum capability of the grid

CHAPTER 1: INTRODUCTION

1.1 Background

1.1.1 Demand Side Management of Commercial Buildings

Commercial Demand side management (CDSM) is an optional matching tool for bridging the gap between the grid supply and demand in commercial buildings. Eissa, 2011; Atzeni *et al.* (2013); Vadabhat and Banerjee (2014); Warren (2014), defined DSM. CDSM programs (Figure. 1.1), include demand response (DR), as well as on-site generation and storage systems (Hohne, Kusakana and Numbi, 2019; Hohne, Kusakana and Numbi, 2020). Commercial buildings include education, hospitals, hotels, malls, offices, restaurants and retail buildings. In this context, DR refers to the response of commercial consumers to electricity price changes or incentive payments. It encourages commercial electricity consumers to reduce or shift their consumption to the periods when the price of electricity is more affordable. On-site generation and storage response systems include either off-grid hybrid energy system (HRES) or grid-tied HRES. In CDSM of hybrid grid-tied hybrid energy systems, consumers may benefit, by selling the surplus generated power to the utility grid, when the electricity price is high.

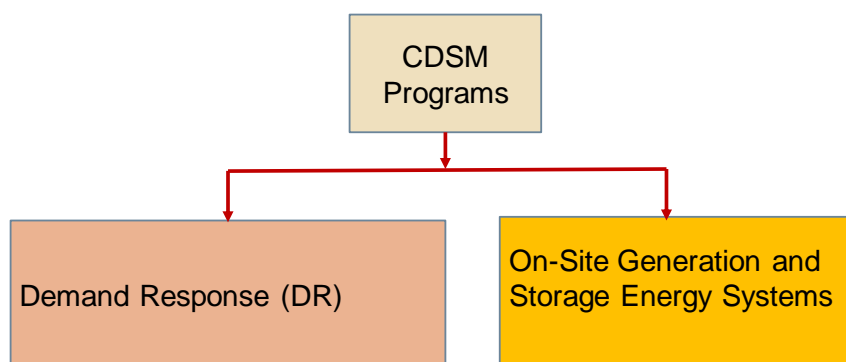


Figure 1.1 Commercial Demand Side Management

An HRES integrates one or more renewable energy systems, such as photovoltaic (PV), a storage system, such as battery and a conventional system, such as a diesel generator (DG). A battery storage system (BSS) or DG, or a combination of both, are required as a backup for unreliable and intermittent electrical power supply. Off-grid HRESs find their application in commercial buildings without access to the grid (Olatomiwa, 2016); while grid-connected HRESs are used in commercial buildings that have access to the grid (Sichilalu and Xia, 2015; Mariaud *et al.*, 2017; Hohne, Kusakana and Numbi, 2020).

1.1.2 Demand Response

DR (Figure 1.2) comprises price-based and incentive-based programs (Albadi and El-Saadany, 2008; Eissa, 2011; Warren, 2014; Aghajani, Shayanfar and Shayeghi, 2017; Hohne, Kusakana and Numbi, 2018). Price-based CDR programs provide commercial consumers time-varying rates that reflect the value and the cost of electricity, during a differentiated period. Conversely, incentive-based DR programs reward participating commercial consumers for reducing their consumptions at times requested by the utility, triggered by either a grid reliability problem or high electricity rates. DR programs may reduce electricity prices, improving system reliability and reducing price volatility (Albadi and El-Saadany, 2008; Eissa, 2011).

Price based DR programs are categorised into real time pricing (RTP), time of use (TOU), critical peak pricing (CPP), extreme day pricing (EDP) and extreme day CPP (ED-CPP). The TOU pricing scheme has the highest price during the peak period, medium price during the standard period and the lowest price during the off-peak period. The RTP pricing scheme has prices that change on hourly or sub-hourly, for the year and it may be for a certain portion or the entire load of the consumer. In contrary to TOU, RTP does not fix the price or the time. CPP has high rates during a few critical hours of the day or year. EDP is like CPP, with the exception that higher rates are implemented in hours of the day, for all critical days of the year. In ED-CPP, the peak rates only to the critical peak hours on extreme days. However, there is no TOU for the rest of the days.

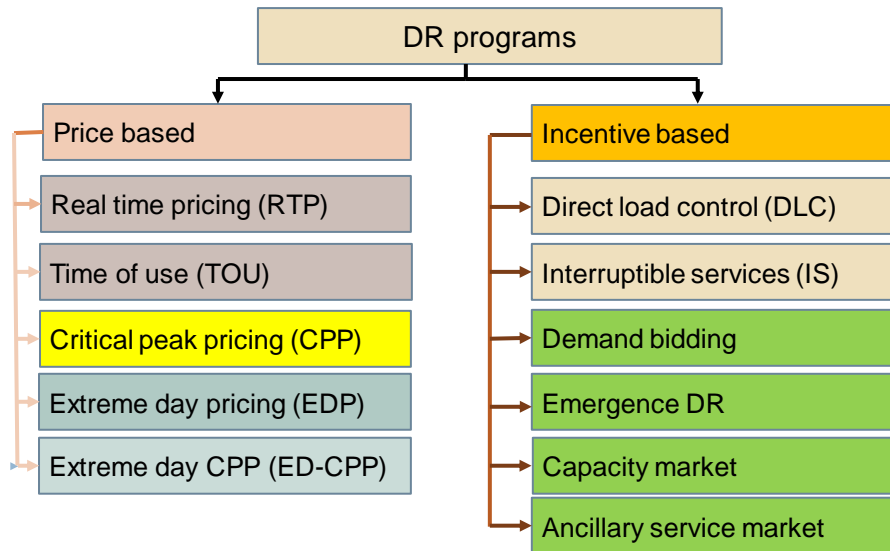


Figure 1.2 Commercial Demand Response

The incentive-based programs include direct load control (DLC), interruptible services (IS), demand bidding, emergence DR (EDRP), capacity market programs (CMP) and ancillary market service (AMS). In DLC, utility controls the switching off and on of participating electrical appliances, on short notice. This applies to small commercial consumers. In IS, participating consumers receive a bill credit as a trade-off, as per agreement with the utility. Demand bidding programs are mostly offered to large consumers, consuming 1 MW or more. These programs encourage participating consumers to offer bids, to minimise their loads in line with the wholesale electricity market prices. EDRP are called upon during the reliability-triggered events that cause reserve shortfalls, and the payment rate is usually specified ahead of time. Utilities offer CMP pricing schemes to consumers who commit to providing pre-specified consumptions, during systems contingencies. ASM programs allow consumers to bid on consumption reduction in the spot market, as an operating reserve.

1.1.3 Hybrid Energy Systems for Commercial Buildings

The promising on-site option for supplying commercial buildings, is a hybrid energy system. Factors affecting the design of hybrid energy systems for commercial buildings include the location of the building, decision on off-grid or grid-tied, the building's load profile, techno-economic assessment and optimal sizing of the hybrid system. Off-grid

hybrid energy systems are suitable for commercial buildings, in which grid electricity is not available, while grid-connected hybrid energy systems are suitable for commercial buildings where the grid electricity is available. A hybrid energy system for commercial buildings, may integrate photovoltaic (PV), diesel generator (DG) sources and a battery storage (BS) system. The hybrid PV/DG/BS energy systems have been proposed in (Ashok, 2007; Mohammed, Mustafa, and Bashir, 2014; Ameen, Pasupuleti, and Khatib, 2015; Sichilalu and Xia, 2015; Tazvinga, Zhu and Xia, 2015). The hybrid PV/DG/BS energy system is reliable and economical.

1.1.4 Smart Grid Technologies for CDSM

Smart grid technologies for CDSM, comprise communication systems, monitoring systems, control devices and on-site HRESs.

Communication systems consists of Communication Technologies, Standards and Networks. Güngör *et al.* (2011); Kuzlu, Pipattanasomporn and Rahman (2014); Shaukat *et al.* (2018) provide an overview of Communication Technologies, Standards and Networks for CDSM. Wired and wireless communication technologies are currently available for transmitting data from or to smart meters at commercial consumer's buildings and electric utilities. Available wired technologies for CDSM applications, comprise fibre optic, power line communication and Ethernet cables (Güngör *et al.*, 2011; Kuzlu, Pipattanasomporn and Rahman, 2014; Shaukat *et al.*, 2018). Optical fibre communication provides quality of service and reliable data transmission. Available wireless communication technologies for CDSM applications, include ZigBee, Wi-Fi, Wireless Mesh, WiMAX, Cellular (includes Global system for Mobile Communications (GSM), GPRS, 3G, 4G), microwave and satellite communication technologies, which enable commercial consumers to take action that minimises their peak load and their overall electricity consumption, resulting in reduced demand charges on bills.

Factors influencing the choice between wired and wireless technologies, include acceptable attenuation, speed of transmitted data, type of terrain, interference and initial infrastructure costs. Information flow may be from the sensors and electrical appliances to smart meters or between smart meters, at the commercial consumer's building and utility's data centres (Güngör *et al.*, 2011). Important parameters for these technologies, include

spectrum, theoretical data rate, coverage range, applications and limitations. Smart grid communications' requirements comprise security, system's reliability, robustness, availability, scalability, as well as quality of service (Güngör *et al.*, 2011; Kuzlu, Pipattanasomporn and Rahman, 2014; Shaukat *et al.*, 2018).

Available networks for CDSM, include Business Area Network for usage in commercial buildings, Neighborhood Area Network, which supports information flow between a commercial building and utility, and Wide Area Network for remote sensing, monitoring, control and energy management of commercial buildings (Güngör *et al.*, 2011; Kuzlu, Pipattanasomporn and Rahman, 2014). Business Area Network further supports the implementation of intelligent buildings, with full integration of computer-based building automation and control systems.

Commonly used smart grid standards at commercial consumer's premises, include 802.3x for Ethernet, IEEE 802.15.4 for ZigBee, 802.11x for Wi-Fi and RF mesh, 802.11, 802.15, 802.16, for Wireless Mesh (Güngör *et al.*, 2011; Kuzlu, Pipattanasomporn and Rahman, 2014; Shaukat *et al.*, 2018).

Monitoring systems comprises smart meters, Advanced Metering Infrastructure (AMI), Energy Management Systems (EMSs) and energy information systems (Siano, 2014). A smart meter consists of an electronic box and a communication link. It electronically measures the consumer's electricity consumption, and other parameters, in a certain time interval and transmits a signal over a communication network to the utility or other person responsible for metering. An AMI (Siano, 2014), comprises several integrated technologies and applications, including smart meters, Building Area Networks, neighbourhood area networks, wide area network and protocols, meter data management systems, operational gateways, as well as systems for data integration into software application platforms. Commercial consumers benefit by obtaining an opportunity to interact with the markets, through the Business Area Network and smart meter connectivity. Energy management system permits monitoring, analysing, as well as controlling building systems and equipment, by means of sensors, switches, controls and algorithms (Siano, 2014). An energy management is intended to improve building energy performance, by saving energy and/or reducing peak demand. The energy information

system may operate as a gateway for two-way communication between a utility and existing energy management system or run independently from an energy management system.

Interaction (Siano, 2014) between commercial consumers and on-site HRESs, may be provided, by means of active DR systems which are located within a commercial building. The DR systems facilitate distinct functions, such as automatic reduction of the energy consumption as a result of the high energy process. Mbungu, Naidoo and Bansal (2017) have proposed an optimal adaptive model of minimising the cost of electricity, for commercial buildings, in a smart grid. The model proved to be robust enough to manage a system full of constraints and the reference turning parameter has a significant effect on the optimal cost of electricity to pay.

1.2 Problem Statement

Many countries in the world experience the high demand of electricity in commercial buildings (Shaahid and Elhadidy, 2007; Pérez-Lombard, Ortiz, and Pout, 2008; Liu, Pistikopoulos and Li, 2010; Chung and Rhee, 2014). Commercial buildings include education, hospitals, hotels, malls, offices, restaurants, and retail buildings. Commercial, as well as public sectors of electricity consumption in South Africa, account for 13.37% of the total electricity consumption. In the United States of America (USA), electricity consumption in commercial buildings account for 28.5%. In the USA and the UK, the commercial sector accounts for 18% and 11%, respectively, of the total energy (Pérez-Lombard, Ortiz, and Pout, 2008). Residential and commercial buildings' energy consumption has steadily increased reaching figures between 20% and 40% in developed countries. Electricity consumption in university' buildings is significantly high (Chung and Rhee, 2014). Matching the grid electrical energy supply and demand in real time, has been a significant global challenge (Bajpai and Dash, 2012; Vadabhat and Banerjee, 2014; Aghajani, Shayanfar and Shayeghi, 2017).

On the supply side, the main contributor to this problem, is the aging infrastructure (Gelazanskas and Gamage, 2014; Mahmood *et al.*, 2014; Giglmayr *et al.*, 2015). On the demand side, there are several contributors to the problem. The first, is the increasing demand (Erdinc and Uzunoglu, 2012; Wu and Xia, 2015; Khare, Nema and Baredar, 2016).

In South Africa, the increasing growth of energy demand, resulted in load shedding and power blackouts, in 2007 and 2008. The second contributor is the significant buildings' electrical energy consumption (Pérez-Lombard, Ortiz, and Pout, 2008; Allab *et al.*, 2017). The third contributor is the fluctuating demand (Abdulaal and Asfour, 2016) throughout the day. These challenges require the consumers to adapt their energy consumptions (Lindberg *et al.*, 2014) to the available generated power, to assist in maintaining electricity grid stability and to reduce their electricity bills.

Commercial consumers need a system that enables them to minimise their consumption of electricity, which they buy from the grid. Such a system should address the increasing demand, increasing growth of energy demand, fluctuating demand throughout the day, as well as load shedding.

1.3 Research Aim and Objectives

With the high electricity cost of the commercial buildings in mind, the aim of this study is to develop an optimal energy management model, which minimises the cost of the purchased electricity from the grid utility during normal operating conditions, as well as during load shedding.

To achieve this aim, the specific objectives of this research are as follows:

- To optimally size a grid-tied hybrid PV-battery-DG energy system, which meets the load demand of a commercial building.
- To model and simulate the performance of the optimised grid-tied PV-battery-DG system, for the demand side management of a commercial building, during normal operating conditions, as well as during load shedding.
- To assess the economic impact of scheduled grid load shedding, on commercial consumers.

1.4 Research Scope

This research work focuses on the development of an optimal energy management model, to minimise the electricity cost of the targeted commercial building supplied by the grid-tied hybrid photovoltaic/diesel generator/battery storage system (PV/DG/BSS) energy system.

1.5 Research Methodology

Achievement of the aim and objectives of this study requires several methodological steps:

1. Literature related to optimal sizing of on-site HRESs, for determining the optimal sizes of HRES components, commercial DSM of HRESs for minimising the cost of electricity purchased from the utility grid, DSM of HRESs under scheduled grid loading for economic impact of scheduled grid load shedding on commercial consumers, DR for determining a suitable DR program for minimising the cost of electricity bought from the utility grid and DSM of hybrid energy systems for future smart commercial buildings, has been reviewed.
2. Choice of the case study. The second floor of Engineering Technology Building (ETB), at Central University of Technology, Free State, South Africa, has been selected for the case study. The energy consumption of ETB's second floor has been measured in 1-hour time intervals, from 01 January 2018 to 31 December 2018, using the EG3000 real time web-based energy meter. The 31 July 2018 (Tuesday) has been selected, as it is the day with the highest load demand for the entire year. The hourly average Global Horizontal Irradiation data has been obtained from the Southern African Universities Radiometric Network (SAURAN), Bloemfontein, South Africa, from January to December 2016. Since the measured data was incomplete for 2018 from the source, it is assumed that 2018 data is akin to that of 2016.
3. HRES component sizing. Optimal sizing of a grid-tied hybrid PV-battery-DG energy system has been conducted, to ensure that the HRES meets the load demand of a commercial building, with possible minimum operating costs and reduced carbon

emissions. Several optimum sizing approaches considered, include commercially available software tools, such as Hybrid Optimization Model for Electric Renewable (HOMER), genetic algorithm, particle swarm optimisation, simulated annealing, ant colony algorithm and artificial immune system algorithm, graphic construction methods, probabilistic methods, analytic methods, iterative methods, artificial intelligence methods and hybrid methods. HOMER has been selected for optimal sizing of grid-tied hybrid PV-battery-DG energy system, as it is user-friendly and may provide powerful graphical outputs. Its limitation is that it models hybrid components with linear equations, that do not represent the source characteristics accurately.

4. Development of a proposed system model and simulations using realistic and measured data. Commercial buildings require reliable HRESs, which should be optimised. In this regard, the aim of the optimisation model in this study, is to minimise the cost of the purchased grid energy under TOU tariff, to minimise the cost of running the DG during the back-up periods and maximise the potential surplus power generated by the on-site HRES, which may be sold to the utility grid. As both the objective function and constraints have linear and non-linear models, the control problem is expressed as a mixed integer nonlinear problem (MINLP). The MINLP problem is solved using an optimisation solver known as Solving Constraint Integer Programs (SCIP), which is available in the MATLAB interface OPTI toolbox.
5. Economic impact assessment of scheduled grid load shedding on commercial consumers. To study the impact of scheduled grid load shedding, four commercial consumers' buildings in Bloemfontein, South Africa, are considered for South African Stage 4 load shedding, on 31 July 2018. The buildings are described as follows: Area B (scheduled load shedding: 00:00 to 04:00), Area C (scheduled load shedding: 06:00 to 10:00), Area D (scheduled load shedding: 12:00 to 16:00) and Area E (scheduled load shedding: 18:00 to 22:00).

1.6 Contribution to Knowledge

This research has contributed in the following ways:

1. The first contribution is in the development and implementation of a mathematical model for an optimal operation of a grid-connected PV-Battery-DG energy system, that enables the commercial consumers, to address the increasing demand, increasing growth of energy demand, fluctuating demand throughout the day, as well as load shedding. The developed model has been validated by means of case studies, using practical and realistic daily fluctuations in the load demand.
2. In this research, the effect of scheduled load shedding for the consumers which are located at different areas has been investigated. It was found that the daily scheduled grid load shedding impacts differently on commercial consumers; this is due to the available renewable resource, battery SOC, as well as the amount of DG energy used.

1.7 Publications

The conference contributions and journal publications from this research are:

- 1) Moji, L.P., Kusakana, K. and Numbi, B.P., 2018, October. Demand Side Management of Grid-Tied Hybrid Photovoltaic-Diesel-Battery Energy System for a University Engineering Building. In *2018 Open Innovations Conference (OI)* (pp. 271-274). IEEE.
- 2) Moji, L.P., Kusakana, K. and Numbi, B.P., Sizing and Operation Control of a Grid-Interactive Photovoltaic-Battery-Diesel System for Commercial Buildings. In *2020 6th IEEE International Energy Conference (ENERGYCon)* (pp. 401-406). IEEE.
- 3) Moji, L. P., Hohne, P.A., Kusakana, K., & Numbi, B. P. Optimal operation of a hybrid multisource energy system considering grid load shedding. *Accepted to be published in Energy reports.*

1.8 Thesis Structure

The thesis has been organized in six distinct Chapters, as follows:

Chapter 1 is the introductory chapter of the Thesis. It has provided the background, problem statement, research aims and objectives, research scope, contribution to knowledge, as well as the publication on the study.

Chapter 2 presents a comprehensive literature review on this research and shows how this study relates to commercial demand side management.

Chapter 3 proposes an optimal sizing and operation control of a grid tied HRES which meets the load requirements of a commercial building with the possible minimum NPC and LCOE for a commercial building.

Chapter 4 presents optimal demand side management of grid-tied hybrid system under TOU tariff, for a commercial building. An optimisation mathematical model is formulated with the aim of minimising the cost of the purchased grid energy under time of use (TOU) tariff and minimising the cost of running the DG during the back-up periods. The daily economic analysis and the validity of the model are investigated as well.

Chapter 5 provides optimal operation of a grid-tied hybrid energy system under scheduled grid load shedding for a commercial building. An optimisation mathematical model is formulated with the aim of mitigating scheduled load shedding. The daily scheduled grid load shedding impact assessment on commercial consumers as well as the validity of model are investigated.

Chapter 6 presents all the summaries and conclusions presented in this research. In addition, recommendations for the future work are provided as well.

CHAPTER 2: LITERATURE REVIEW

2.1 Introduction

This Chapter presents a literature review on commercial demand site energy management strategy, within the thesis topic. The Chapter provides the literature review on on-site hybrid renewable energy systems (HRES), demand response (DR) and concludes with the discussions and summary.

2.2 On-site Hybrid Renewable Energy Systems

On-site hybrid renewable energy systems (HRESs) are a promising option for managing the high electricity consumption in commercial buildings.

2.2.1 Optimal Sizing of On-site Hybrid Renewable Energy Systems

Grid-tied hybrid PV-battery systems are extensively used in optimal control of HRESs in commercial buildings (Mariaud *et al.*, 2017; Hohne, Kusakana and Numbi, 2020). These systems are attractive in this application, as they are environmentally friendly, noiseless, cost effective, have low operation and maintenance cost. In a grid-connected hybrid PV-battery system, PV operates as the primary source while the utility grid and the battery are backups making for a reliable electricity power supply. dos Santos, Sechilariu and Locment (2016), focused on the application of grid-tied PV-battery systems to mitigate the scheduled grid load shedding in commercial buildings. The PV and the battery bank are employed to mitigate the load shedding.

A grid-tied PV-battery-DG hybrid is employed in (Sichilalu and Xia, 2015), to power heat pump heaters in a hotel building. The PV is the primary source, while the grid, battery and the diesel generator (DG), are backups, ensuring reliability of the HRES. The DG operates when either the PV or grid energy is unable to meet the load demand or uneconomical.

Ndwali, Njiri and Wanjiru (2020) focused on a grid-connected PV-DG hybrid system, for mitigating the scheduled load shedding in commercial buildings. The HRES employs the PV and the DG for mitigating the scheduled grid load shedding.

The optimal hybrid system's configuration aims at a combination of generator types and sizes, that produce the lowest life cycle costs and/or emissions (Erdinc and Uzunoglu, 2012). Optimal sizing of the hybrid system ensures that the designed hybrid system meets the load requirements of the building, with possible minimum operating costs. Optimal sizing techniques are required for designing reliable and economical hybrid energy systems (Askarzadeh, 2017; Abushnaf and Rassau, 2018). Sizing techniques have been reviewed in (Erdinc and Uzunoglu, 2012; Upadhyay and Sharma, 2014; Abushnaf and Rassau, 2018). al Garni, Awasthi and Ramli (2018), propose a commercially available software known as Hybrid Optimization Model for Electric Renewable (HOMER), for optimal sizing of hybrid energy systems. HOMER is user-friendly and provides powerful graphical outputs. Its limitation is that it models hybrid components with linear equations, that do not represent the source characteristics accurately. Probabilistic optimal sizing has been proposed in (Celik, 2003). Its limitation is that the dynamic performance of the hybrid energy system is misrepresented. Some several studies (Dufo-López and Bernal-Agustín, 2008; Mondol, Yohanis and Norton, 2009), have suggested analytical optimal sizing. This technique is less flexible in designing of the system, as the computational models assess performance. Further studies (Ashok, 2007), have proposed iterative optimal sizing. An iterative technique results in suboptimal solutions, as the computation involves linearly changing of the decision variables. It does not cater for the photovoltaic module slope angle and the wind turbine installation height. In Koutroulis *et al.* (2006), artificial intelligence optimal sizing, has been suggested. Its limitation is that the hybrid system's design becomes complex. Studies in Borowy and Salameh, (1996) have suggested graphic construction optimal sizing. This technique does not cater for the photovoltaic module slope and the wind turbine's height. In Katsigiannis, Georgilakis and Karapidakis (2012; Alsayed *et al.* (2013), hybrid optimal sizing has been proposed. Its limitation is that the hybrid system's design becomes complex.

2.2.2 DSM of hybrid renewable energy systems for commercial buildings

Literature has a few studies on optimal Commercial DSM (CDSM) of grid-connected hybrid renewable energy systems for commercial buildings (Sichilalu and Xia, 2015; Wu, Tazvinga and Xia, 2015; Mariaud *et al.*, 2017; Hohne, (Sichilalu and Xia, 2015; Wu, Tazvinga and Xia, 2015; Mariaud *et al.*, 2017; Hohne, Kusakana and Numbi, 2019; Kusakana and Numbi, 2020). Hohne, Kusakana and Numbi (2020) research work, validated the optimal power dispatch model of a grid-interactive hybrid PV-battery system for minimising the grid, the maximum demand charges and daily costs of a hospital in South Africa, under the TOU tariff. Both the grid and battery ensure the reliability of the HRES. This HRES is prone to total power failure, depending on whether the grid power outage may last long enough, to a point whereby the battery is no longer able to meet the load demand. The authors modelled the system as a nonlinear problem and solved it using the MATLAB Optimization toolbox, with the algorithm Interior Point. This study considered the economic analysis of the proposed system.

In (Mariaud *et al.*, 2017), an integrated optimisation of grid-tied hybrid PV-battery energy, for minimising the grid costs and payback period for UK commercial buildings, was proposed. The authors present a Technology Selection and Operation (TSO), for determining the optimal selection and operation of a decentralised grid-tied hybrid PV-battery system in commercial buildings. Both the grid and battery bring about reliability to the HRES. The HRES is exposed to total power failure if the grid power failure lasts long enough to drain the battery. This approach simultaneously optimises the selection, the capacity and operation of grid-tied hybrid PV-battery system. The economic analysis of the proposed system was considered.

The study in (Sichilalu and Xia, 2015), developed an optimal control strategy of power dispatch of grid-tied hybrid PV-battery DG, to supply the heat pump water heaters (HPWH), at a Pretoria hotel, in South Africa. The battery, grid and DG, ensure the reliability of the HRES. The DSM of the HRES minimises the energy purchased from the grid and the fuel cost for running the DG and maximises the surplus PV energy that is sold to the grid, during the peak periods of the TOU tariff. The system was modelled as nonlinear problem and the MINLP optimization solver OPT toolbox in MATLAB was used. The work considers the economic analysis.

Wu, Tazvinga and Xia (2015) presented an optimal power flow management algorithm of grid-connected hybrid PV-battery system, to supply a residential or commercial building, in South Africa. The HRES uses the battery storage and the grid for its reliability. The HRES design, does not account for the grid power outage that lasts long enough to drain the battery. This is due to the fact, that the battery energy is limited to a certain period only, so, if this period is exceeded, an additional standby source such as the DG, may be considered. The optimal operation of the HRES minimises the cost of electricity bought from the grid within the DSM framework, maximises the surplus PV electricity sold to the grid and minimises the wear out cost. The authors developed an optimal control method, to schedule the power flow of HRES and model predictive control to dispatch the power flow in real-time, when uncertain disturbances occur. The control problem was expressed as a linear programming problem. The economic analysis of the hybrid system was accounted for in this study.

2.2.3 Demand side management of hybrid renewable energy systems under scheduled grid load shedding

Researchers are currently striving to discover effective strategies, to mitigate scheduled grid load shedding. In (dos Santos, Sechilariu and Locment, 2016), the optimal grid-connected PV-battery hybrid systems, which mitigate the scheduled load shedding in commercial buildings, are presented. The systems use the PV and the battery bank to mitigate the load shedding. The studies do not consider the economic impact assessment of the load shedding on commercial consumers.

Ndwali, Njiri and Wanjiru (2020) proposed an optimal grid-connected PV-DG hybrid system, which mitigates the scheduled load shedding in commercial buildings. The system uses the PV and DG for mitigating the scheduled grid load shedding. This work does not account for the economic impact assessment of load shedding on commercial consumers.

Bakht *et al.* (2021) presented an optimal operation of a grid-connected PV-battery-DG hybrid system, that mitigates the scheduled load shedding in residential buildings. The hybrid system uses PV, battery bank and DG, for mitigating the scheduled grid load

shedding. This strategy does not account for the economic impact assessment of load shedding on commercial consumers.

Hijjo, Felgner and Frey (2016) proposed an optimal operation of grid-connected PV-battery-DG hybrid system, to mitigate the scheduled load shedding in commercial buildings. The system employed the PV, battery bank and DG, for mitigating the scheduled grid load shedding. The strategy did not consider the economic impact assessment of load shedding on commercial consumers.

2.3 Demand Response

Demand response (DR) consists of price-based and incentive-based programs (Albadi and El-Saadany, 2008; Aghajani, Shayanfar and Shayeghi, 2017). DR programs may reduce electricity prices, improve system reliability and reduce price volatility. Price-based DR programs provide commercial consumers with time-varying rates that reflect the value and the cost of electricity during differentiated periods. They comprise time of use (TOU), real time pricing (RTP), critical peak pricing, extreme day pricing and extreme day CPP.

TOU pricing scheme has the highest price during the peak period, medium price during the standard period and the lowest price during the off-peak period. It is the popular DR program used with HRESs (Sichilalu and Xia, 2015; Hohne, Kusakana and Numbi, 2020; Ndwali, Njiri and Wanjiru, 2020), to minimise the cost of purchased electricity from the grid. In (Hohne, Kusakana and Numbi, 2020), DR has been integrated in an optimal HRES power flow management strategy that minimises the grid energy costs and maximum demand, at a health facility based on the TOU tariff. It ensures that the grid supplies the load during the off-peak and standard periods of TOU, for the price of grid electricity is more affordable than during the peak periods. In Ndwali, Njiri and Wanjiru (2020), TOU tariff enables the optimal operation control of a microgrid connected PV-DG to mitigate the scheduled grid load shedding at a university facility.

A real time pricing scheme has prices that change on hourly or sub-hourly, for the year and it may be for a certain portion or the entire load of the consumer. Contrary to TOU, real time pricing does not fix the price or the time. Real time pricing has been proposed and implemented in (Mbungu, Naidoo and Bansal, 2017), to minimise the cost

of electricity for a commercial building. Integration of a smart grid, real time pricing and energy management system, in the framework of a model predictive control, have been used for the demand side management. The strategy permits commercial consumers to decide on the amount of money they prefer to pay for the grid electricity. Mays and Klabjan (2017) propose a new rate structure, real time pricing +, to denote hourly prices that optimally combine energy and capacity costs.

Critical peak pricing has high rates during a few critical hours of the day or year. Participating consumers in the critical peak pricing program, receive price discounts during noncritical peak periods (Meyabadi and Deihimi, 2017). Critical peak pricing and TOU rates have been compared in (Wang and Li, 2016), to analyse annual costs and greenhouse gas emissions.

EDP is akin to CPP, however, it differs in higher rates applied in all hours of the day, for all critical days of the year. The difference between the ED-CPP and CPP, is that in ED-CPP, CPP rates for peak and off-peak periods are solely called during the extreme days (Albadi and El-Saadany, 2008).

The incentive-based DR programs, include direct load control, interruptible services, demand bidding, emergence DR, capacity market programs and ancillary market service. Direct load control programs, enable the utilities to remotely shut down participating residential and small commercial consumer's equipment, on short notice (Albadi and El-Saadany, 2008; Aghaei and Alizadeh, 2013). In interruptible services (Albadi and El-Saadany, 2008), participating consumers receive upfront incentive payment or rate discount. Demand Bidding programs allow consumers to bid on specific load reductions in the electricity wholesale market. Participating consumers are paid incentives for measured load reductions during emergency conditions in emergence DR programs. Consumers who commit to providing pre-specified reductions, when system contingencies arise are offered Capacity Market Programs by utilities. In ancillary services market programs consumers are permitted to bid on load curtailment in the spot market as an operating reserve (Albadi and El-Saadany, 2008).

Potential benefits of DR (Albadi and El-Saadany, 2008; Siano, 2014), include: electricity bill savings and incentive payments for participating consumers, bill savings for other consumers, reliability benefits, market performance, consumers have more options

for electricity costs management and system security. On the hand, DR has costs (Albadi and El-Saadany, 2008), which include: enabling technology, response plan, inconvenience, lost business; rescheduling, on-site generation, administration, marketing, incentive payments and evaluation.

2.4 DSM of hybrid energy systems for smart commercial buildings.

Enabling smart technologies for commercial DR (Siano, 2014) include on-site HRESs, communication systems, monitoring systems and control devices (Hohne, Kusakana and Numbi, 2020). Eltamaly *et al.* (2021), propose an internet of things (IoT) based architecture for HRES, consisting of a grid, wind turbine, PV, BSS, and DG. This study defines communication models for HRES based on the IEC 61850 standard. A university campus is employed as a case study, in which critical parameters, such as network topology, link capacity and latency, are studied and discussed. In (Setiawan *et al.*, 2015), a ZigBee-Based communication system for data transfer within future microgrids has been presented. All local controllers, which control each hybrid component, are operated by a central controller. The ZigBee communication system transmits and receives data amongst the controllers. The ZigBee technology has a low cost and low power, and its limitation is the low data transfer rate. Demand side management in a smart micro grid, in the presence of renewable generation and demand response, has been presented in (Aghajani, Shayanfar and Shayeghi, 2017). To resolve the intermittence of the power produced by the wind and PV, the use of demand response program, with the participation of commercial consumers, has been proposed. The authors recommend the use of incentive-based payments as price offer packages, to implement demand response programs. Dagdougui, Ouammi and Benchrifa (2020), propose an effective approach for the modelling and optimisation of a smart building integrated microgrid. The study's objective is the development of a smart building energy management system, which optimally controls the operation of a building-integrated-microgrid. The smart building microgrid, consists of a PV, wind turbine, energy storage unit, electric vehicle, metering infrastructure, micro-CHP and loads. Scheduling distributed energy resources and smart buildings of a microgrid, via a multi-time scale and model predictive control method, has been proposed in Jin *et al.* (2019). In this paper, a

two-stage scheduling framework has been proposed. During the first stage, a day-ahead dynamic optimal economic scheduling method, has been proposed, to minimise the daily operating cost of the microgrid, while a model predictive control based intra-hour adjustment method, is proposed to reschedule the distributed energy resources and smart buildings to cope with the uncertainties during the second stage. An optimisation strategy is proposed (Ullah *et al.*, 2020), to minimise the operation costs and carbon emissions, with and without DR programs in the smart grid integrated with renewable energy sources. Commercial, residential and industrial consumers are encouraged to participate in the energy optimisation actively through the offered incentive-based DR programs.

2.5 Chapter discussions and summary

The reviewed research work, shows that the integration of on-site optimised grid-connected hybrid energy systems and TOU DR, is potentially able to minimise the high electricity consumption in commercial buildings. However, solely (Sichilalu and Xia, 2015) accounts for a grid outage which lasts long enough to exhaust the battery capacity. Similarly, this research accounts for a grid outage which lasts long enough to exhaust the battery capacity. In addition, this research work is taken further, to assess the economic impact of grid scheduled load shedding on commercial consumers.

The related studies show that the integration of on-site optimised grid-connected hybrid energy systems and TOU DR, may mitigate the scheduled load shedding in commercial buildings. However, they do not consider the economic impact assessment of load shedding on commercial consumers. Table 2.1 provides a comparative summary on related studies and this study, on scheduled grid load shedding. This study considers load shedding mitigation backup strategies, optimal load shedding control, application of grid load shedding to commercial buildings and the economic impact assessment of scheduled load shedding, as shown in Table 2.1. The contributions of this study are as follows:

1. The first contribution is the development and implementation of a mathematical model for an optimal operation of a grid-connected PV-Battery-DG energy system, that enables the commercial consumers, to address the increasing demand, increasing growth of energy demand, fluctuating demand throughout the day, as well as load

shedding. The developed model has been validated by means of case studies, using practical and realistic daily fluctuations in the load demand.

Table 2.1 Comparative summary on related studies and this study

Reference	Load shedding mitigation backup strategy	Optimal load shedding control	Optimal load shedding applied to:	Economic impact assessment of scheduled load shedding on commercial consumers
Bakht et al., (2021)	Photovoltaic, battery bank and diesel generator.	Yes	Residential buildings	No
Hijjo et al., (2016)	Photovoltaic, battery bank and diesel generator.	Yes	Commercial buildings	No
Ndwali et al., (2020) Grid-tied PV-DG	Photovoltaic and diesel generator	Yes	Commercial buildings	No
Trigueiro dos Santos et al., (2016)	Photovoltaic and Battery bank	Yes	Commercial buildings	No
Hohne, Kusakana and Numbi (2020)	Photovoltaic and Battery bank	No	No application	No
Mariaud <i>et al.</i> , (2017)	Photovoltaic and Battery bank	No	No application	No
Sichilalu and Xia, (2015)	Photovoltaic, battery bank and diesel generator.	No	No application	No

Wu, Tazvinga and Xia (2015)	Photovoltaic and Battery bank	No	No application	No
This study	Photovoltaic, battery bank and diesel generator.	Yes	Commercial buildings	Yes

2. In this research, the effect of scheduled load shedding for the consumers which are located at different areas has been investigated. It was found that the daily scheduled grid load shedding impacts differently on commercial consumers; this is due to the available renewable resource, battery SOC, as well as the amount of DG energy used.

This Chapter has covered a comprehensive literature review on commercial demand side management, under which this thesis falls.

CHAPTER 3: OPTIMAL SIZING AND OPERATION CONTROL OF A GRID-TIED HYBRID RENEWABLE ENERGY SYSTEM FOR A COMMERCIAL BUILDING

3.1 Introduction

The objective of this Chapter is to optimally size a grid-tied hybrid PV-battery-DG energy system, to have a minimum Net Present Cost (NPC) and minimum Levelized Cost of Energy (LCOE), while meeting the load demand of a commercial building. The optimally sized HRES configuration, is the one that has the minimum total NPC. Optimal sizing techniques have been considered in this Chapter for designing a reliable and economical HRES.

The rest of this chapter is organised as follows: Section 3.2 presents information for the case study. Section 3.3 provides HRES description and model. Simulation results are presented and discussed in Section 3.4, while a conclusion is presented in Section 3.5.

3.2 Case Study Description and Data Inputs

The second floor of the Engineering Technology Building (ETB), at Central University of Technology, Free State, South Africa, has been selected for the case study. This floor has Electronics and Electrical Engineering Laboratories, as well as staff offices. Its load comprises laboratory equipment, air conditioners, printing and photocopying machines, data projectors, computers, as well as lights. The energy consumption of ETB's second floor has been measured in 1-hour time intervals, from 01 January 2018 to 31 December 2018 using the EG3000 real time web-based energy meter. The author accessed the measured load profile using the local area network of the institution. The 31 July 2018 (Tuesday) has been selected, as it is the day with the highest load demand for the entire year. The load demand varies in accordance with the periods when the equipment and computers are in use, i.e., summer, winter, weekdays weekends, university's holidays, and

public holidays. Figure 3.1 shows that the load demand reached its maximum value of 15.13 kW, in July 2018. This is due to the high usage of air conditioners, laboratory equipment and computers. July is the coldest month in Bloemfontein, therefore there is a need for the use of air conditioners. Laboratory equipment and computers are further frequently used this time for the academic work. The lowest load demand was reached in December, when staff and students were on vacation. The recorded average energy consumed by the load, is 102 kWh/day.

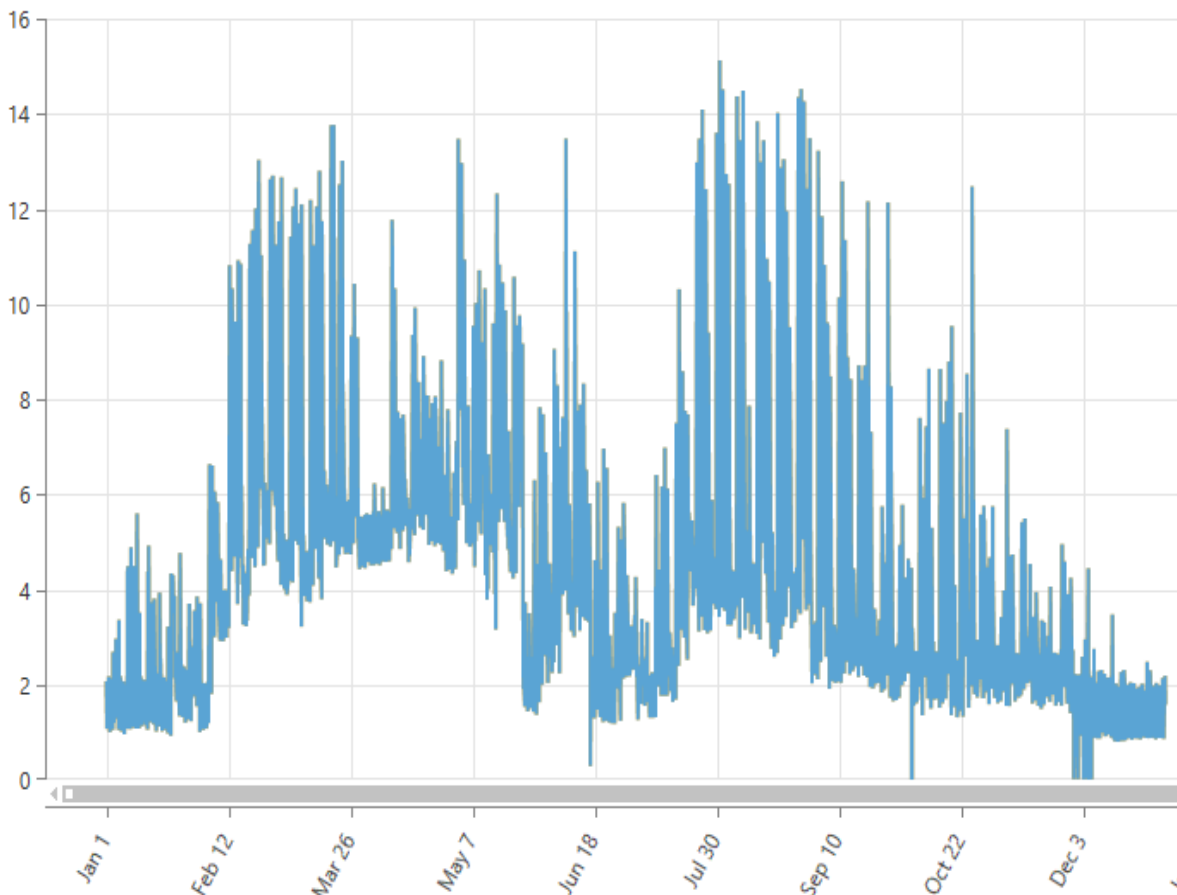


Figure 3.1 Energy consumption of ETB second floor for 2018

The hourly average Global Horizontal Irradiation data has been obtained from the Southern African Universities Radiometric Network (SAURAN), Bloemfontein, South Africa, from January to December 2016. Since the measured data was incomplete for 2018 from the source, it is assumed that 2018 data is like that of 2016, as the difference between the hourly average Global Horizontal Irradiation for the two years would not affect the

optimal size of the PV system significantly. The monthly average solar irradiance (Figure 3.2), varies from 3.6 kW/m²/d in June, to 8 kW/m²/d in December, with the annual average of 5.83 kW/m²/d.

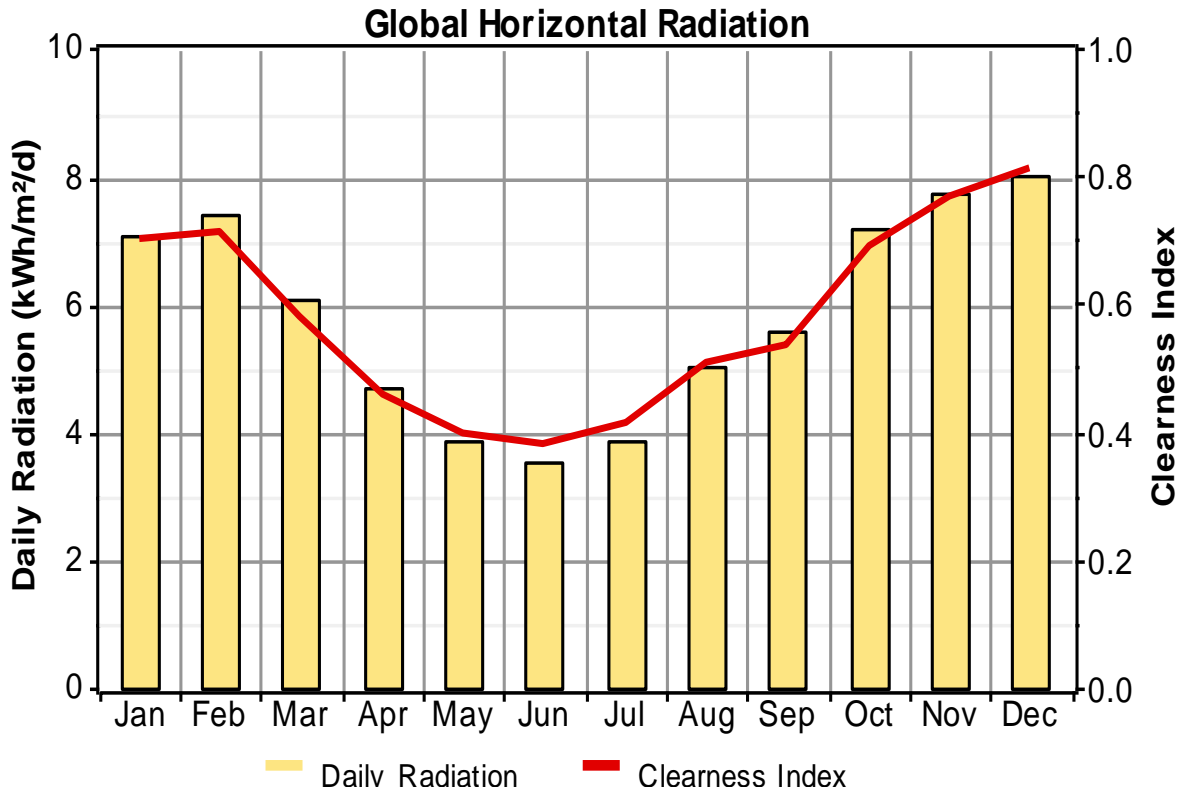


Figure 3.2 Bloemfontein 2016 global horizontal irradiance data

All prices in this study are expressed in USD, using the 28 December 2018 exchange rate of \$1 to R14.42, as South African Rand (ZAR) fluctuates extensively.

The High Season TOU Tariff for Mangaung Municipality, used in this study, is outlined on Table 3.1.

Table 3.1 High Season TOU Tariff for Mangaung Municipality

Charge	Time interval	Energy Price
Peak	07:00-10:00, 18:00-20:00	0.20 (USD/kWh)
Standard	06:00-07:00, 10:00-18:00, 20:00-22:00	0.10 (USD/kWh)
Off-peak	00:00-06:00, 22:00-24:00	0.09 (USD/kWh)
Network access		3,21(USD/kVA)
Demand charge		8.72(USD/kVA)
Basic charge	Monthly	141.40 (USD)

3.3 HRES Description and Model

3.3.1 Introduction to HOMER

al Garni, Awasthi and Ramli (2018); Kusakana and Vermaak (2012) have proposed a commercially available software known as Hybrid Optimization Model for Electric Renewable (HOMER) for optimal sizing of hybrid energy systems. HOMER is user-friendly and may provide powerful graphical outputs. Its limitation is that it models hybrid components with linear equations, that do not represent the source characteristics accurately. To determine the best HRES configuration which has the minimum total NPC, HOMER uses equations (3.1) and (3.2).

$$TNPC(\$) = \frac{C_A}{CRF} \quad (3.1)$$

$$CRF = \frac{i(1+i)^n}{(1+i)^n - 1} \quad (3.2)$$

HOMER uses equation (3.3) to determine the system total levelized cost of energy (LCOE)

$$LCOE(\$) = \frac{C_A}{E_{AC}} \quad (3.3)$$

Where: C_A is the Total Annualised Cost including components' capital costs, replacement costs, operational costs as well as fuel costs; CRF is the capital recovery factor; i is the annual rate of interest for the project life; n is the project lifetime and E_{AC} is annualised AC load supplied by the HRES. The major constraints during the simulation and optimisation process are the project lifetime, the minimum renewable fraction, as well as the operating reserve.

3.3.2 PV System

The CS6U-335P model (335 W) photovoltaic panel, has been selected for the simulation for its high output power, high efficiency and 25 years lifetime (Siecker, Kusakana and Numbi, 2017). Its capital cost, with assumptions for replacement, operating and maintenance (O & M) costs, are given in Table 3.2. Based on this selection, three panels are required to generate 1 kW, with the capital cost of \$454.44. The PV generated power is the main supply of the load. In cases of surplus output, the excess power is used to charge the battery storage and it may be sold to the grid, when the battery storage is fully charged.

3.3 Battery Storage System

The battery storage system may be charged by the optimal power flow from the PV, solely when the surplus power has been generated by the PV system (Kusakana, 2020). It may further be charged by the optimal power flow from the Utility grid, during the off-peak and standard periods of the TOU tariff. The battery storage system may be used to supply the load during peak periods of the TOU, as it is uneconomical to supply the load from the grid during these periods. In this study, the Surrette 6CS25P lead acid battery has been selected for simulation. Its specification, capital cost with assumptions for replacement and O & M costs, are given in Table 3.2. HOMER supports the load following dispatch strategy, in which generators are operated to meet the primary load and cycle charging, in which generators are operated to meet the primary load first and the surplus power flows to other components. The charge and discharge of batteries in HOMER, depends on dispatch strategy. If load following strategy is employed, generators solely

operate at a power to meet the load demand. Conversely, when cycle charging strategy is used, the generator works at its full load and after meeting the load requirements, the surplus electricity carries over to other components.

3.3.4 Inverter

The inverter used in this study is a grid-tied bidirectional converter (Kusakana, 2021). Based on the measured peak load of 15 kW, the author has selected Solis-3P15K-4G, a 15 kW 3-phase inverter for simulation. Its capital cost, with assumptions for replacement, O & M costs are given in Table 3.2. This inverter is suitable for grid-tied hybrid energy systems and smart grid operations.

3.3.5 DG

The Ricardo-HL, 18 kW model diesel generator has been selected for the simulation. Its capital cost, with assumptions for replacement, O & M costs are given in Table 3.2. The price of the diesel impacts significantly on the running costs of a grid-tied hybrid PV-Battery-DG energy system (Kusakana, 2015). The cost of diesel solely takes place when the diesel generator is used to supply the load, when both the photovoltaic array and grid are unavailable. In South Africa, the diesel price fluctuates throughout the year. The inland prices fluctuated from \$0.84 (R12.15/l) to \$1.1 (R15.69/l) in 2018.

Technical and economic data of the HRES parameters with assumptions, are summarised in Table 3.2.

Table 3.2 Technical and economic data of the HRES parameters with assumptions

Description	Parameter	Description	Parameter
Photovoltaic Panel		Diesel Generator	
Model	CS6U-335P	Model	Ricardo-HL
Power (peak)	335 W)	Rated power	18 kW
Capital cost	\$447.51	Capital cost	\$2000
O & M cost	\$0/year	O & M cost	\$0.05/h
Replacement cost	\$447.51	Replacement cost	\$2000
Efficiency	18%	Lifetime	15000h
Lifetime	25 years	Minimum load ratio	30% of rated power
Battery Storage		Converter	
Model	Surrette 6CS25P	Model	Solis-3P15K- 4G
Nominal voltage	6 V	Rated power	15 kW
Capacity	1156 Ah@100h rate	Capital cost	\$1800.07
Capital cost	\$1375	O & M cost	\$22.50/year
O & M cost	\$23.57/year	Replacement cost	\$1800.07
Replacement cost	\$1178.58	Lifetime	25 years
		Conversion efficiency	98%

The load profile presented in Figure 3.1, the Global horizontal irradiance data provided in Figure 3.2, the High Season TOU Tariff in Table 3.1, the diesel price provided in section 3.3.5, as well as the technical and economic data of the HRES parameters in Table 3.2, are applied to the HOMER model of Figure 3.3, for simulations. Figure 3.3 shows the HOMER model of the proposed grid-tied hybrid energy system.

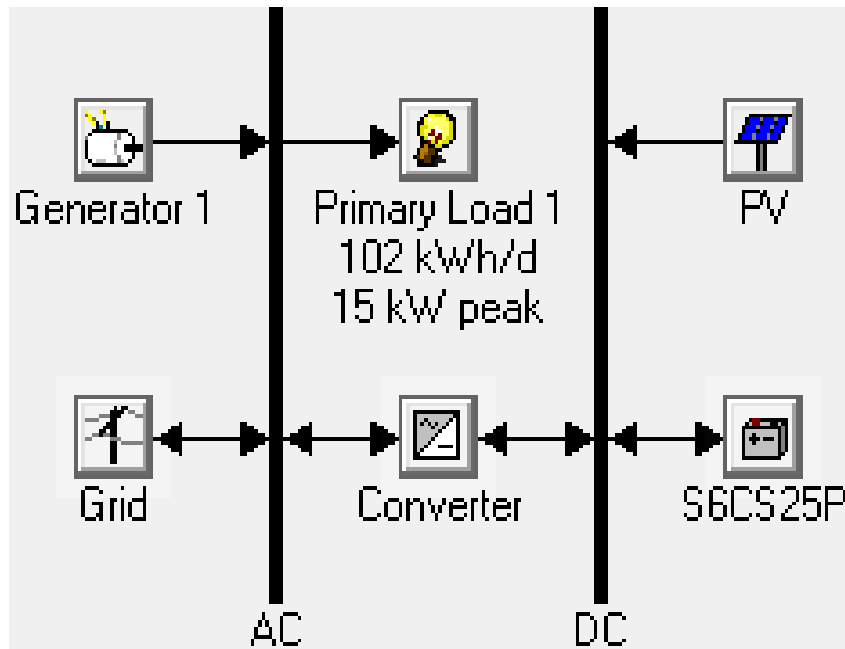


Figure 3.3 HOMER model of grid-tied hybrid PV-Battery-DG energy system

3.4 Simulation Results and Discussions

Table 3.3 provides the HRES cost in detail. HOMER predicts the total NPC of the system over 25 year's operation of the optimum PV-Battery, as 85195 (USD), while the LCOE is 166 (USD). On the other hand, the total NPC for optimum PV-Battery-DG, is 86740 (USD), while the LCOE is 169 (USD). The share of various costs of the optimum PV-Battery system, is shown in Figure 3.4.

For the grid-tied optimum PV-Battery system, the optimum sizes are 18 kW for the PV, 6 Surrrette 6CS25PS batteries and 15 kW for the bidirectional converter. Conversely, for the grid-tied optimum PV-Battery-DG system, the optimum sizes are 18 kW for the PV, 18 kW for the DG, 6 Surrrette 6CS25PS batteries and 15 kW for the bidirectional converter.

Table 3.3 Comparisons of the first five of sixty feasible grid-tied hybrid configurations using HOMER

Configuration	Grid	PV (kW)	DG (kW)	Batteries (number)	Converter (kW)	NPC (USD)	O & M (USD)	LCOE (USD/kWh)
PV-Battery	√	18	0	6	15	85195	5247	166
PV-Battery	√	16	0	6	15	85974	5379	170
PV-Battery-DG	√	18	18	6	15	86740	5212	169
PV-Battery	√	14	0	6	15	86885	5520	174
PV-Battery-DG	√	16	18	6	15	87520	5343	173

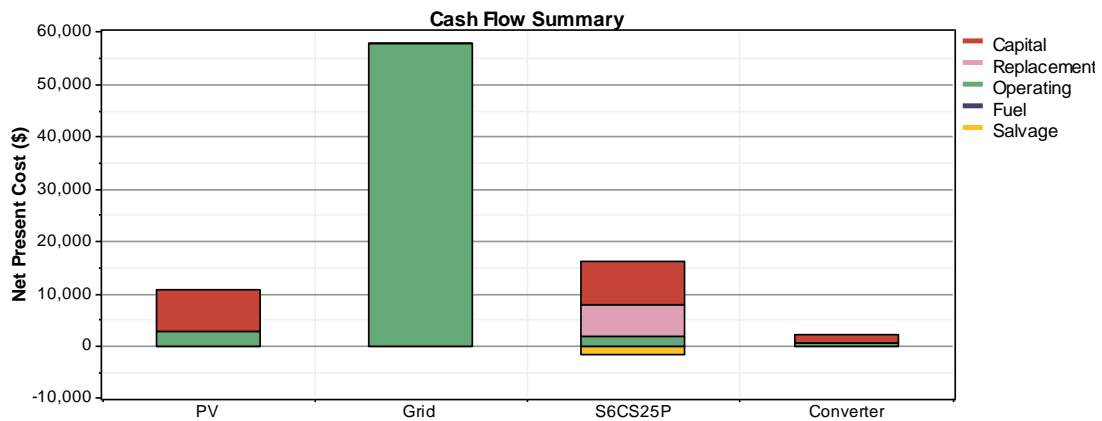


Figure 3.4 The share of various costs of optimum PV-Battery system during the project life

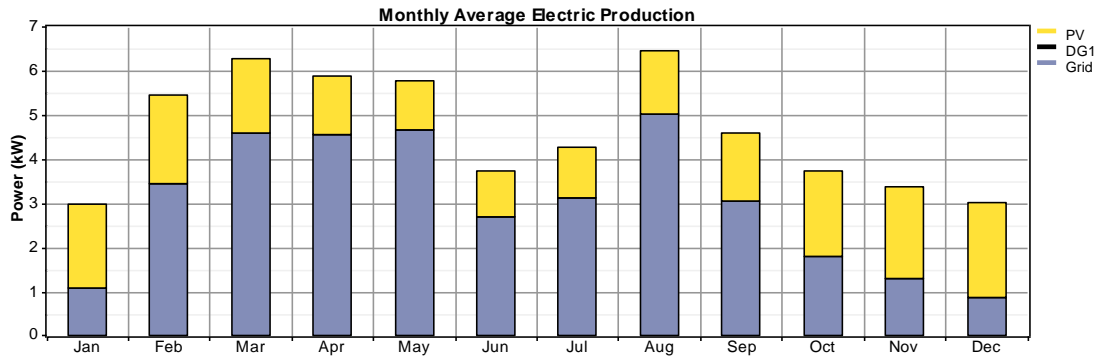


Figure 3.5 Power generated by the PV-Battery optimally sized system

Figure 3.5 shows the power generated by the optimally sized hybrid system, throughout the year. The monthly average generated power varies from 3 kW in January and December, to approximately 6.5 kW, in August. The power purchased from the grid, varies from 1 kW in January and December to 5 kW in August. The power generated by the PV array ranges from 1 kW in June to 2 kW in January and December. This is because solar irradiance is lowest in June and highest in January and December. Energy produced by PV array is 14134 kWh/year (35% of the total energy). Energy purchased from the grid is 26400 kWh/year (65% of the total energy). On the other hand, the energy consumed by the AC primary load, sold to the grid, is 37230kWh/year and 3003 kWh/year, respectively. Simulation results show that the unmet load demand is 0%, while the capacity shortage is 0%.

Figure 3.6 indicates the power generated by the PV (PV-Battery HRES). This power varies from 0 kW to 5.76 kW, with the average value of 1.61kW. The power is generated from 06:00 – 18:00 per day. The total electric production is 14134 kWh/year. The PV array operates 4380 h/year, with the penetration on 38%.

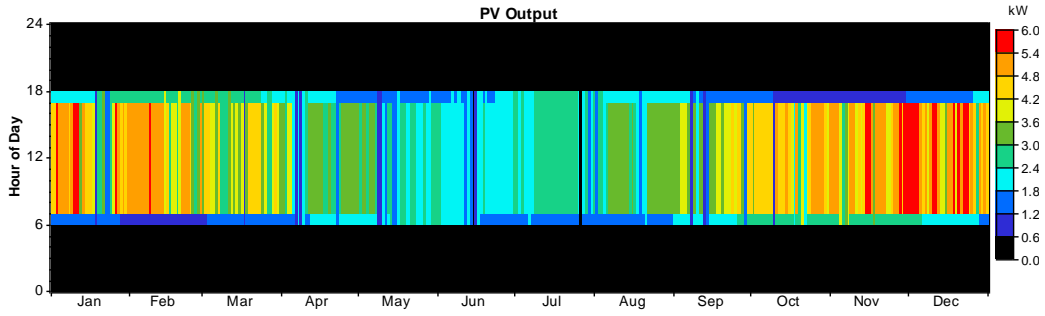


Figure 3.6 Power generated by the optimally sized PV (PV-Battery HRES) during the year

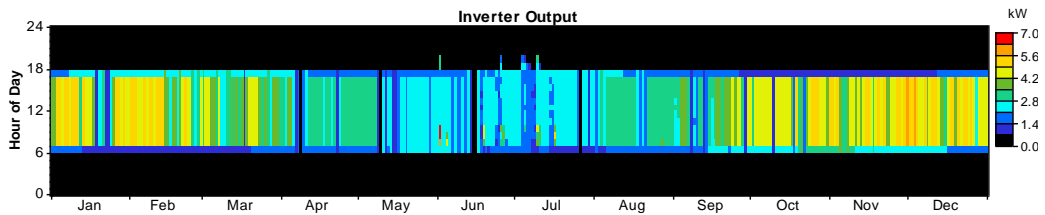


Figure 3.7 Converter (PV-Battery HRES) optimal power flow to the AC bus

Figure 3.7 shows the power flow from the converter (PV-Batter HRES) to the AC bus. The output power ranges from 0 kW to 6.9 kW, with the average value of 1.6 kW. The inverter operates for 4450 hours/year. The input energy to the inverter is 14116 kWh/year, while the output energy to the AC bus is 13 833 kWh/year, with 282 kWh/year (2%) losses, due to the load following dispatch strategy.

3.5 Conclusion

The objective of this Chapter is to optimally size a grid-tied hybrid PV-battery-DG energy system, to meet the load demand of a commercial building with possible minimum NPC and LCOE. To achieve this objective, the HOMER software has enabled the author to optimally size the proposed HRES, to obtain the minimum NPC and LCOE. For the proposed grid-tied optimum PV-Battery-DG system, the optimum sizes are 18 kW for the PV, 18 kW for the DG, 6 Surrerte 6CS25PS batteries and 15 kW for the bidirectional converter. The most economic NPC for the grid-tied PV-Battery configuration obtained in this study using HOMER, is \$85195, while the LCOE is \$166/kWh, and the operating

cost is \$5247 for the 25-year period. Alternatively, the most economic NPC for the grid-tied PV-Battery-DG configuration obtained in this study using HOMER, is \$86740, while the LCOE is \$169/kWh and the operating cost is \$5212, for the 25-year period. The load following dispatch strategy has been employed in this study. The optimally sized grid-tied PV-Battery-DG, is required in the following Chapters.

CHAPTER 4: DEMAND SIDE MANAGEMENT OF GRID-TIED HYBRID SYSTEM FOR A COMMERCIAL BUILDING

4.1 Introduction

The objective of this Chapter is to model and simulate the performance of the optimised grid-tied PV-battery-DG system, for the demand side management of a commercial building. To achieve this objective, this study proposes the development of an optimisation model for grid connected HRES for a commercial building. The purpose of the optimisation model is to minimise the cost of the purchased grid energy under time of use (TOU) tariff and to minimise the cost of running the DG during the back-up periods. The main benefit of reduced electricity purchased from the grid, is the potential reduced electricity bill for the commercial consumers. To validate the performance of the optimised grid-tied PV-battery-DG system, a case study has been conducted for a commercial building, at the Central University of Technology, in Bloemfontein, South Africa.

The remainder of this Chapter is organised as follows: Section 4.2 focuses on the model development; Section 4.3 presents information for the case study; simulation results are presented and discussed in Section 4.4; while a conclusion is presented in Section 4.5.

4.2 System Model Development

In this Section, the proposed hybrid system (Figure 4.1), is presented and modelled. It comprises the photovoltaic (PV), battery storage system (BSS), the grid and the diesel generator (DG). The PV generator is the primary renewable energy source for supplying the commercial building, while the BSS, grid, and DG function as the backups. The backups are required due to the unpredictability and intermittence of the PV. They contribute to reliability of grid-tied hybrid PV-Battery-DG energy system. The DG supplies the load solely when the PV, BSS and the grid are unable to meet the load demands

or are uneconomical, depending on the time of use (TOU). The arrows indicate the direction of the power flow. The mathematical models for the PV system, the BSS, the DG, and the TOU tariff, are formulated. Furthermore, the parameters from the mathematical models are defined. The system components' operation and mathematical models are presented in the following Sections.

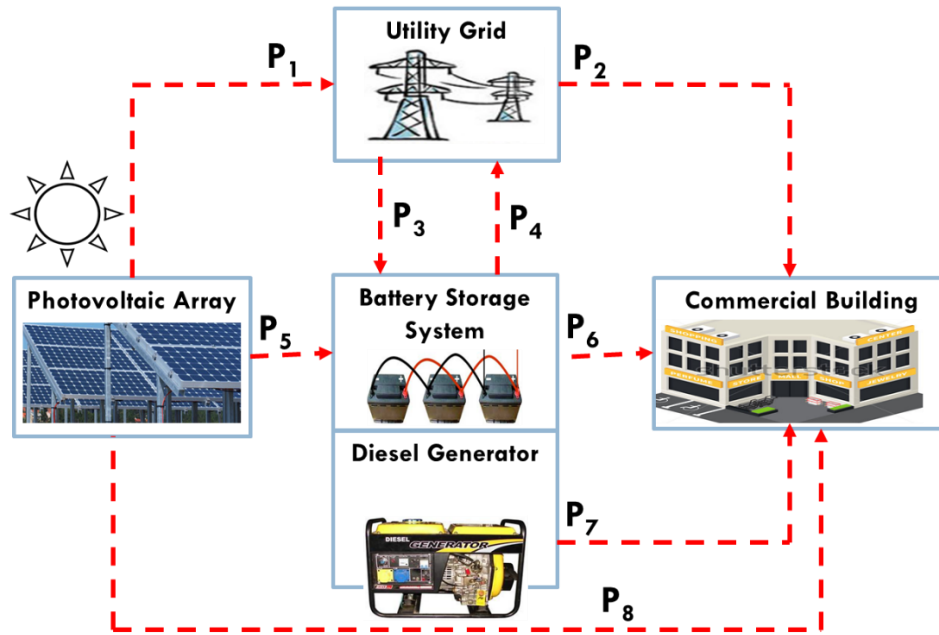


Figure 4.1 Proposed grid-tied hybrid PV-battery-DG energy system

4.2.1 PV model

The PV system consists of several solar cells, which convert solar irradiation into direct current power. For P_{PV} , the hourly output power from a PV system for a specific solar array area; I_{PV} , the hourly solar irradiation incident on the PV panels (kW/m^2); η_{PV} , the efficiency of PV generator; A_{PV} , the total PV surface area (m^2). The hourly output power of the PV system for a given area (Tazvinga, Xia and Zhang, 2013), is formulated as:

$$P_{PV} = I_{PV}\eta_{PV}A_{PV} = P_1 + P_5 + P_8 \quad (4.1)$$

For η_R , the PV generator efficiency is measured at reference cell temperature T_R (25°C); β , is the temperature coefficient for cell efficiency (typically) 0.004-0.005/°C); $I_{Pv,NT}$, the average hourly solar irradiation incident on the array at normal temperature, NT (0.8kW/m²); $T_{c,NT}$, is the cell temperature at NT (typically 45°C) and $T_{A,NT}$, is the ambient temperature (20°C) at NT. The efficiency of the PV generator (Tazvinga, Xia and Zhang, 2013; Hohne, Kusakana and Numbi, 2021), may be expressed as:

$$\eta_{Pv} = \eta_R \left[1 - 0.9\beta \left(\frac{I_{Pv}}{I_{Pv,NT}} \right) (T_{c,NT} - T_{A,NT}) - \beta(T_A - T_R) \right] \quad (4.2)$$

For the hourly global irradiation, I_B (kWh/m²); the hourly diffuse irradiation, is I_D (kWh/m²) and R_B is the geometric factor representing the ratio of beam irradiance incident on a tilted plane to the incident on a horizontal plane. The solar irradiation incident on the PV, may be expressed as (Hohne, Kusakana and Numbi, 2018):

$$I_{Pv}(t) = (I_B(t) + I_D(t))R_B + I_D(t) \quad (4.3)$$

4.2.2 BSS model

The BSS is used as an energy backup in this study. The battery is charged with P_3 from the grid, during the off-peak and standard periods of the TOU and with P_5 from the PV. P_4 is the discharge power to the grid and P_6 is the discharge power to the load. The battery performance (Belfkira, Zhang and Barakat, 2011; Tazvinga, Xia and Zhang, 2013; Sichilalu and Xia, 2015), depends on the state of charge (SOC), $SOC(t - 1)$ and this is influenced by charging/discharging power. The study has adopted the battery SOC from Ashook, (Ashok, 2007), for any given time t. For 24-hour horizon, the power flow from (t-1) to t is expressed in (4.4), where: $t = 1, \dots, 24$.

$$SOC(t) = SOC(t - 1)(1 - \sigma) + \eta_c(P_3(t) + P_5(t)) - \frac{1}{\eta_d}(P_4(t) + P_6(t)) \quad (4.4)$$

Where: η_c is the BSS charging efficiency and η_d is the BSS discharging efficiency.

The BSS is charged with the sum of $P_3(t)$ from the grid and $P_5(t)$ from the PV. For model simplicity, both the self-discharged factor, σ and the inverter efficiency, are ignored. The discrete (Hohne et al., 2020) BSS dynamics, are expressed as:

$$SOC(j) = SOC(0) + \frac{\Delta t}{C_b} \times (\eta_c \times \sum_{j=1}^N (P_3(j) + P_5(j))) \left(-\frac{1}{\eta_d} \times \sum_{j=1}^N (P_4(j) + P_6(j)) \right) \quad (4.5)$$

Where: $SOC(0)$ is the initial SOC of the BSS; Δt is the sampling time; C_b is the BSS capacity; $\frac{\eta_c \times \Delta t}{C_b} (P_3(j) + P_5(j))$ is the power accepted by the BSS; $\frac{\Delta t}{C_b \times \eta_d} (P_4(j) + P_6(j))$ is the power discharged by the battery; j is the sampling interval; $j = 1, \dots, N$ and N is the horizon period. The BSS should be operated within its nominal range, expressed as:

$$SOC^{min} < SOC(j) \leq SOC^{max} \quad (4.6)$$

Where: SOC^{min} is the minimum SOC, and SOC^{max} is the maximum SOC, which is equal to the battery capacity to prolong its life.

4.2.3 Grid model

In this study, the grid is used as a backup to supply the load, when both the PV power flow (P_8) and the BSS power flow (P_6) to the load are unable to meet the load demand. Furthermore, it is used to charge the BSS during the off-peak and standard periods of TOU. It should be capable of receiving power flow (P_1) from the PV and from the BSS (P_4), when the sum of (P_6) and (P_8) is greater than the load demand. It is modelled (Sichilalu and Xia, 2015; Yang and Xia, 2017; Kusakana, 2017) as an infinite busbar.

The available grid power is formulated as:

$$P_{grid}(t) = (P_2(t) + P_3(t)) \quad (4.7)$$

The following constraint should be satisfied by the dispatched power from the grid:

$P_{disp-grid}$.

$$P_{disp-grid}(t) \leq (P_2(t) + P_3(t)) \quad (4.8)$$

4.2.4 DG model

DG is commonly used as a backup in commercial buildings. In this study, the DG should be operated solely if the PV, the BSS and the grid are unable to meet the load demand. The benefits of using the DG, are that it may be operated at any time and has low initial cost, compared to alternatives for commercial facilities. Factors affecting the choice of the DG, include the load demand peak and fuel consumption characteristics. The DG fuel consumption may be minimised by operating the DG at a high efficiency (say 75%-100%). The DG fuel consumption (Makhdoomi and Askarzadeh, 2020; Kusakana and Vermaak, 2014), is given by:

$$F_c = C_f(QP_7^2 + RP_7 + S) \quad (4.9)$$

Where: P_7 is the DG power delivered to the load; C_f is the diesel fuel cost (\$/L); Q (L/(kW)²h), R (L/(kWh)) and S (L/h) are the coefficients of the selected DG. The daily fuel consumption, may be obtained from:

$$F_c = \int_{t=1}^{24} C_f (QP_7^2 + RP_7 + S) (t) \quad (4.10)$$

The DG power output is usually within its lower and upper bounds, as indicated in (4.11).

$$P_{DG}^{min} \leq P_7(t) \leq P_{DG}^{rated} \quad (4.11)$$

Where: P_{DG}^{rated} is the rated power output of the DG.

4.2.5 TOU tariff model

TOU is a DR program of DSM, which is used in this study. During a High Season (For June-August day), the TOU Tariff for Mangaung Municipality used in this study, is modelled as follows:

$$\rho(t) = \begin{cases} p_o = \frac{\$0.09}{kWh} \text{ if } t \in [0,6] \cup [22,24], \\ \rho_s = \frac{\$0.10}{kWh} \text{ if } t \in [6,7] \cup [10,18] \cup [20,22], \\ \rho_p = \frac{\$0.20}{kWh} \text{ if } t \in [7,10] \cup [18,20] \end{cases} \quad (4.12)$$

Where: p_o is the off-peak price; ρ_s is the standard price and ρ_p is the peak price.

4.2.6 Aim of the optimisation model

Commercial buildings require reliable hybrid renewable energy sources, which should be optimised. In this regard, the aim of the optimisation model in this study, is to minimise the cost of the purchased grid energy under the TOU tariff and to minimise the cost of running the DG during the back-up periods.

4.2.7 Objective function model

The objective of the optimisation model is to minimise the energy cost of the grid-tied hybrid PV-Battery-DG system under TOU tariff. The proposed multi-objective function presented in (4.13), for the 24-hour horizon, minimises the purchased electricity from the grid (first term), minimises the diesel fuel used to run the DG (second term) and maximises the potential surplus electricity that may be sold to the grid (third term). The control parameters of the objective function are the TOU electricity tariff ($\rho(t)$), the diesel cost (C_f) and the feed in tariff (ρ_{fi}). The multi-objective function, is expressed as:

$$J = t_s \left[\begin{array}{l} \rho(t) \sum_{j=1}^N (P_2(j) + P_3(j)) + C_f \sum_{j=1}^N (QP_7^2(j) + RP_7(j) + S) \\ -\rho_{fi} \sum_{k=1}^N (P_1(k) + P_4(k)) \end{array} \right] \quad (4.13)$$

Where: t_s is the sampling time (delta); $\rho(t)$ is the TOU price (\$/kWh); j is the sampling interval; $j= 1, \dots, N$, C_f is the diesel cost (\$/L) and ρ_{fi} is the feed-in tariff (\$/kWh), subject to the constraints outlined in 4.2.8.

4.2.8 Model constraints

The proposed grid-tied hybrid PV-Battery-DG system comprises linear and nonlinear constraints. The system is subject to the following technical and operational constraints.

- Load balance constraint:

The total power of the grid, BSS, DG and PV should precisely satisfy the load demand of a commercial building as:

$$P_L(j) = P_2(j) + P_6(j) + P_7(j) + P_8(j) \quad (0 \leq j \leq N) \quad (4.14)$$

- Final fixed state constraint for the BSS:

This should be equal to zero for the considered optimisation horizon, which is 24 hours in this case, as given in (4.15).

$$\sum_{j=1}^N (P_3 - P_4 + P_5 - P_6) = 0 \quad (4.15)$$

- PV's output constraint:

The PV's surplus power sold to the grid, power for charging the battery and for supplying the load directly, should be less than the PV's output power generated as given by:

$$0 \leq P_1(j) + P_5(j) + P_8(j) \leq P_{pv}^{max}(j) \quad (0 \leq j \leq N) \quad (4.16)$$

- Grid's power constraint:

The excess power sold to the grid from the PV, grid power to the load, grid power for charging the battery and the discharge power from the battery, should be less than the grid power, as given by:

$$0 \leq -P_1(j) + P_2(j) + P_3(j) - P_4(j) \leq P_{grid}^{max}(j) \quad (0 \leq j \leq N) \quad (4.17)$$

- Battery's power constraint:

The charging power from the grid, discharge power from the battery, charging power from the PV and discharging power from the battery, should be less than the grid power, as given by:

$$0 \leq -P_3(j) + P_4(j) - P_5(j) + P_6(j) \leq P_{BSS}^{rated}(j) \quad (0 \leq j \leq N) \quad (4.18)$$

- SOC boundary constraint:

The $SOC(j)$ of the battery should be less than the battery's capacity SOC^{max} and larger than the minimum allowable value SOC^{min} , as follows:

$$SOC^{min} < SOC(j) \leq SOC^{max} \quad (4.19)$$

- Non-Linear Constraints:

The power flow for charging and discharging the BSS, should not take place simultaneously, since power flows in one direction. As a result, the product of charging power flows and discharging power flows, should be zero and this is expressed as:

$$(P_3(j) + P_5(j)) \times (P_4(j) + P_6(j)) = 0 \quad (4.20)$$

Similarly, the power flow to and from the grid, should not take place simultaneously for power flows in one direction. Consequently, the product of power bought from the grid and power sold to the grid, should be zero and this is expressed as:

$$(P_1(j) + P_4(j)) \times (P_2(j) + P_3(j)) = 0 \quad (4.21)$$

- Variable boundaries

The optimisation model has continuous control variables. These control variables are exceptionally critical for the safety purposes of the generation, battery storage and stable operation of the on-site hybrid renewable energy systems. They enable the HRES to operate within its minimum and maximum electrical power capacities at any given time. The continuous control variable limits measured in kW, at each j^{th} sampling interval, are expressed as:

$$0 \leq P_{PV}(j) \leq P_{PV}^{max} \quad (0 \leq j \leq N) \text{ for the PV} \quad (4.22)$$

$$0 \leq P_{grid}(j) \leq P_{grid}^{rated} \quad (0 \leq j \leq N) \text{ for the grid} \quad (4.23)$$

$$0 \leq P_{DG}(j) \leq P_{DG}^{rated} \quad (0 \leq j \leq N) \text{ for the DG} \quad (4.24)$$

$$0 \leq P_{BSS}(j) \leq P_{BSS}^{rated} \quad (0 \leq j \leq N) \text{ for the BSS} \quad (4.25)$$

4.2.9 Model solver selection

An optimisation model is formulated based on the multi-objective function (4.13), subject to constraints (4.14-4.25). As both the objective function and constraints have linear and non-linear models, the control problem is expressed as a mixed integer nonlinear problem (MINLP). The MINLP problem is solved using an optimisation solver, known as Solving Constraint Integer Programs (SCIP), which is available in the MATLAB interface OPTI toolbox. The SCIP is one of the fastest, non-commercial solvers for mixed integer (linear and nonlinear) programming solver and constraint programming framework. It employs Interior Point Optimizer (IPOPT) and SoPlex algorithms. IPOPT, is a non-commercial solver for large-scale nonlinear programming. SoPlex, is well suited for advanced implementation of the revised simplex algorithm, for solving linear programs. Its features include pre-processing, exploits sparsity and it provides primal and dual solving routines. The SCIP solver solves problems of the form:

$$\min_x f(x) \text{ (objective function)}$$

Subject to the following constraints:

$Ax \leq b$ (linear inequality constraints)

$A_{eq}x = b_{eq}$ (linear equality constraints)

$l_b \leq x \leq u_b$ (upper and lower boundaries)

$c(x) \leq d$ (nonlinear inequality constraints)

$c_{eq}(x) = d_{eq}$ (nonlinear equality constraints)

$x_i \in Z$ (integer decision variables)

$x_j \in \{0,1\}, i \neq j$ (binary decision variables)

4.3 Case Study

In this Section, load description, hybrid system sizing, generated PV output power data and simulation parameters for the case study, are presented.

4.3.1 Load description

The second floor of Engineering Technology Building (ETB), at Central University of Technology, Free State, South Africa, has been selected for the case study. This floor has Electronics and Electrical Engineering Laboratories, as well as staff offices. Its load comprises laboratory equipment, air conditioners, printing/photocopying machines, data projectors, computers and lights. The energy consumption of ETB's second floor has been measured in 1-hour time intervals, from 01 January 2018 to 31 December 2018, using the EG3000 real time web-based energy meter. The worst-case day load demand occurred on 31 July (Tuesday) 2018. Figure 4.2 indicates that the load profile varies from 3.4kW to 15.1kW. The peak consumption of 15.1kW (from 10:00 to 11:00), is characterised by the high usage of power in the laboratories, offices and air conditioners, throughout July. The off-peak periods, standard periods and peak periods, are presented in green, yellow and red, respectively.

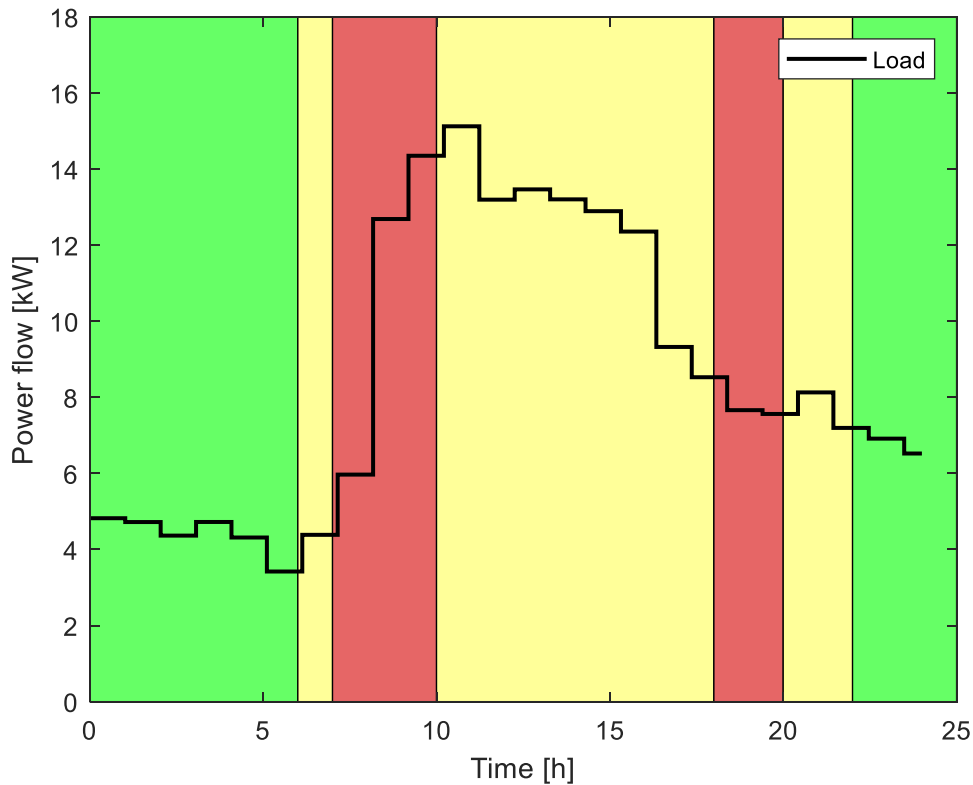


Figure 4.2 Load profile of the second floor CUT ETB building on 31 July 2018.

4.3.2 Hybrid system sizing

The PV fixed system optimal sizing is based on the available space on the institution's premises and the load profile of the building. The battery storage system optimal sizing is based on the minimisation of the electricity bill for the building. The DG optimal sizing is based on the importance of avoiding power outages during the academic calendar. The study has adopted optimal sizing of the grid-tied PV-Battery-DG, based on HOMER from (Moji, Kusakana and Numbi, 2020), in which PV array: 18kW; battery storage system: 6 Surrette 6CS25P batteries; inverter: 15kW and DG: 18kW. HOMER is preferred for optimal hybrid sizing, as it is user friendly and may provide powerful graphical outputs. However, it models hybrid components with linear equations, which fail to represent the source characteristics accurately.

4.3.3 Generated PV output power

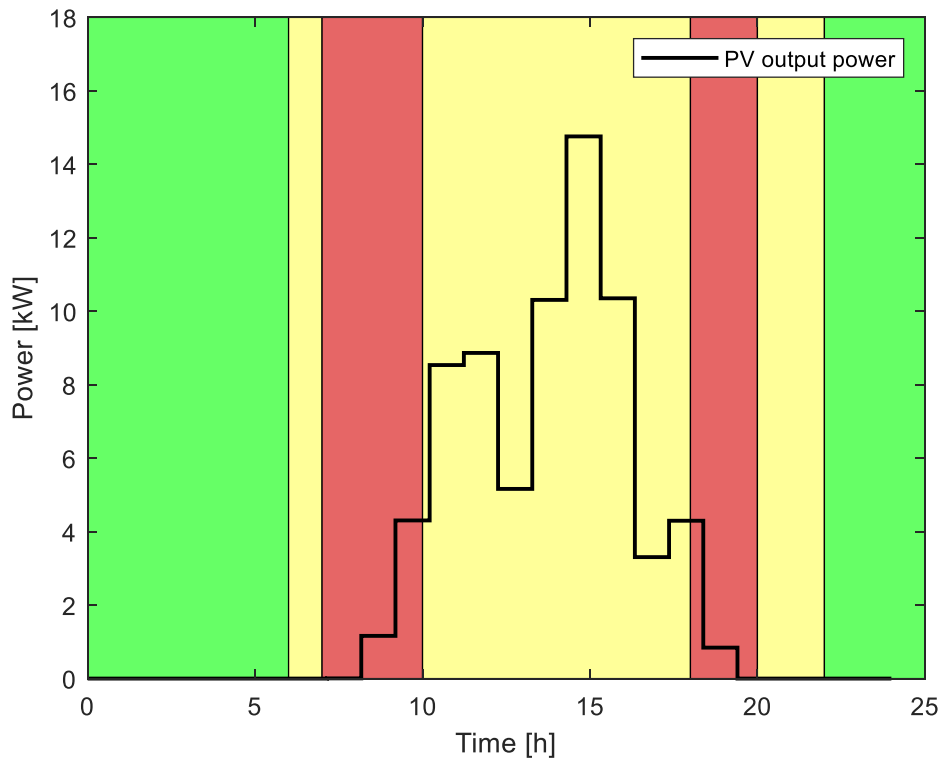


Figure 4.3 Generated PV output power for 31 July 2018

The hourly average Global Horizontal Irradiation data (Southern African Universities Radiometric Network) has been obtained from the Southern African Universities Radiometric Network (SAURAN), Bloemfontein, South Africa, from January to December 2016. Since the measured data was incomplete for 2018 from the source, it is assumed that 2018 data is like that of 2016. The value of the hourly measured irradiance for the 31 July 2018, the assumed efficiency of 18% and assumed PV array area of 135m², have been substituted in (4.1), to obtain the hourly generated PV power. It should be noted that the generated PV power depends on the parameters in the (4.1) model. The generated PV output power (Figure 4.3), for 31 July 2018, ranges from 0kW (00:00-08:00, 19:30-24:00) to 14.8kW (14:00-15:00). The three colours indicate TOU periods, namely, green for off peak, yellow for standard and red for peak periods.

4.3.4 Simulation parameters

Simulation parameters are provided in Table 4.1.

Table 4.1 Simulation parameters

Item	Value
t_s =Delta (sampling time)	30min
Q (fuel consumption coefficient)	4.166e-3(L/(kW) ² h)
R (fuel consumption coefficient)	0.18(L/(kWh)
S (fuel consumption coefficient)	0.8102(L/h)
C_f (diesel fuel cost)	\$1.1/L
C_b (BSS capacity)	16kWh
η_c (BSS charging efficiency)	85%
η_d (BSS discharging efficiency)	95%
SOC^{max} (maximum battery state of charge)	100%
SOC^{min} (minimum battery state of charge)	20%
SOC.0 (initial battery state of charge)	0.9 x SOC^{max}
p_o (Winter off-peak tariff)	\$0.09/kWh
ρ_s (Winter standard tariff)	\$0.10/kWh
ρ_p (Winter peak tariff)	\$0.20/kWh
ρ_{fi} (Feed-in tariff)	\$0.65/kWh

The simulation horizon for this study is 24h (31 July 2018), with a sampling time (t_s =Delta) of 30 minutes in (4.13), as shown in Table 4.1. To minimise the running cost of the DG, the fuel consumption coefficients Q, R and S, in equation (4.13) are set to 4.166e-3L/h, 0.18L/h and 0.8102L/h, respectively, as shown in Table 4.1. The study uses South Africa's inland diesel price of 2018, \$1.1/L (Table 4.1). The BSS capacity (C_b) in Table 4.1, is set to 16kWh. The battery charging (η_c) and discharging (η_d) efficiencies, are set to 85% and 95%, respectively, in Table 4.1. As the utilization of the battery should be within its nominal range, the minimum state of charge SOC^{min} is set to 20%, the maximum

state of charge SOC^{max} , is equal to the battery capacity and the initial battery state is set to 90% of SOC^{max} , in Table 4.1. The winter TOU tariff for Centlec Mangaung, is used in which the off-peak p_o value is \$0.09/kWh, the standard period ρ_s value is \$0.10/kWh and the peak period ρ_p value is \$0.20/kWh (Table 4.1). The feed-in tariff ρ_{fi} , is set to \$0.65/kWh in Table 4.1.

4.4 Simulation Results and Discussions

The optimal operation of the hybrid grid-tied PV-Battery-DG, is based on the load profile in Figure 4.2, generated PV output (Figure 4.3) and simulation parameters in Table 4.1. The PV system is the primary source, while the grid, battery storage, and DG are the back-up systems that ensure that the building does not experience power outages. Figure 4.4 shows the optimal power flow from the PV to the grid, when a surplus of PV power is available. Figure 4.5 shows the optimal power flow from the grid to the load. Figure 4.6 shows the SOC of the battery storage system. Figure 4.7 indicates the optimal power flow from the grid to the battery storage system. Figure 4.8 shows the optimal power flow from the battery storage system to the grid. Figure 4.9 indicates the optimal power flow from the PV to the battery storage system. Figure 4.10 shows the optimal power flow from the battery storage system to the load. Figure 4.11 shows the optimal power flow from the DG to the load when the PV, the battery storage and the grid are unable to meet the load demand. Figure 4.12 indicates the optimal power flow from the PV to the load. Figure 4.13 compares the baseline cost (solely when the load demand is met by the grid) and the optimal cost.

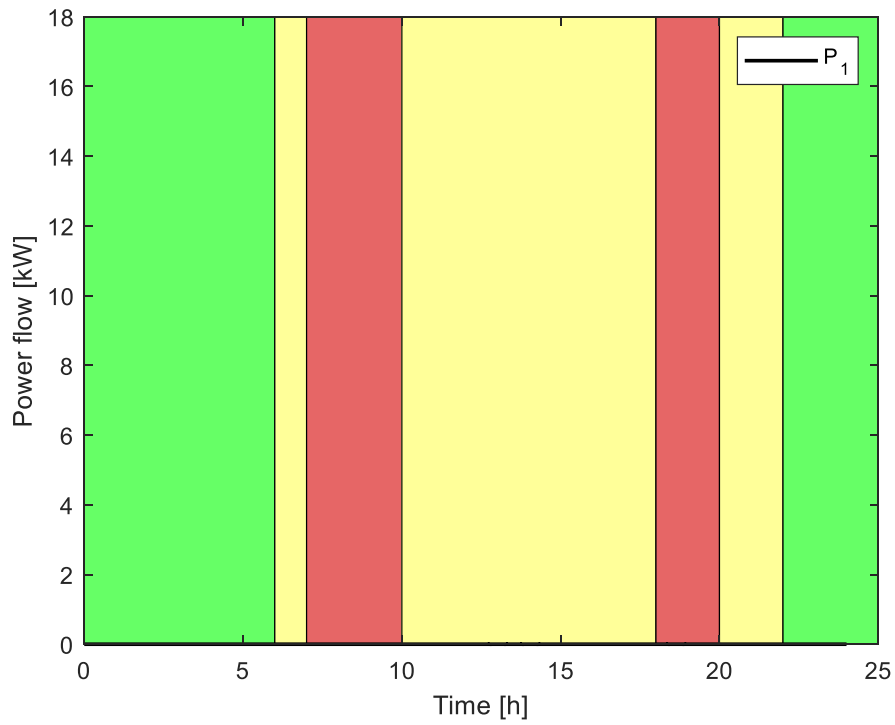


Figure 4.4 Optimal power flow from the PV to the grid

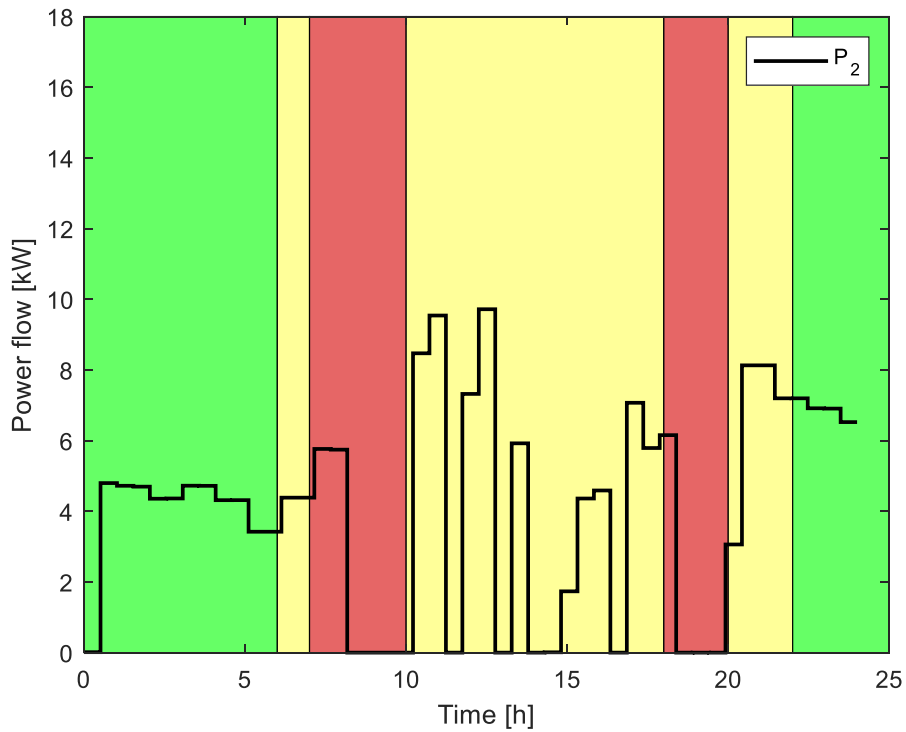


Figure 4.5 Optimal power flow from the grid to load

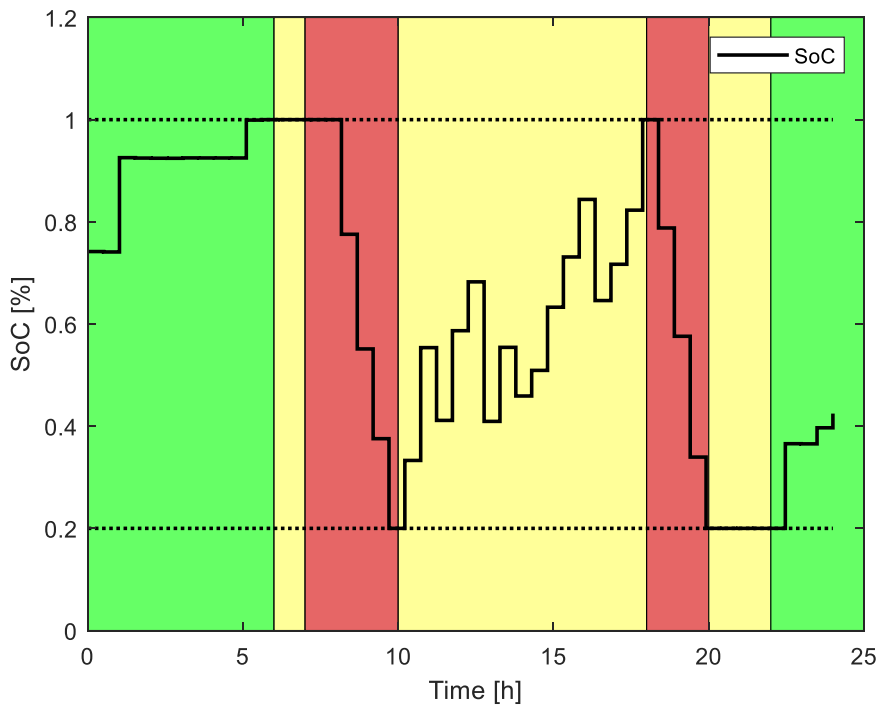


Figure 4.6 Optimal SOC

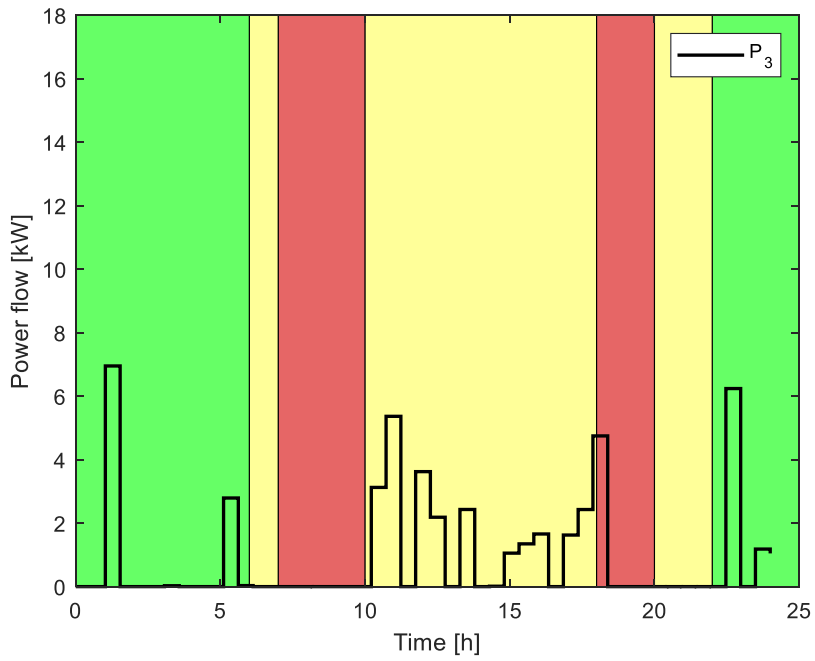


Figure 4.7 Optimal power flow from the grid to the BSS

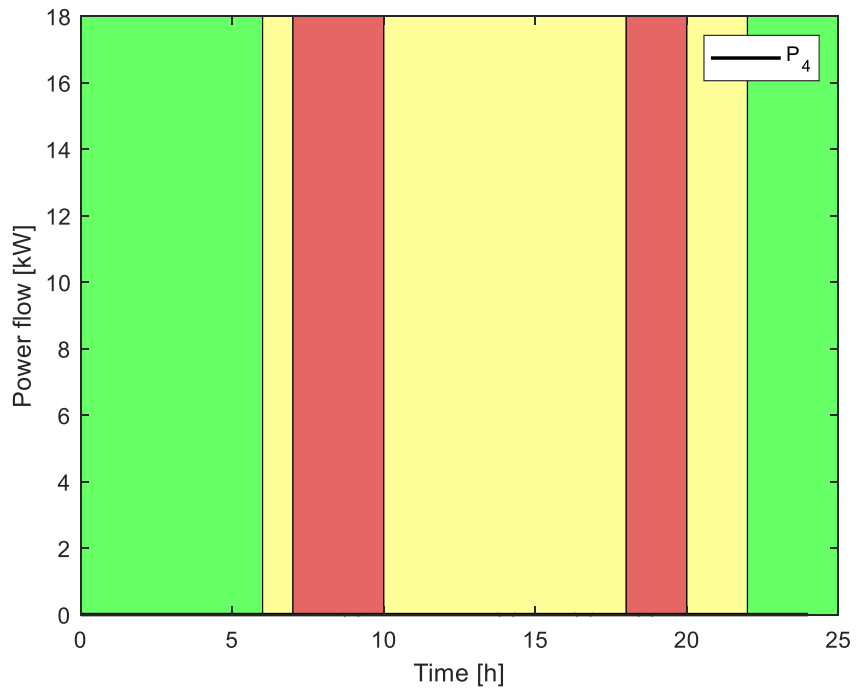


Figure 4.8 Optimal power flow from the BSS to the grid

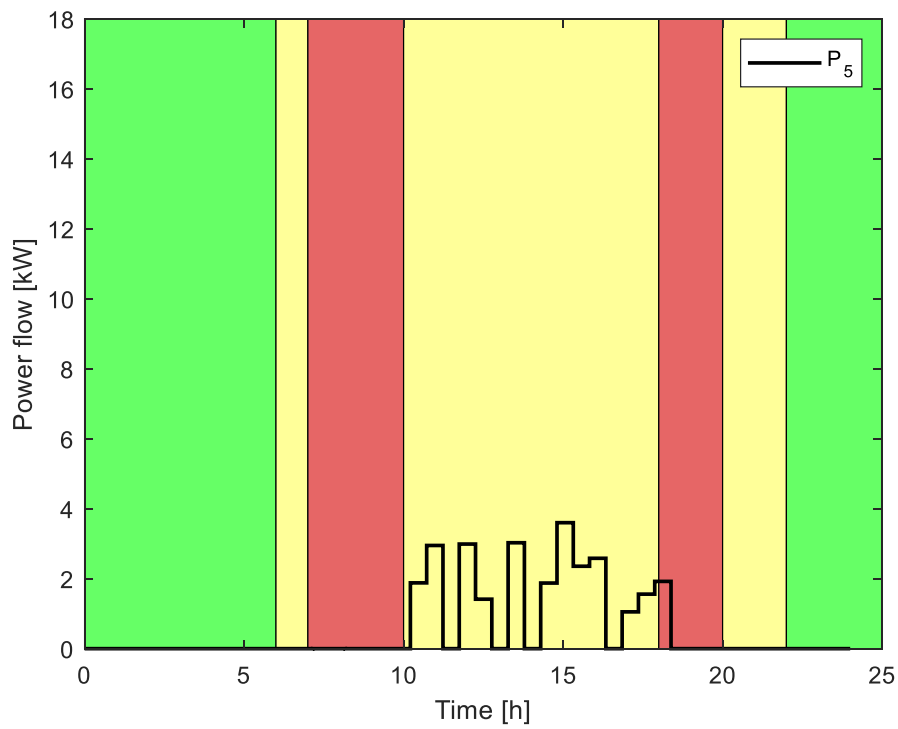


Figure 4.9 Optimal power flow from the PV to the BSS

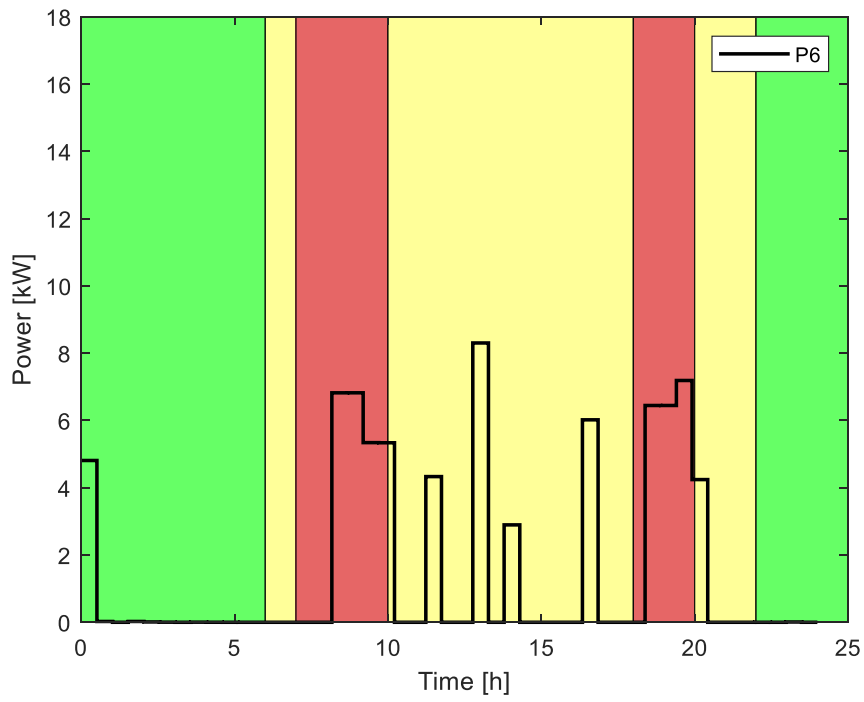


Figure 4.10 Optimal power flow from the BSS to the load

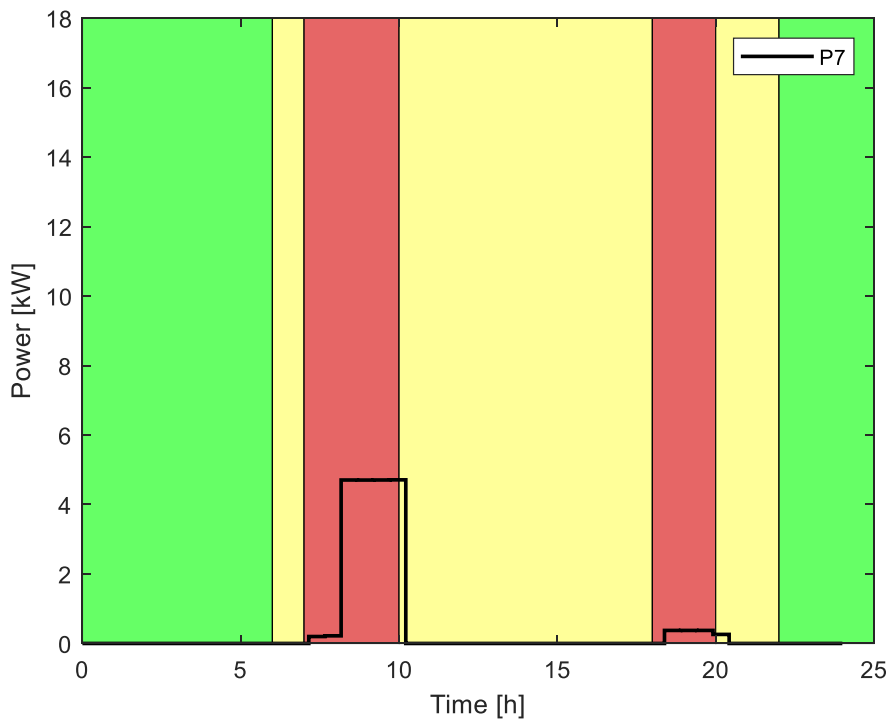


Figure 4.11 Optimal power flow from the DG to the load

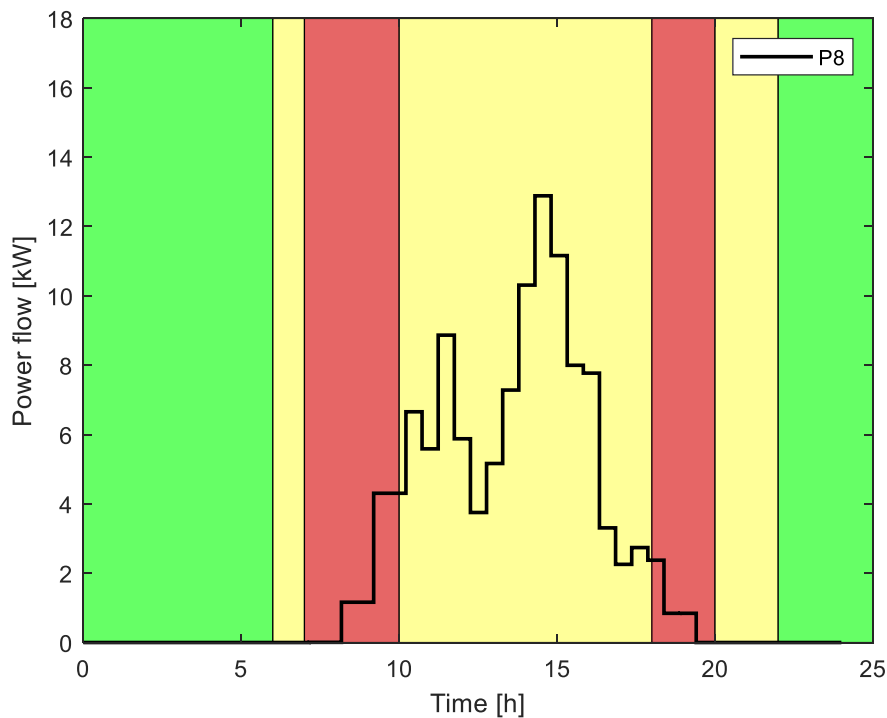


Figure 4.12 Optimal power flow from the PV to the load

4.4.1 During the first off peak period (00:00-06:00)

During this period, the load demand is met by the optimal power flows from both the grid (Figure 4.5) and the BSS (Figure 4.10). BSS supplies 100% of the load, from 00:00 to approximately 00:30 and from 00:30-06:00 the load is supplied 100% from the grid. The optimal power flow from the PV (Figure 4.12) is zero as the PV output power (Figure 4.3) is zero. The grid power is required, as optimal power flows from both the PV and the BSS are unable to meet the load demand. The BSS is charged by the optimal power flow from the grid (Figure 4.7), solely because the PV output power is zero. Since there is a lack of surplus power that may be sold to the grid, both the optimal power flows from the PV to the grid (Figure 4.5) and from the BSS to the grid (Figure 4.8), are zero.

4.4.2 During the first standard period (06:00-07:00)

During this period, the load demand (4kW) is met by the optimal power flow from the grid (Figure 4.5), solely because the optimal power flow from the PV to the load (Figure 4.12) is zero and for the PV output power (Figure 4.3) is zero. The BSS power output

(Figure 4.10) is zero, as there is no discharge on SOC (Figure 4.6). Since the BSS is fully charged (Figure 4.6), the power flows from both the grid to the BSS (Figure 4.7) and from the PV to the BSS (Figure 4.9), are zero. As there is a lack of surplus power that may be sold to the grid, both the optimal power flows from the PV to the grid (Figure 4.5) and the power flow from the BSS to the grid (Figure 4.5), are zero.

4.4.3 During the first peak period (07:00-10:00)

During this period, the load demand is met by the optimal power flows from the PV (Figure 4.12), from the BSS (Figure 4.10), due to the SOC (Figure 4.6) discharge, from the grid (Figure 4.5) and from the DG (Figure 4.11). From 07:00-08:00, the grid supplies 100% of the load and it is off for the rest of the period, to minimise the electricity bill. From 08:00-09:00, the PV supplies 10% of the load, the BSS supplies 55% of the load and the DG supplies 35% of the load. From 09:00-10:00, the PV supplies 28% of the load, BSS supplies 42% of the load and the DG supplies 30% of the load. Both the optimal power flows from the grid (Figure 4.5) and the DG (Figure 4.11) are required, as both the optimal power flows from the PV (Figure 4.12) and the BSS (Figure 4.10), are unable to meet the load demand. Both the optimal power flows from the PV to the grid (Figure 4.4) and from the BSS to the grid (Figure 4.5) are zero, indicating that there is a lack of surplus power that may be sold to the grid.

4.4.4 During the second standard period (10:00-18:00)

During this period, the load demand is met by the optimal power flows from the PV (Figure 4.12), from the BSS (Figure 4.10), from the grid (Figure 4.5) and from the DG (Figure 4.11). Both the optimal power flows from the grid (Figure 4.5) and the DG (Figure 4.11), are required, as both the optimal power flows from the PV (Figure 4.12) and the BSS (Figure 4.10), are unable to meet the load demand. Figure 4.3 shows that load demand peak for the day, is 15.1kW and this is met by 53% from the PV (Figure 4.12) and 47% from the grid (Figure 4.5). As there is a lack of surplus power that may be sold to the grid, both the optimal power flows from the PV to the grid (Figure 4.4) and the power flow from the BSS to the grid (Figure 4.5), are zero.

4.4.5 During the second peak period (18:00-20:00)

During this period, the load demand is met by the optimal power flows from the PV (Figure 4.12), from the BSS (Figure 4.10) due to the SOC (Figure 4.6) discharge, from the grid (Figure 4.5) and from the DG (Figure 4.11). From 18:00:00-18:30, the grid (Figure 4.5) supplies 67% of the load and it is off for the rest of the period, to minimise the electricity bill. Both the optimal power flows from the grid (Figure 4.5) and the DG (Figure 4.11) are required, as both the optimal power flows from the PV (Figure 4.12) and the BSS (Figure 4.10), are unable to meet the load demand. Both the optimal power flows from the PV to the grid (Figure 4.4) and from the BSS to the grid (Figure 4.5), are zero, indicating that there is a lack of surplus power that may be sold to the grid.

4.4.6 During the third standard period (20:00-22:00)

During this period, the load demand is met by the optimal power flows from the BSS (Figure 10), from the grid (Figure 4.5) and from the DG (Figure 4.11) from 20:00-20:30, alone. Both the optimal power flows from the grid (Figure 4.5) and the DG (Figure 4.11) are required, as both the optimal power flows from the PV (Figure 4.12) and the BSS (Figure 4.10), are unable to meet the load demand. As there is a lack of surplus power that may be sold to the grid, both the optimal power flows from the PV to the grid (Figure 4.4) and the power flow from the BSS to the grid (Figure 4.5), are zero.

4.4.7 During the second off period (22:00-24:00)

During this period, the load demand is met by the optimal power flows from the grid (Fig.5), solely because the optimal power flows from both the PV (Fig. 12) and the BSS (Fig. 10) cannot meet the load demand. The BSS is charged by the optimal power flow from the grid (Fig. 7) only because the PV output power (Fig. 3), is zero. Since there is a lack of surplus power that may be sold to the grid, both the optimal power flows from the PV to the grid (Fig.4) and from the BSS to the grid (Fig.5), are zero.

4.4.8 Daily Economic Analysis

An economic analysis has been conducted, to establish the possible energy savings of the proposed optimised energy system for 31 July 2018, the day with maximum load

demand (Hohne, Kusakana and Numbi, 2022). The daily baseline and optimal costs for the optimal energy management of the proposed grid-connected hybrid PV-Battery-DG system, for the ETB, are compared in Figure 4.13. From 00:00 to 01:00, the optimal cost is slightly less than the baseline cost in Figure 4.13, as the load demand is met by the BSS, as indicated in Figure 4.2 (load profile) and Figure 4.10. From 01:00 to 08:00, the difference between the baseline cost and optimal cost in Figure 4.13, is minimal as the load demand is solely met by the grid, as shown in Figures 4.2 and 4.5. From 08:00 to 24:00, the difference between the baseline cost and the optimal cost increases continuously, as the optimised energy from the proposed hybrid system is more affordable than using the grid alone. The overall daily baseline cost is \$25.0102, while the daily optimal cost is \$12.6264; this represents daily savings of \$12.3838. The optimal energy management of the proposed grid-connected hybrid PV-Battery-DG system for the ETB, brings about the possible daily savings of 49.51%.

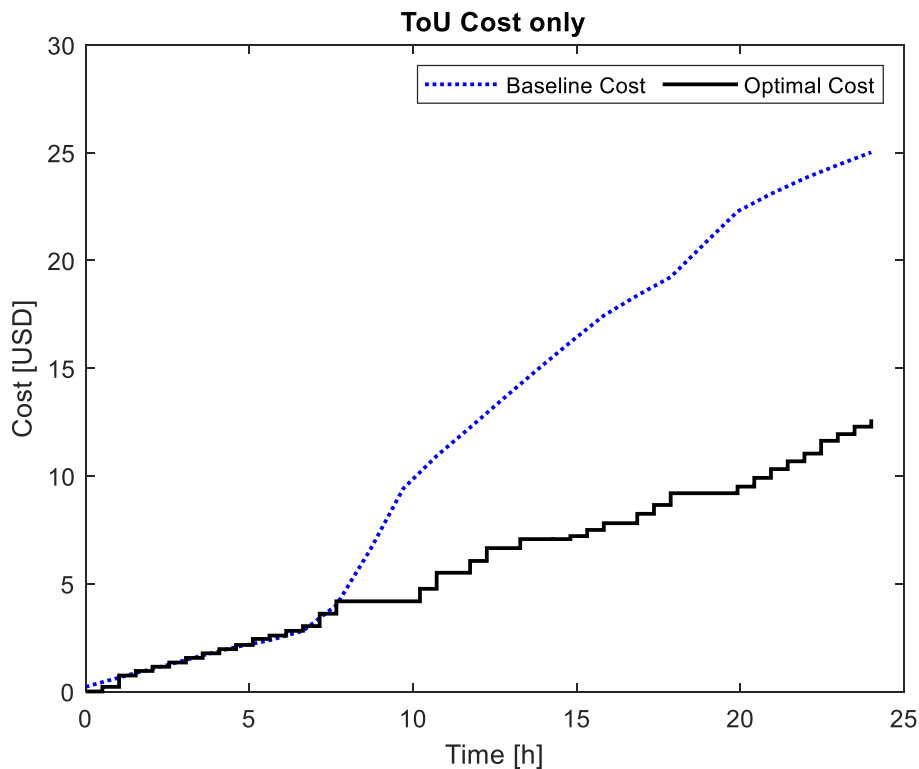


Figure 4.13 Comparison between baseline and optimal costs

4.5 Conclusion

The objective of this Chapter is to model and simulate the performance of the optimised grid-tied PV-battery-DG HRES, for the demand side management of a commercial building. Optimal energy management of hybrid system for a commercial building, has been studied in this Chapter. This chapter investigated the DSM of optimised grid-connected hybrid PV-Battery-DG HRES for a commercial building, which minimised the cost of electricity purchased from the grid, minimised the diesel fuel required for running the DG and maximised the surplus energy generated by the hybrid system, that may be sold to the grid under TOU tariff. The optimal energy management of the proposed hybrid energy system under TOU minimised both the grid consumption and the consumer's bill and the diesel fuel for running the DG. The main benefit of reduced electricity purchased from the grid is the reduced electricity bill for the commercial consumers. There was no surplus energy generated by the hybrid system, for 31 July 2018, as Figure 3.2 showed that the highest load demand for the whole year occurred on this day. The daily economic analysis on using the optimised grid-connected hybrid PV-Battery-DG system under TOU tariff for the commercial building, has been conducted and the results indicate that the optimal energy management of the hybrid system, has potential daily savings of 49.51%, based on the data provided and the assumptions made.

CHAPTER 5: OPTIMAL OPERATION OF GRID-TIED HYBRID ENERGY SYSTEM UNDER SCHEDULED GRID LOAD SHEDDING FOR A COMMERCIAL BUILDING

5.1 Introduction

Scheduled grid load shedding is a major challenge in commercial buildings, in many developing countries, including South Africa. In this Chapter, the operation of grid-tied HRES under scheduled grid load shedding, for a commercial building is optimised and the economic impact of scheduled grid load shedding on commercial consumers is assessed. Researchers are currently striving to find the strategies to mitigate scheduled grid load shedding. On-site grid connected HRESs are the promising alternative solution to the grid load shedding problem. To mitigate the scheduled grid load shedding effectively, the on-site HRES requires backup. This study proposes an optimal operation of grid-tied hybrid PV-Battery-DG HRES, under the TOU tariff, in South African grid load shedding context, in which the PV, battery storage and the DG are the backups, mitigating the scheduled grid load shedding. To study the impact of scheduled grid load shedding, a commercial consumer located in Area A where load shedding is not applied, a consumer in Area B with scheduled load shedding: 00:00- 04:00, a consumer in Area C with scheduled load shedding: 06:00-10:00, a consumer in Area D with scheduled load shedding: 12:00-16:00 and a consumer in Area E with scheduled load shedding: 18:00-22), are considered on 31 July 2018.

This Chapter is arranged into five sections. The current section has provided the overview of the Chapter. The second section is the system's model development. The third section provides the case study information. The fourth section highlights the case study simulation results and discussions. Finally, the fifth section provides the conclusion.

5.2 System Model for Scheduled Grid Load shedding

The system's model extends from the Chapter 4 work. The utility grid model and objective function model, considering scheduled grid load shedding, are presented in 5.2.1 and 5.2.3, below.

5.2.1 Utility grid model under scheduled load shedding

The available grid power under scheduled load shedding, is formulated (Ndwali, Njiri and Wanjiru, 2020) as:

$$P_{grid}(t) = \alpha_{grid}(t)P_{grid(max)} = \alpha_{grid}(t)(P_2(t) + P_3(t)) \quad (5.1)$$

Where: $\alpha_{grid}(t)$ is the grid availability parameter at time t and $P_{grid(max)}$ is the maximum capability of the grid. The grid power is available when $\alpha_{grid}(t)=1$ and in the case of scheduled grid load shedding, $\alpha_{grid}(t) = 0$.

5.2.2 Aim of the optimisation model

The aim of the optimisation model is to optimally operate the on-site grid-tied hybrid photovoltaic (PV)-Battery-diesels generator (DG), system, for the optimisation window, taking load shedding into consideration.

5.2.3 Objective function model

The objective of the optimisation model is to minimise the energy cost of running the DG during the scheduled grid load shedding. The proposed objective function is presented in (5.2), for the 24-hour horizon. The objective function, is given as:

$$J = t_s C_f \sum_{j=1}^N (QP_7^2(j) + RP_7(j) + S) \quad (5.2)$$

Where: t_s is the sampling time (delta); j is the sampling interval; $j= 1, \dots, N$; N is the horizon and C_f is the diesel cost (\$/L).

5.3 Case Study

dos Santos, Sechilariu and Locment (2016), define, load shedding as the amount of load which should be shed, based on operational conditions and priorities. ESKOM, South African Utility, defines load shedding as a strategy to temporarily interrupt electricity supply to certain areas for a specific period, published ahead to consumers when there is a lack of sufficient electricity to meet the load demand. ESKOM applies load shedding when all other options have been exhausted. It has developed eight stages, based on the level of risk, whereby each stage level represents the number of hours per interruption. South African Stage 4 load shedding means that a selected area grid power will be temporarily interrupted by the utility for four hours, for a specified day. To study the economic impact of scheduled grid load shedding, four commercial consumers' buildings in Bloemfontein, South Africa, are considered for grid load shedding, under South African Stage 4 load shedding, on 31 July 2018. The buildings are described as follows: Area B (scheduled load shedding: 00:00 to 04:00), Area C (scheduled load shedding: 06:00 to 10:00), Area D (scheduled load shedding: 12:00 to 16:00) and Area E (scheduled load shedding: 18:00 to 22:00). It is assumed that the simulation parameters for each of the four buildings, Area B, Area C, Area D and Area E, are as outlined in section 4.3.4.

5.4 Scheduled Load Shedding Simulation Results and Discussions

5.4.1 Area B load shedding during 00:00-04:00 schedule

Both Figure 5.3 and 5.4, show that the optimal grid power flow is zero during this period, as expected, while Figure 5.2 indicates that the BSS discharges to supply the load. Both Figure 5.4 and Figure 5.6 are zero, as the BSS cannot be charged during this period. During this schedule, the load demand is met by the optimal BSS power flow (Figure 5.7) and the optimal DG power flow, as shown in Figure 5.8, as the PV power flow (Figure 9), is zero. Both Figure 5.1 and 5.7, show that there is a lack of surplus power that may be sold to the grid during this period. These results indicate that the proposed grid-tied hybrid PV-Battery-DG, has the potential of managing the scheduled grid load shedding for a commercial consumer, in Area B.

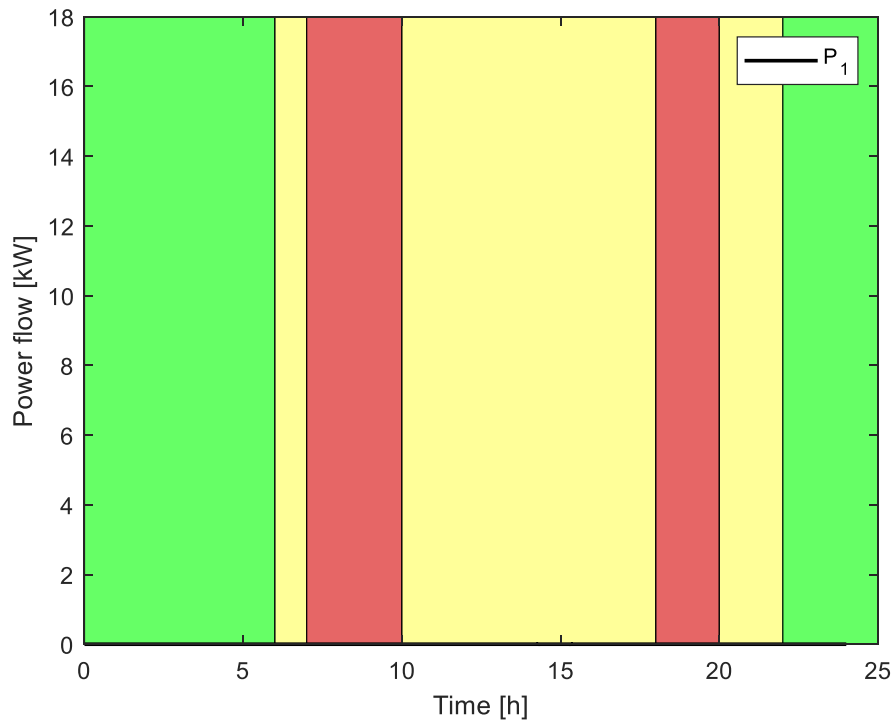


Figure 5.1 Optimal power flow from the PV to the grid for area B

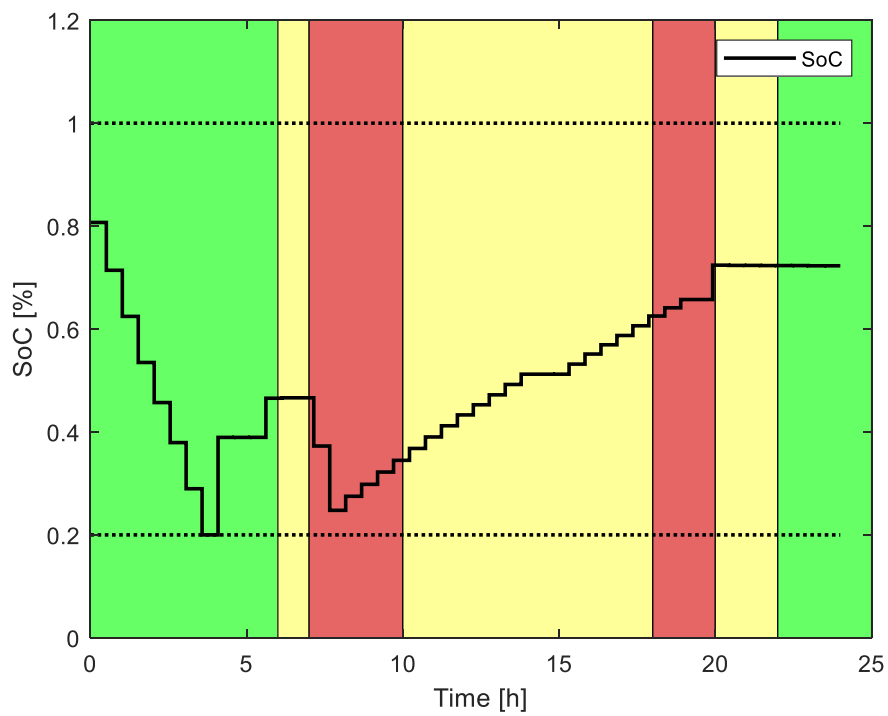


Figure 5.2 SOC power flow for area B

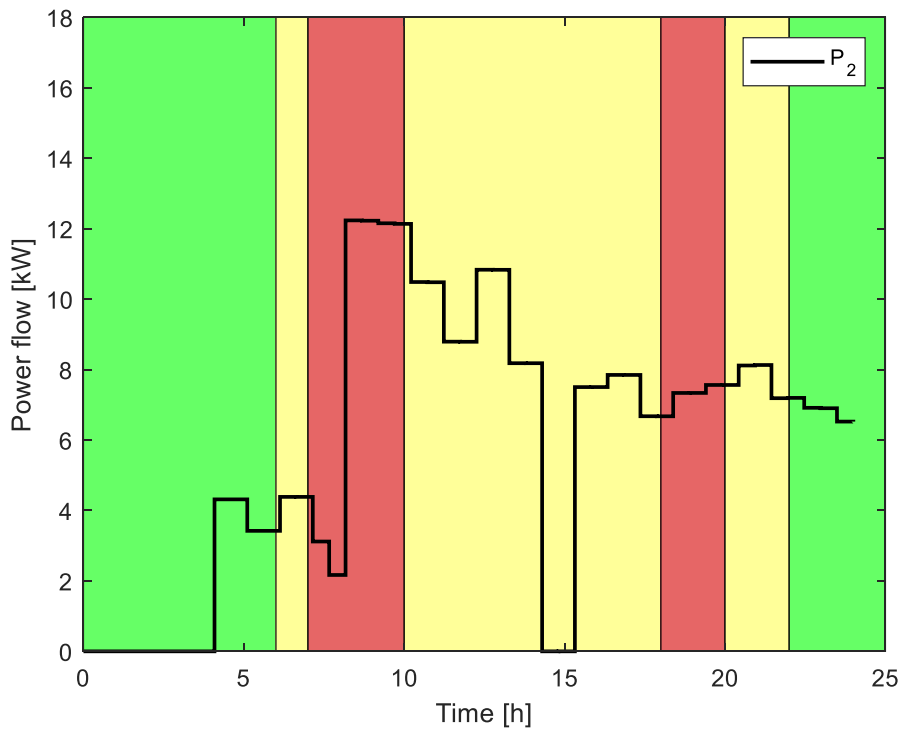


Figure 5.3 Optimal power flow from the grid to the load for area B

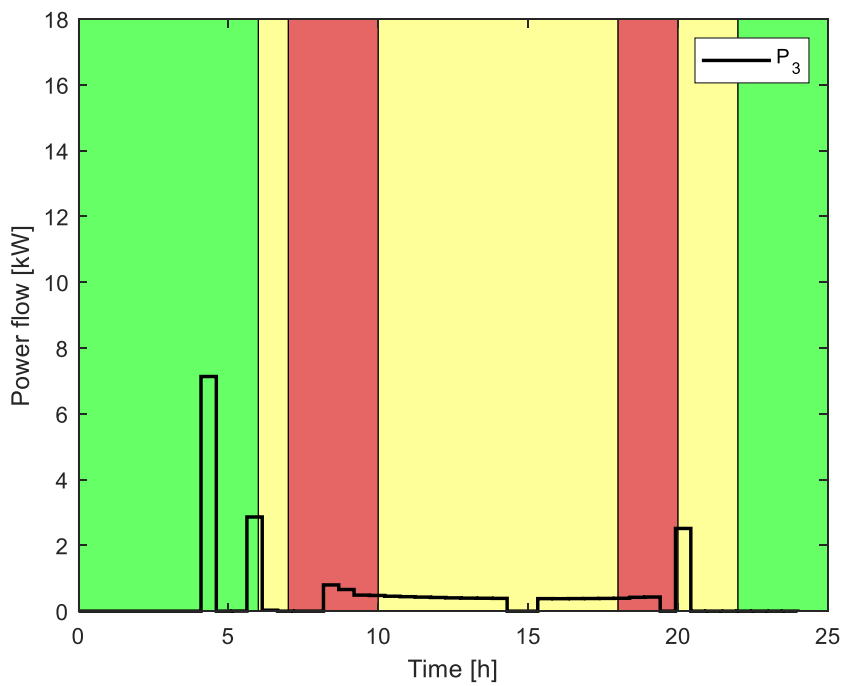


Figure 5.4 Optimal power flow from the grid to the BSS for area B

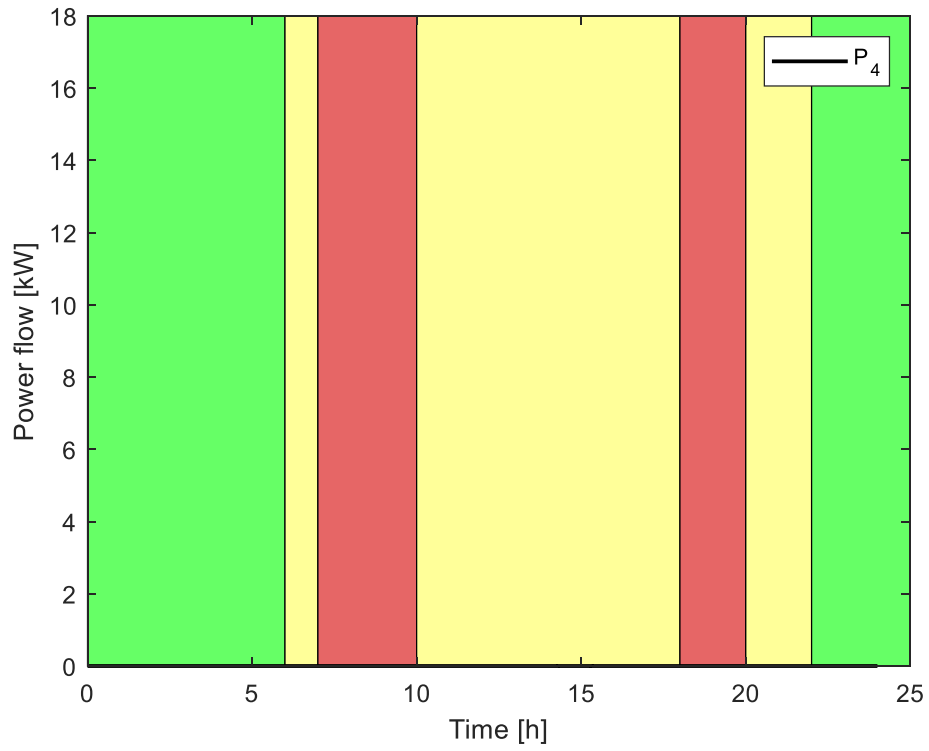


Figure 5.5 Optimal power flow from the BSS to the grid for area B

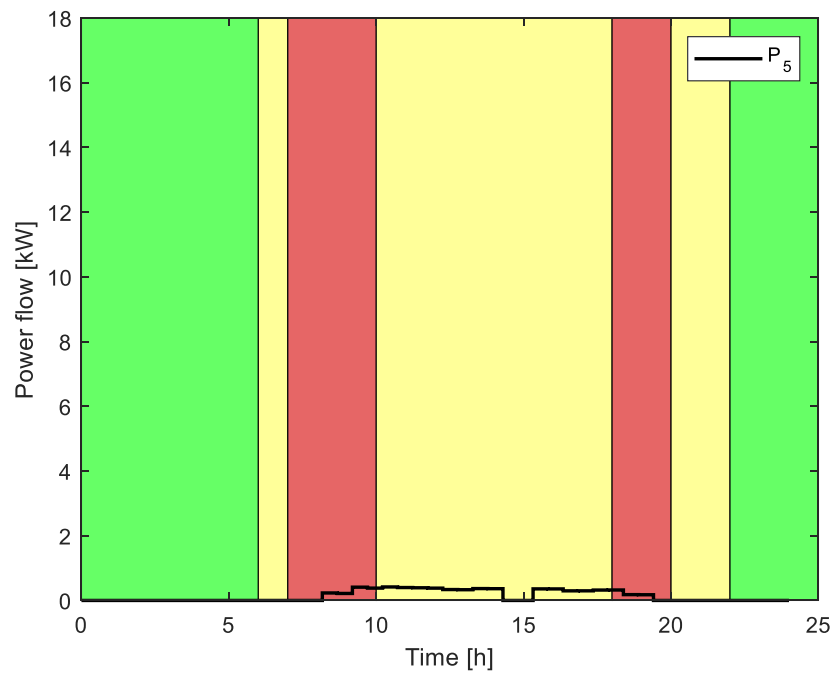


Figure 5.6 Optimal power flow from the PV to the BSS for area B

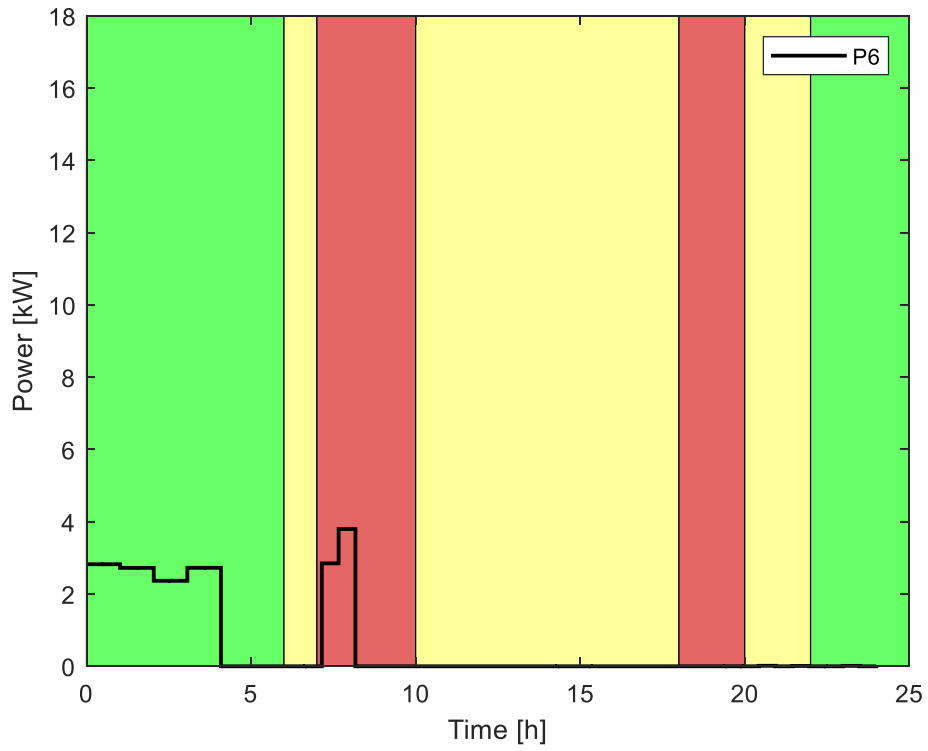


Figure 5.7 Optimal power flow from the BSS to the load for area B

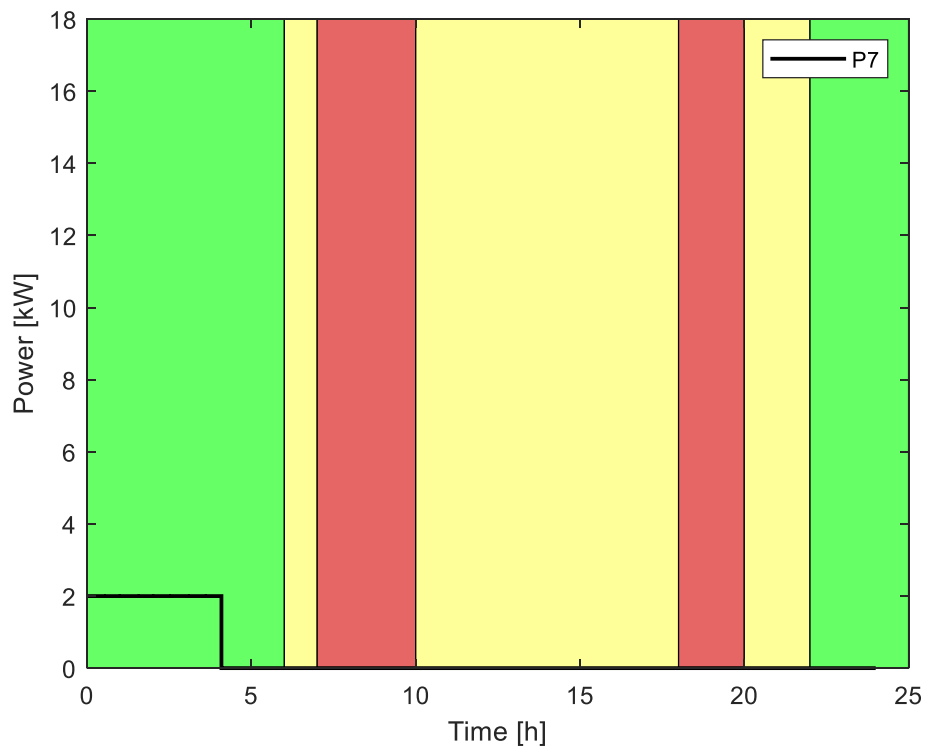


Figure 5.8 Optimal power flow from the DG to the load for area B

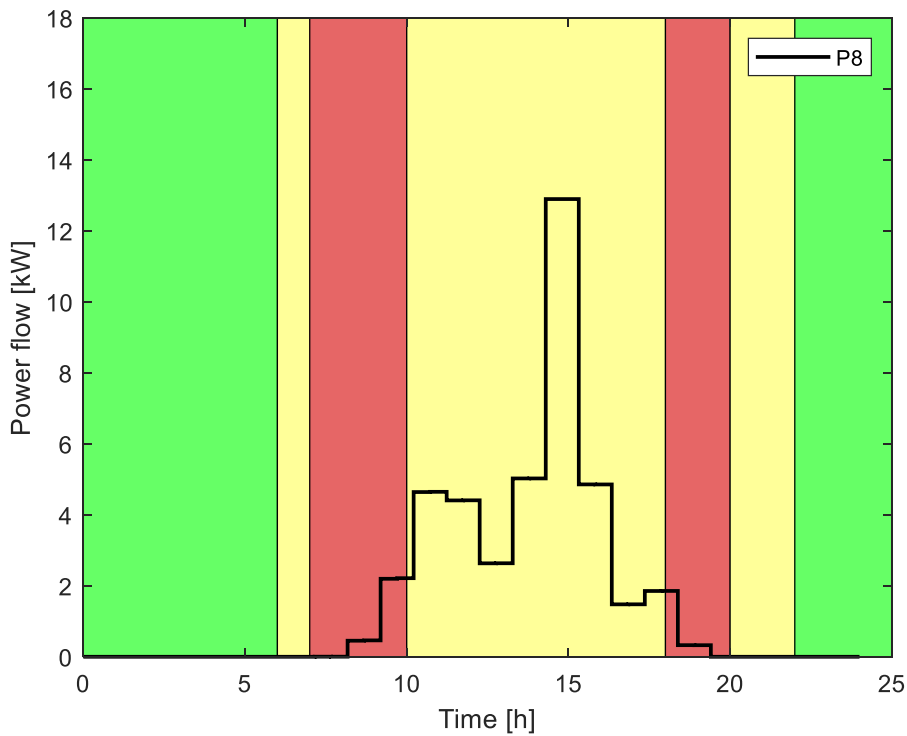


Figure 5.9 Optimal power flow from the PV to the load for area B

5.4.2 Daily economic analysis for Area B scheduled load shedding

A daily economic analysis for Area B has been conducted, to establish the possible energy savings of the proposed optimised energy system for Area B scheduled load shedding (00:00-04:00), on 31 July 2018, the maximum load demand day. The daily baseline and optimal costs for the optimal energy management of the proposed grid-connected hybrid PV-Battery-DG system, for the building, are compared in Figure 5.10. From 00:00 to 08:00, the difference between the baseline cost and the optimal cost is minimal, as the optimised energy cost for the proposed hybrid system is less than solely the grid. From 08:00 to 24:00, the difference between the baseline cost and the optimal cost, increases continuously, as the optimised energy cost for the proposed hybrid system is significantly less than solely the grid cost. The overall daily baseline cost is \$25.0102, while the daily optimal cost is \$19.6008 and this represents daily savings of \$5.4094. The optimal energy management of the proposed grid-connected hybrid PV-Battery-DG system for the building, brings about possible daily savings of 21.63%.

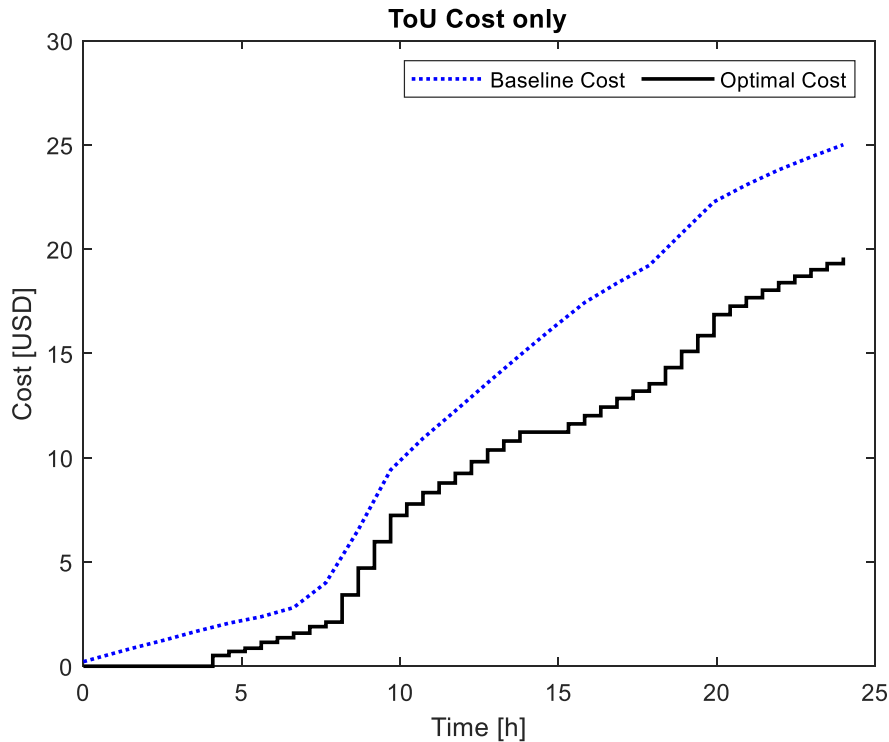


Figure 5.10 Area B (scheduled load shedding: 00:00-04:00) daily energy costs

5.4.3 Area C scheduled load shedding: 06:00-10:00

Both Figures 5.13 and 5.14, show that the optimal grid power flow is zero during this period, as expected, while Figure 5.12 indicates that the BSS discharges, supplying the load. Both Figures 5.14 and 5.16 are zero, as the BSS is incapable of charging this period. During this schedule, the load demand is met by the optimal BSS power flow to the load (Figure 5.17), by the optimal power flow from the PV (Figure 5.19) and by the optimal DG power flow as shown in Figure 5.18. Both Figures 5.11 and 5.15 show that there is a lack of surplus power that may be sold to the grid during the load shedding. These results indicate that the proposed grid-tied hybrid PV-Battery-DG possesses the potential of managing the scheduled grid load shedding, for a commercial consumer in Area C.

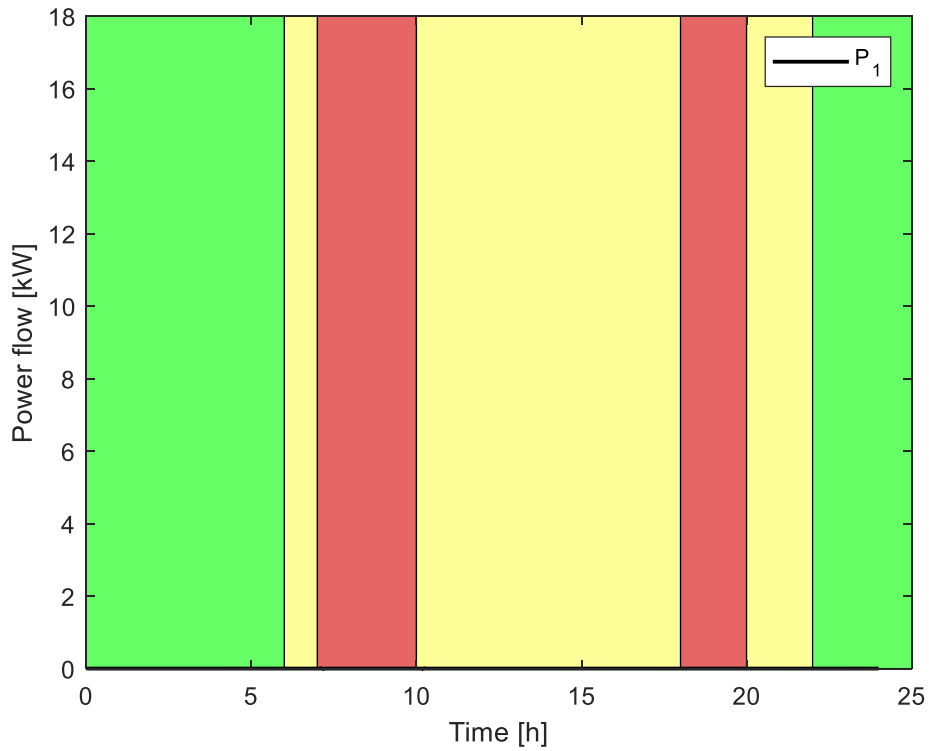


Figure 5.11 Optimal power flow from the PV to the grid for area C

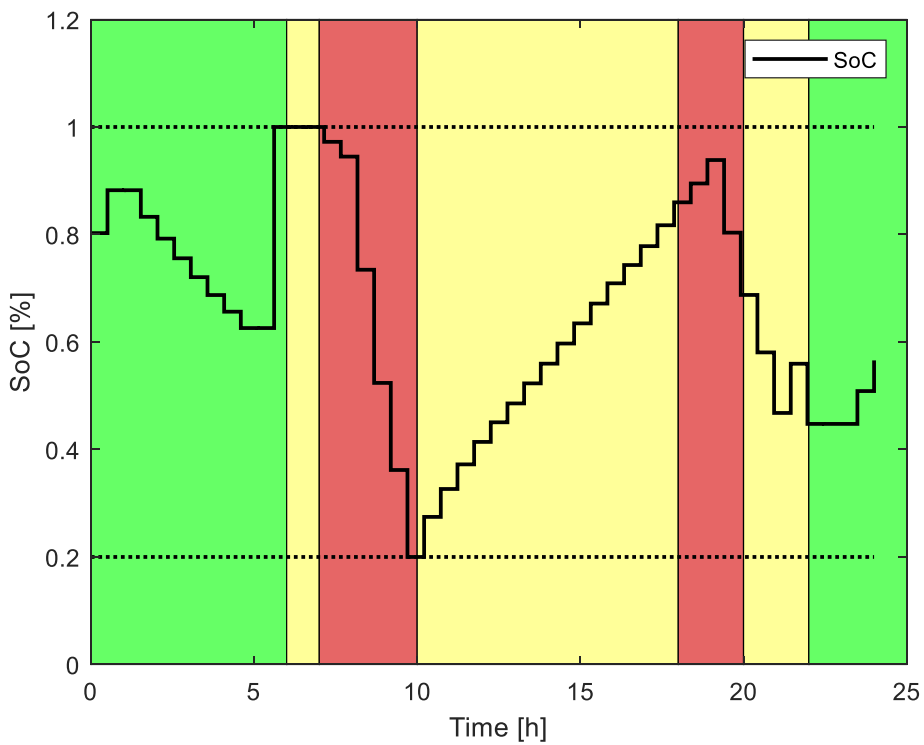


Figure 5.12 SOC power flow for area C

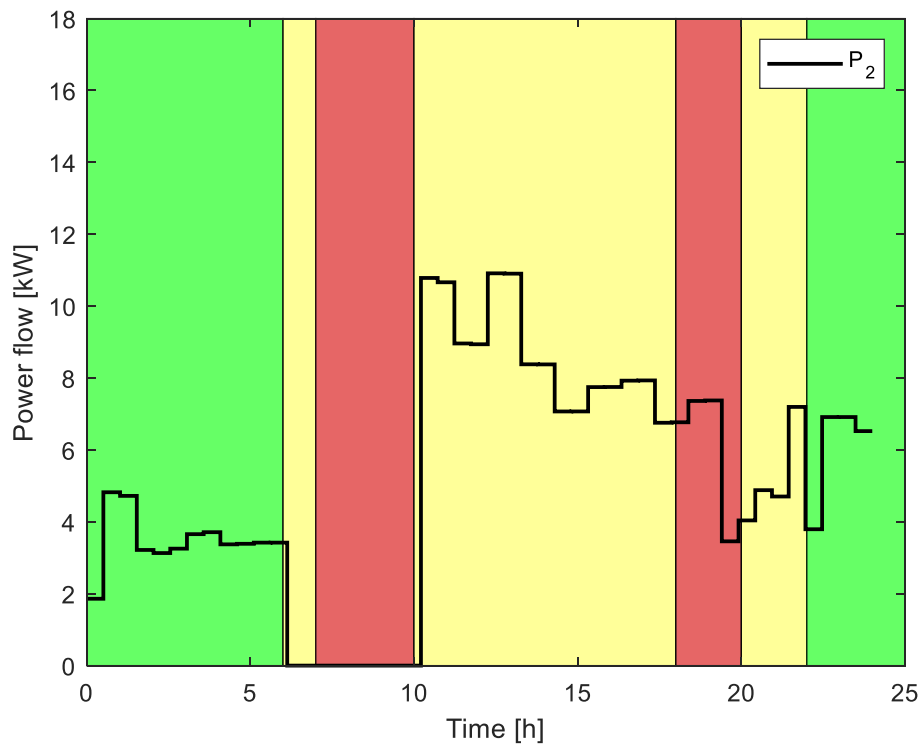


Figure 5.13 Optimal power flow from the grid to the load for area C

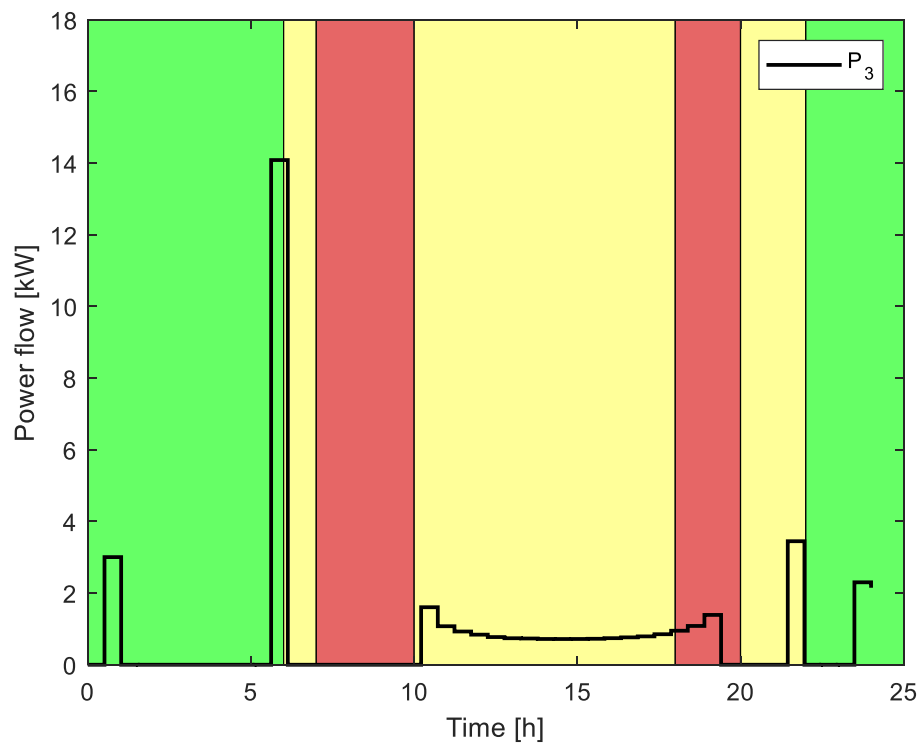


Figure 5.14 Optimal power flow from the grid to the BSS for area C

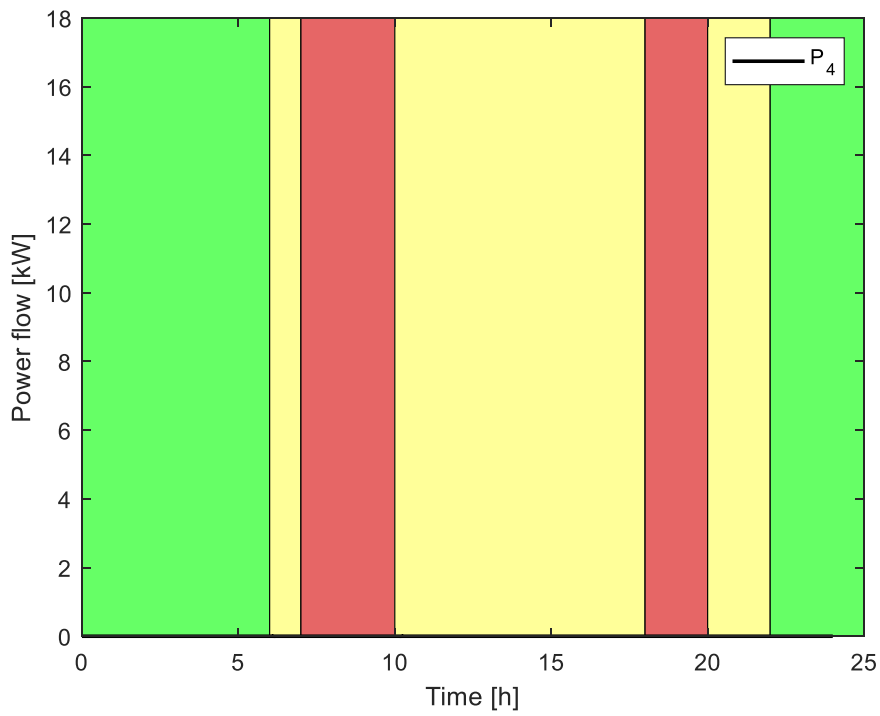


Figure 5.15 Optimal power flow from the BSS to the grid for area C

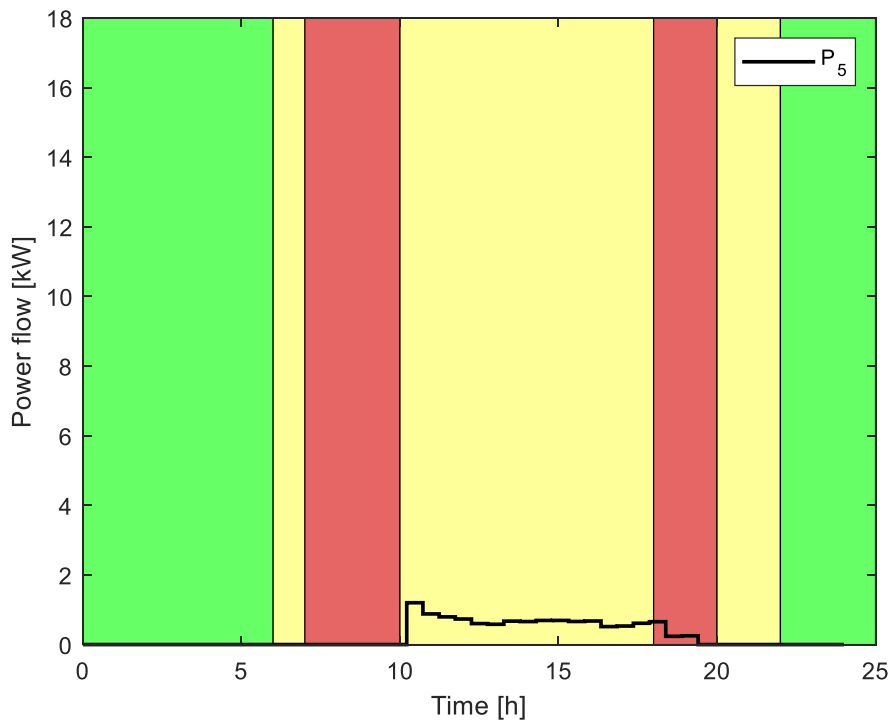


Figure 5.16 Optimal power flow from the PV to the BSS for area C

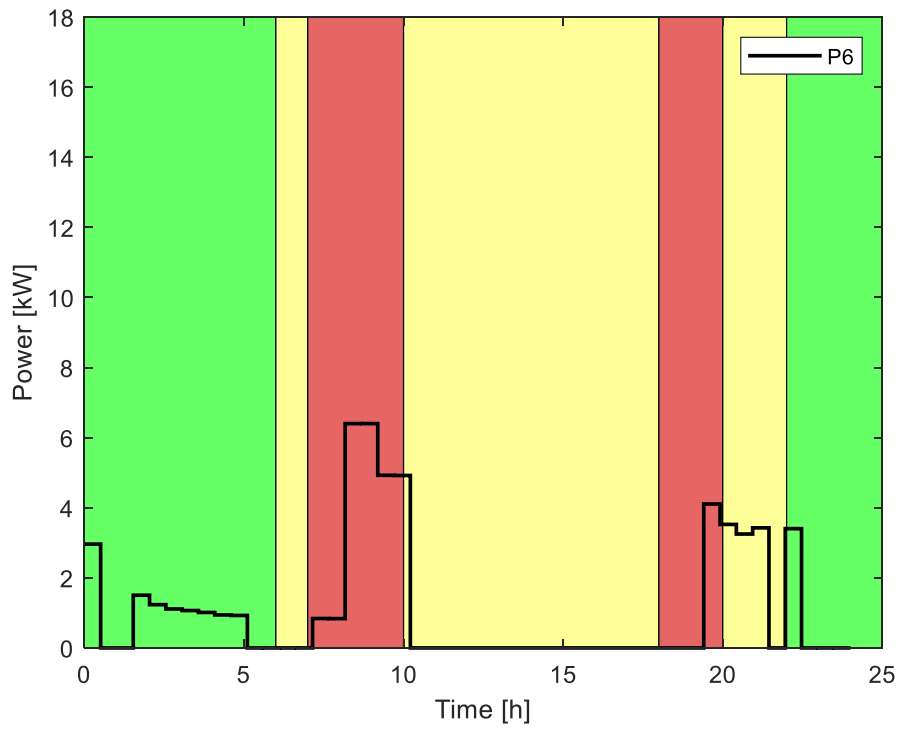


Figure 5.17 Optima power flow from the BSS to the load for area C

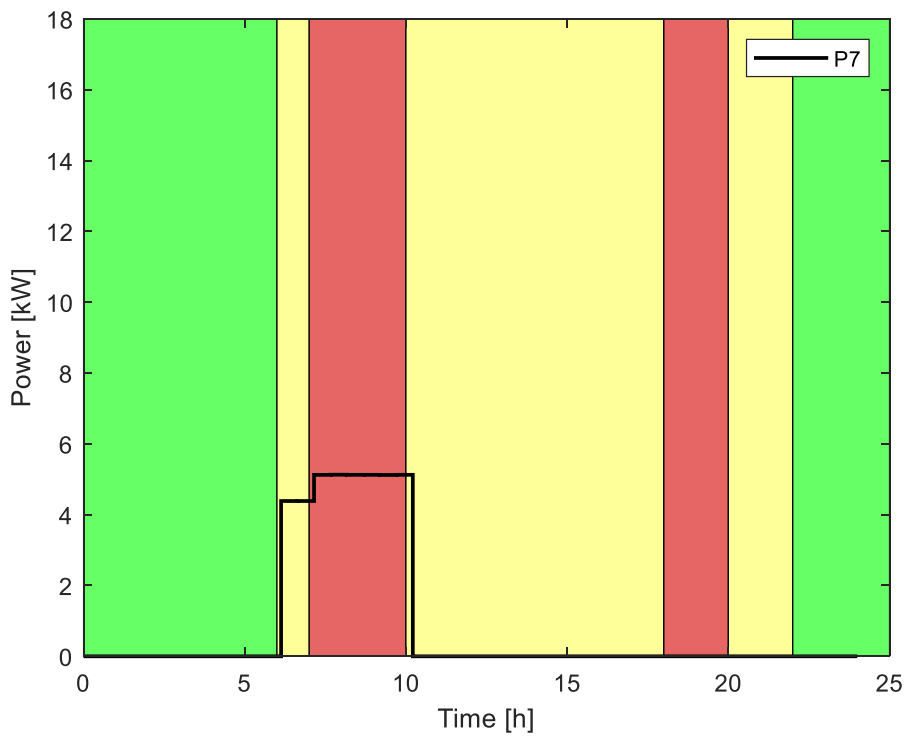


Figure 5.18 Optimal power flow from the DG to the load for area C

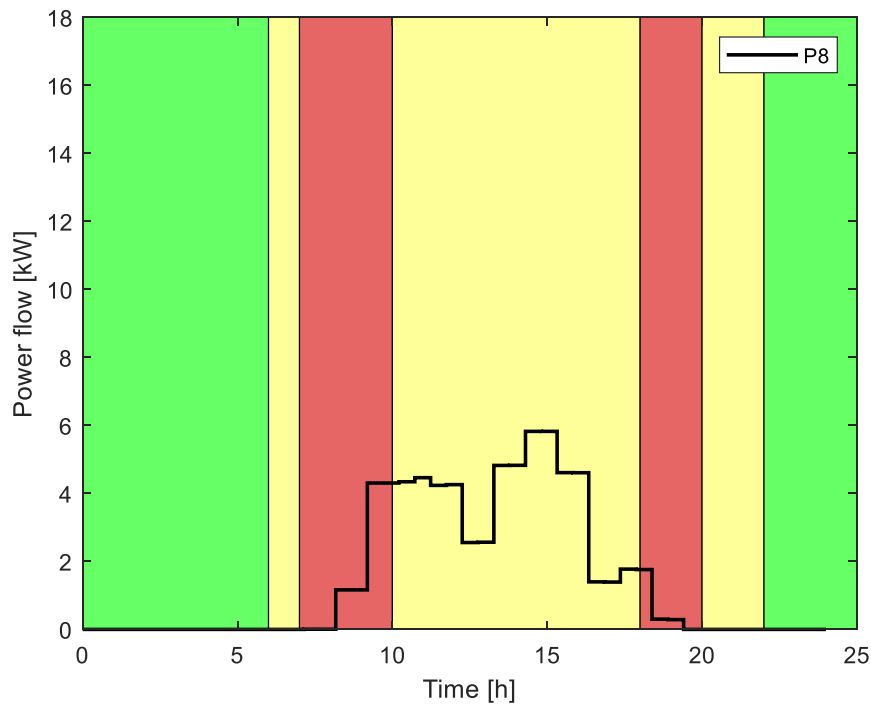


Figure 5.19 Optimal power flow from the PV to the load for area C

5.4.4 Daily economic analysis for Area C scheduled load shedding

An economic analysis has been conducted, to establish the possible energy savings of the proposed optimised energy system for Area C scheduled load shedding (06:00-10:00) on the 31 July 2018, the maximum load demand day. The daily baseline and optimal costs for the optimal energy management of the proposed grid-connected hybrid PV-Battery-DG system for the building, in this area, are compared in Figure 5.20. From 00:00 to 06:00, the difference between the baseline cost and optimal cost, in Figure 5.20, is minimal and the optimised energy from the proposed hybrid system, is less than solely using the grid. From 06:00 to 07:00, the difference between the baseline cost and optimal cost in Figure 5.20 is zero, as the optimised energy cost for the proposed hybrid system is the same as the sole grid cost. From 07:00 to 24:00, the difference between the baseline cost and the optimal cost increases continuously, as the optimised energy cost for the proposed hybrid system is significantly less than the sole grid cost. The overall daily baseline cost is \$25.0102, while the daily optimal cost is \$15.2696, and this represents daily savings of \$9.7406. The optimal energy management of the proposed grid-connected hybrid PV-Battery-DG system for the building in this area, brings about possible daily savings of 38.95%.

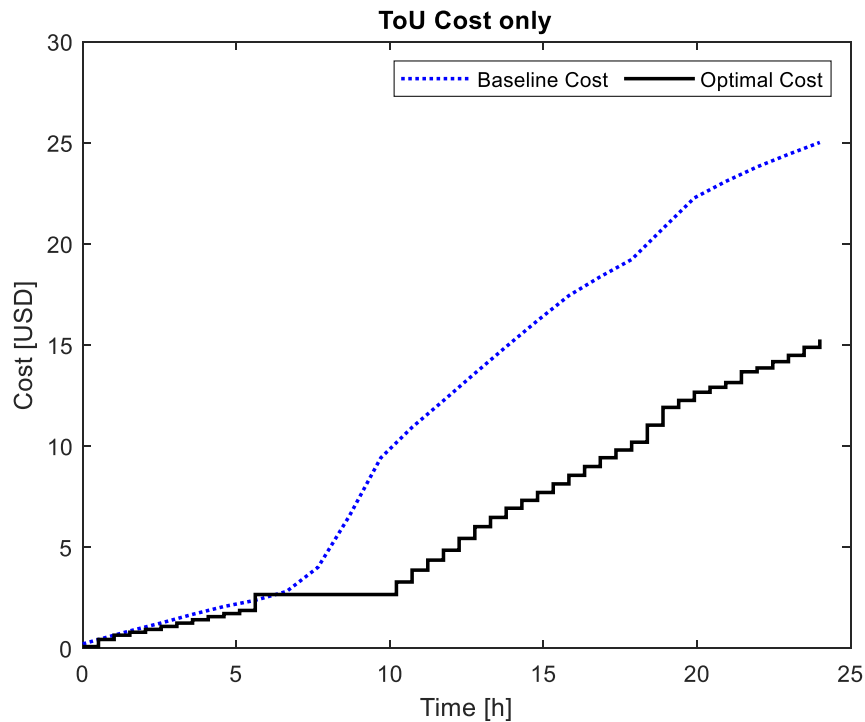


Figure 5.20 Area C (scheduled load shedding: 06:00-10:00) daily energy costs

5.4.5 Area D load shedding during 12:00-16:00 schedule

Both Figures 5.23 and 5.24, show that the optimal grid power flow is zero during this period, while Figure 5.22 indicates that the BSS discharges from 12:00 to 14:00, is charged by the optimal power flow from the PV, between 14:00 and 15:00 and discharges from 15:00 to 16:00. Figure 5.24 is zero during load shedding, while Figure 5.26 is zero between 12:00 and 14:00, as the BSS is discharging optimally to the load, the BSS is charged by the optimal power from the PV between 14:00 and 15:00 and Figure 5.26 is zero between 15:00 and 16:00 because the BSS is discharging optimally to the load. During this schedule, the load demand is met by the optimal BSS power flow to the load (Figure 5.27) and by the optimal power flow from the PV (Figure 5.29). Figures 5.21 and 5.25, show that there is a surplus power that may be sold to the grid from 10:00 to 11:00. Both Figures 5.21 and 5.25, show that there is a lack of surplus power that may be sold to the grid during the load shedding. These results indicate that the proposed grid-tied hybrid PV-Battery-DG, possesses the potential of managing the scheduled grid load shedding for a commercial consumer in Area D.

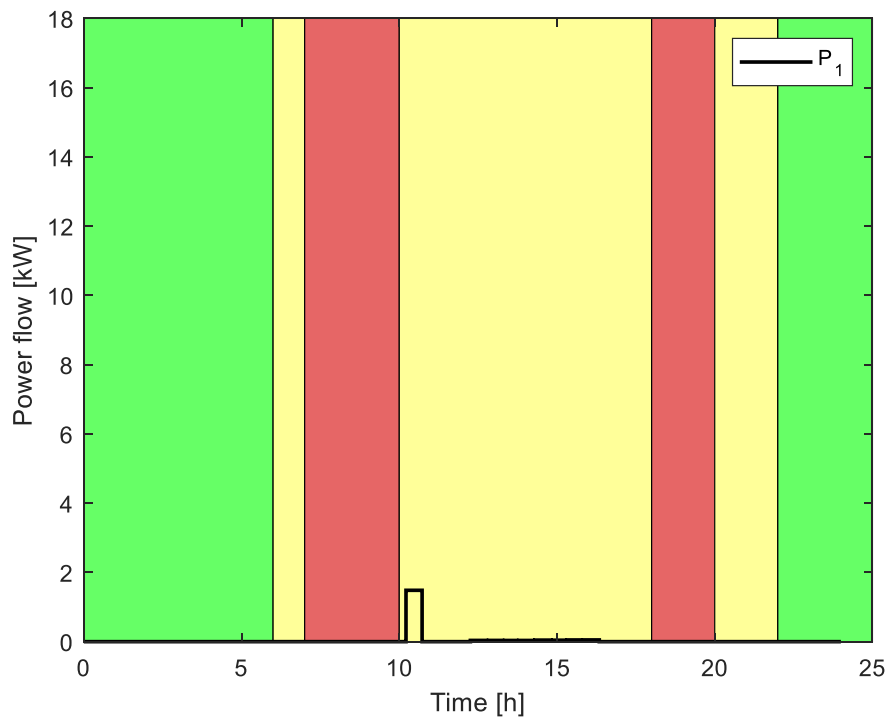


Figure 5.21 Optimal power flow from the PV to the grid for area D

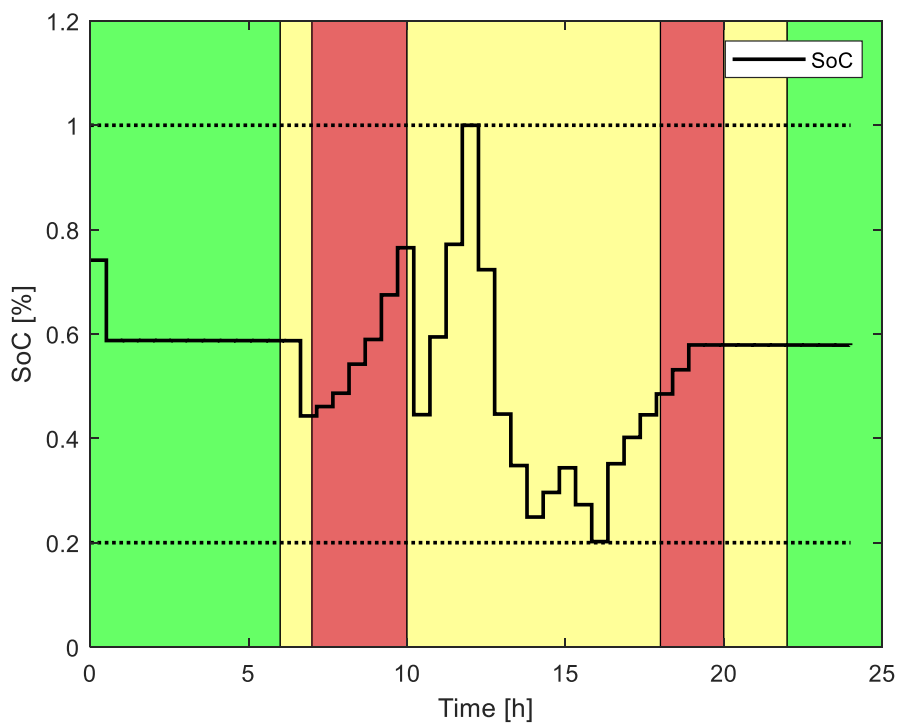


Figure 5.22 SOC power flow for area D

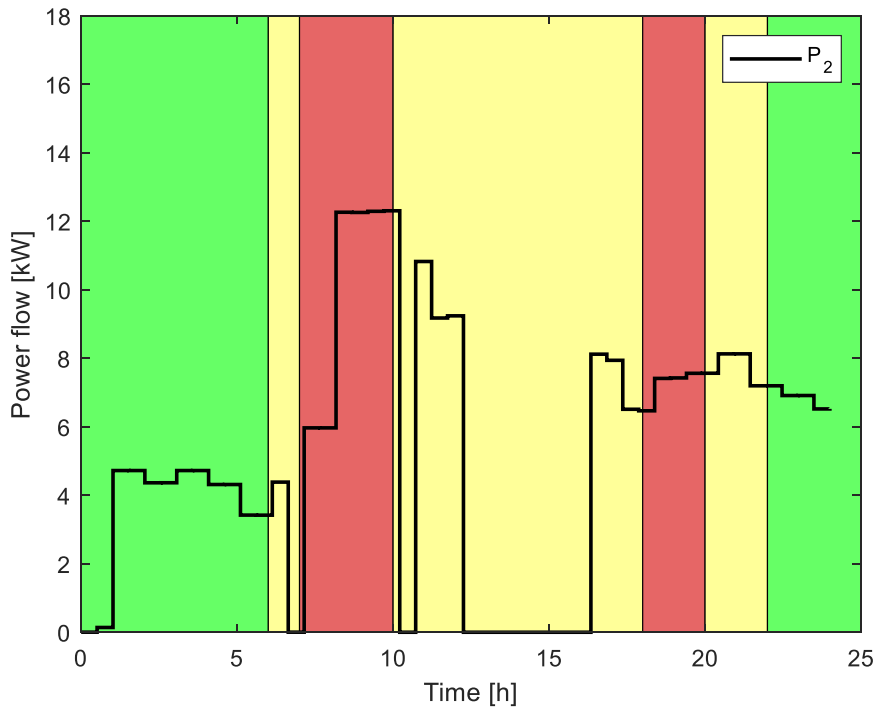


Figure 5.23 Optimal power flow from the grid to the load for area D

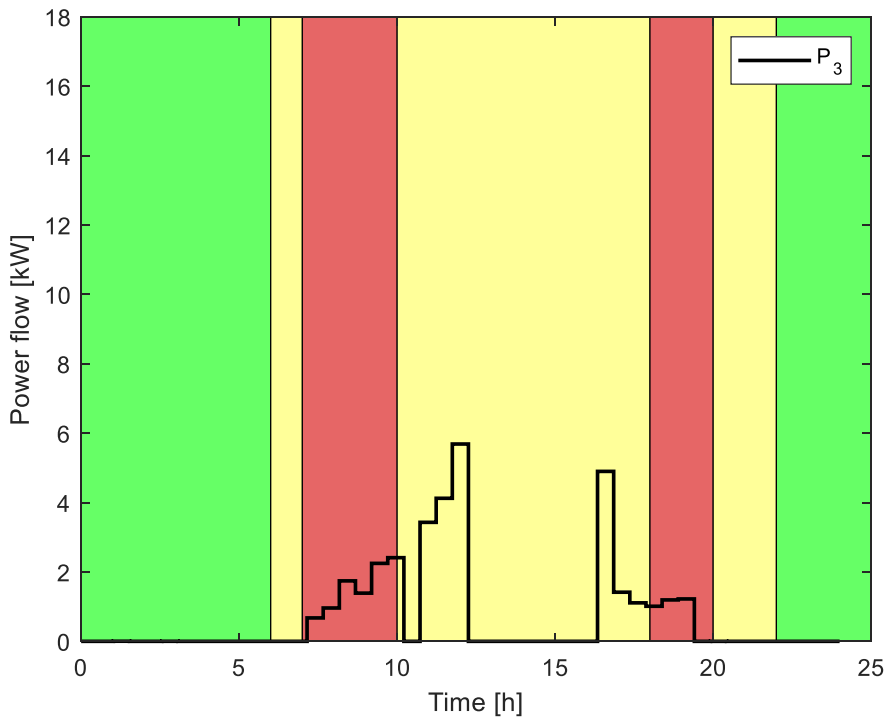


Figure 5.24 Optimal power flow from the grid to the BSS for area D

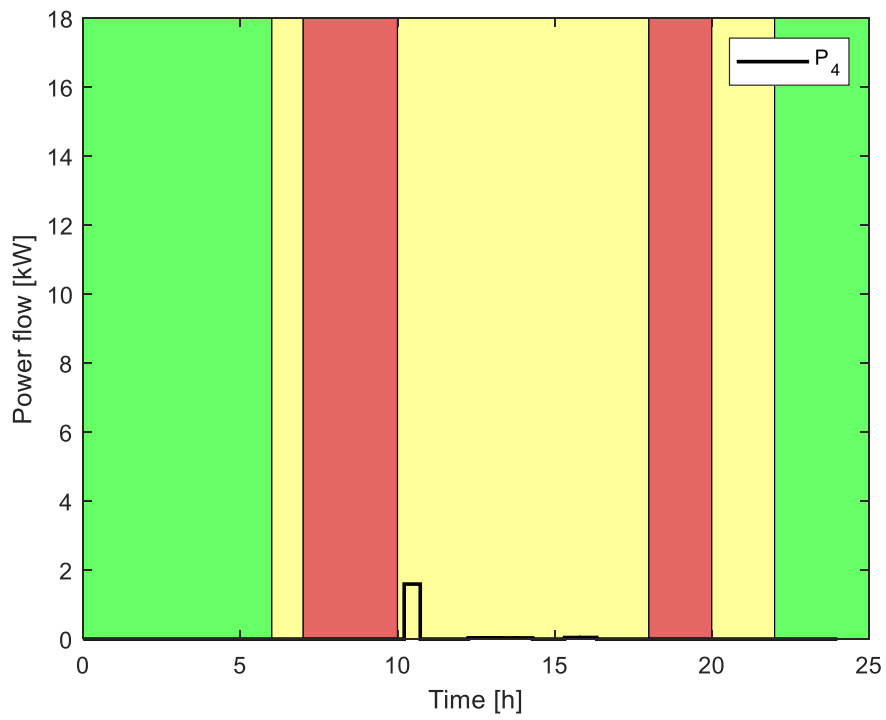


Figure 5.25 Optimal power flow from the BSS to the grid for area D

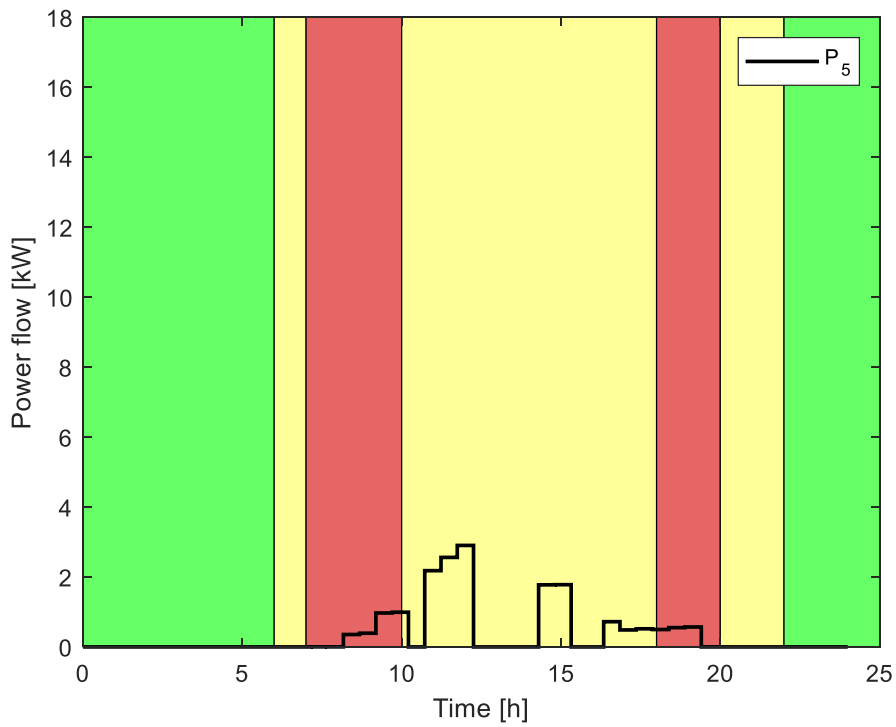


Figure 5.26 Optimal power flow from the PV to the BSS for area D

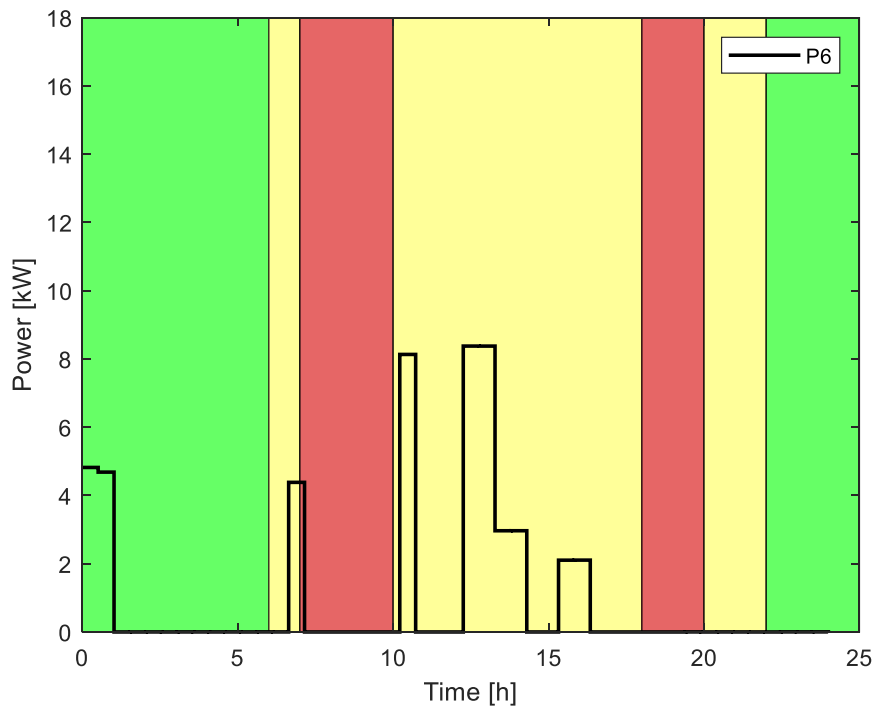


Figure 5.27 Optimal power flow from the BSS to the load for area D

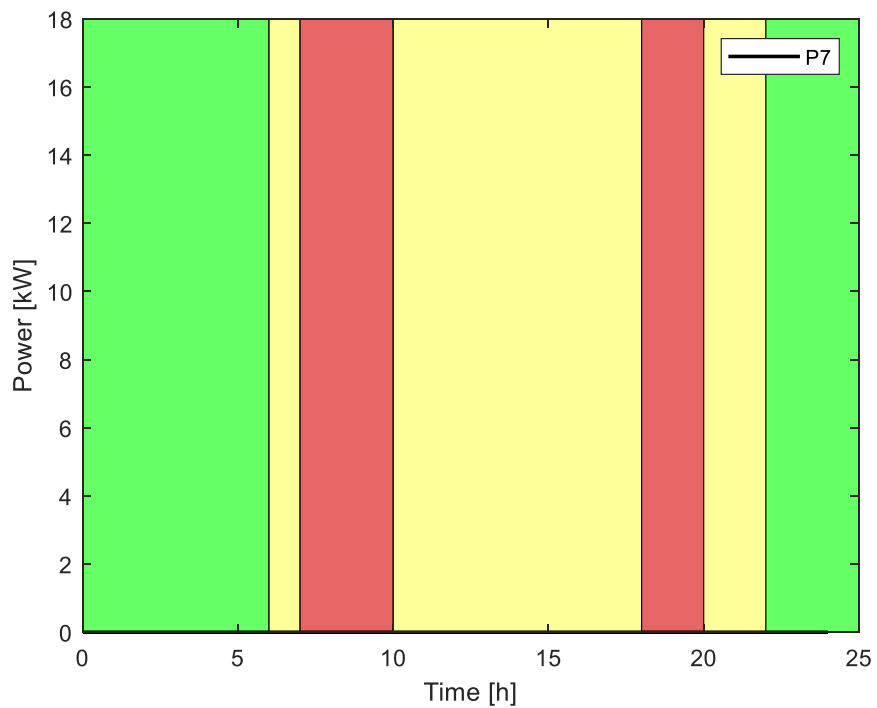


Figure 5.28 Optimal power flow from the DG to the load for area D

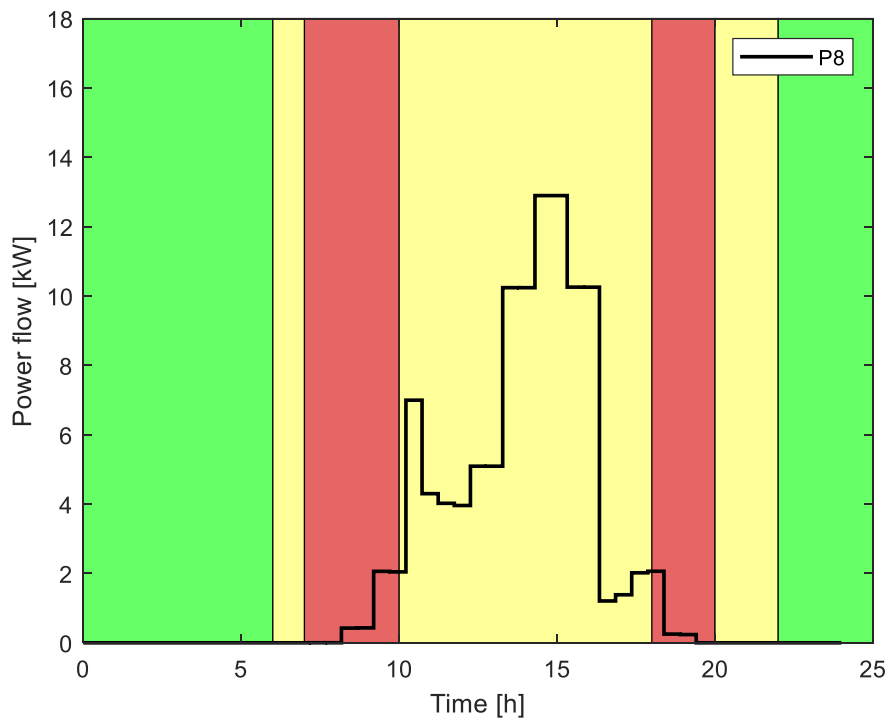


Figure 5.29 Optimal power flow from the PV to the load for area D

5.4.6 Daily economic analysis for Area D scheduled load shedding

An economic analysis has been conducted, to establish the possible energy savings of the proposed optimised energy system for Area D scheduled load shedding (12:00-16:00), on 31 July 2018, the maximum load demand day. The daily baseline and optimal costs for the optimal energy management of the proposed grid-connected hybrid PV-Battery-DG system for the building, are compared in Figure 5.30. From 00:00 to 12:00, the difference between the optimal cost and the baseline cost, is minimal in Figure 5.30, as the optimised energy cost for the proposed hybrid system is less than the sole grid cost. From 12:00 to 24:00, the difference between the baseline cost and the optimal cost increases continuously, as the optimised energy cost for the proposed hybrid system, is significantly less than the sole grid cost. The overall daily baseline cost is \$25.0102, while the daily optimal cost is \$19.1884, and this represents daily savings of \$5.8218. The optimal energy management of the proposed grid-connected hybrid PV-Battery-DG system for the building in this area, brings about the possible daily savings of 23.28%.

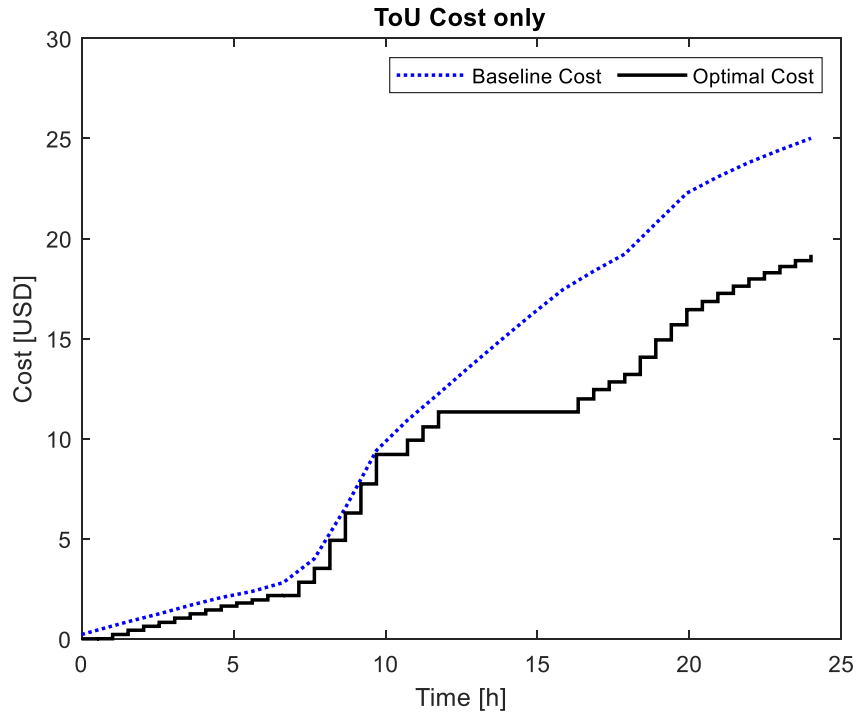


Figure 5.30 Area D (scheduled load shedding: 12:00-16:00) daily energy costs

5.4.7 Area E scheduled load shedding: 18:00-22:00

Both Figures 5.33 and 5.34, show that the optimal grid power flow is zero during this period, as expected, while Figure 5.32 indicates that the BSS discharges to supply the load. Both Figures 5.24 and 5.26 are zero, as the BSS is unable to be charged during this period. During this schedule, the load demand is met by the optimal BSS power flow to the load (Figure 5.27), by the optimal power flow from the PV (Figure 5.29) and by the optimal DG power flow, as shown in Figure 5.28. Figure 5.35 shows that there is a surplus power that may be sold to the grid from 08:00 to 09:00. Both Figures 5.31 and 5.38, show that there is a lack of surplus power that may be sold to the grid during the load shedding. These results indicate that the proposed grid-tied hybrid PV-Battery-DG, possesses the potential of managing the scheduled grid load shedding for a commercial consumer in Area E.

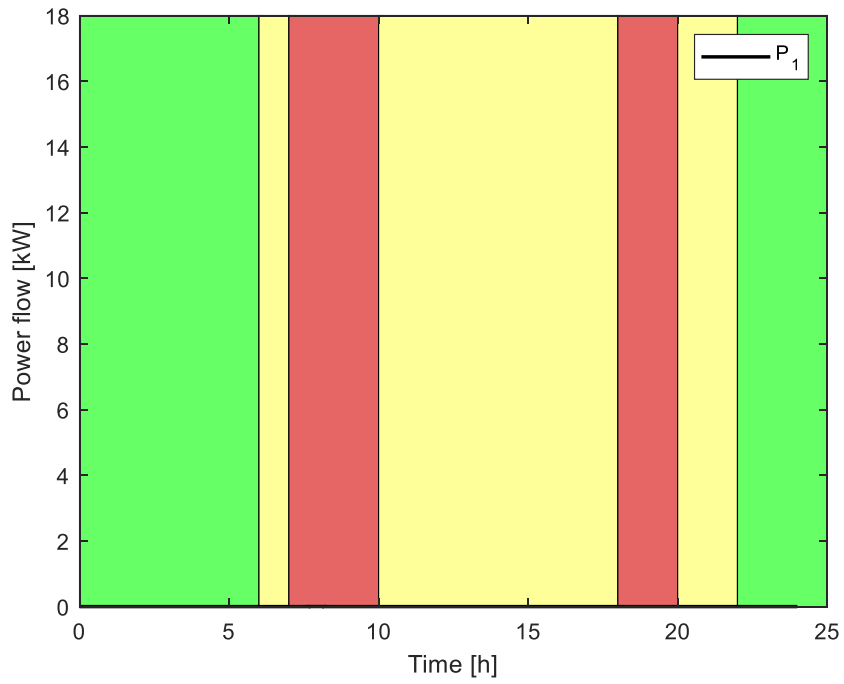


Figure 5.31 Optimal power flow from the PV to the grid for area E

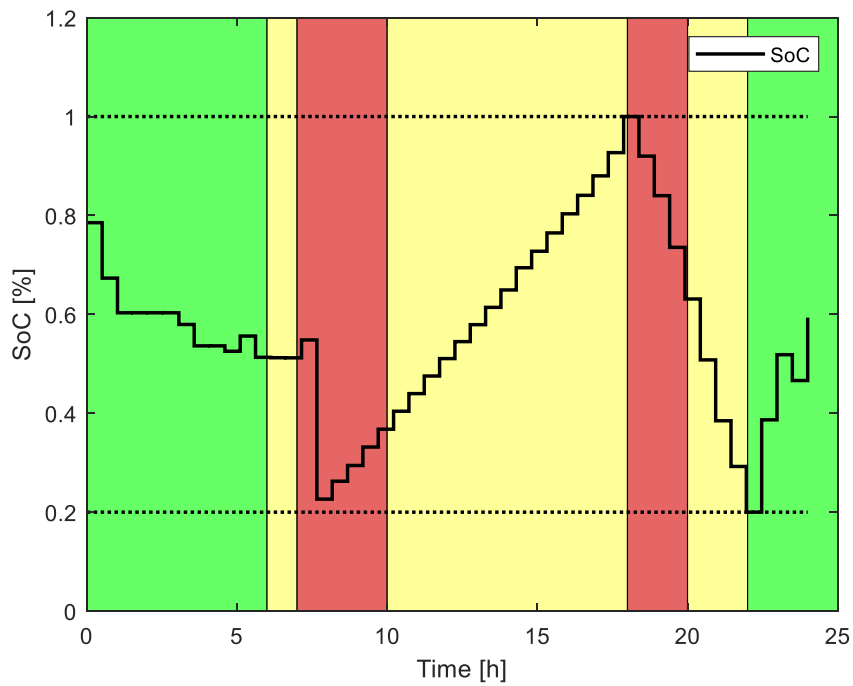


Figure 5.32 SOC power flow for area E

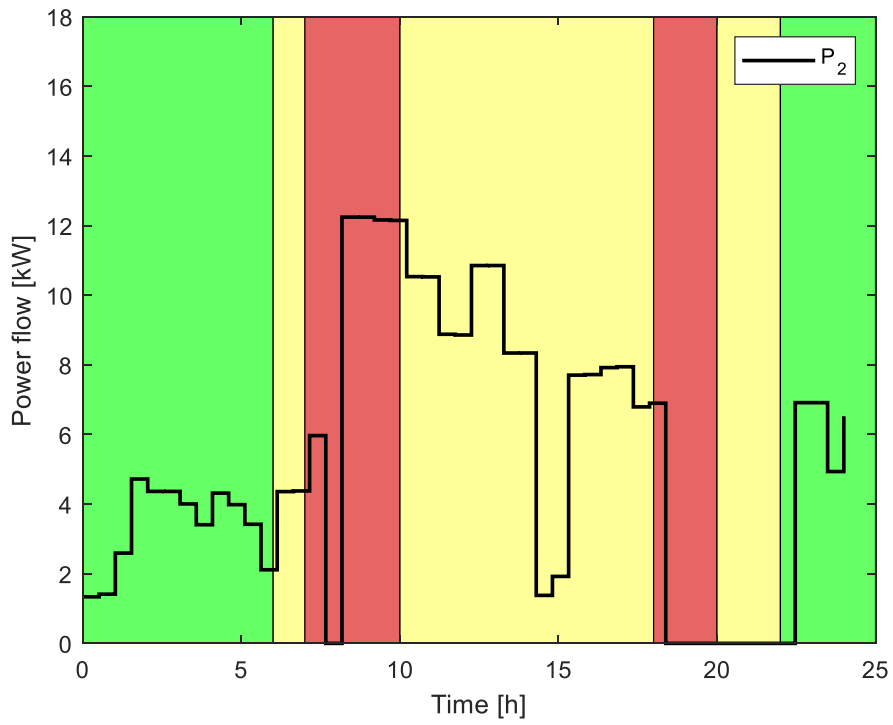


Figure 5.33 Optimal power flow from the grid to the load for area E

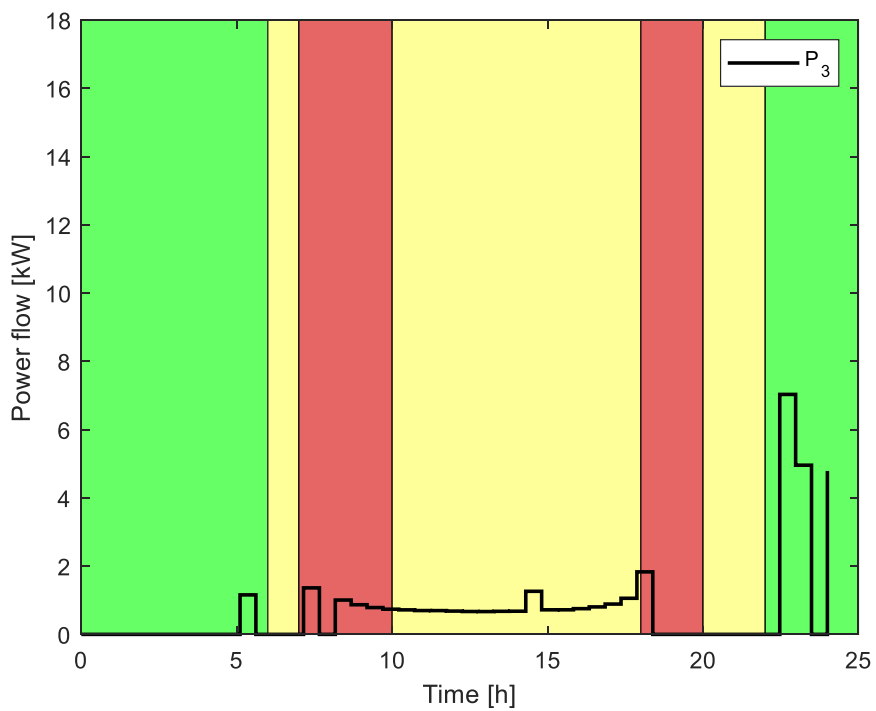


Figure 5.34 Optimal power flow from the grid to the BSS for area E

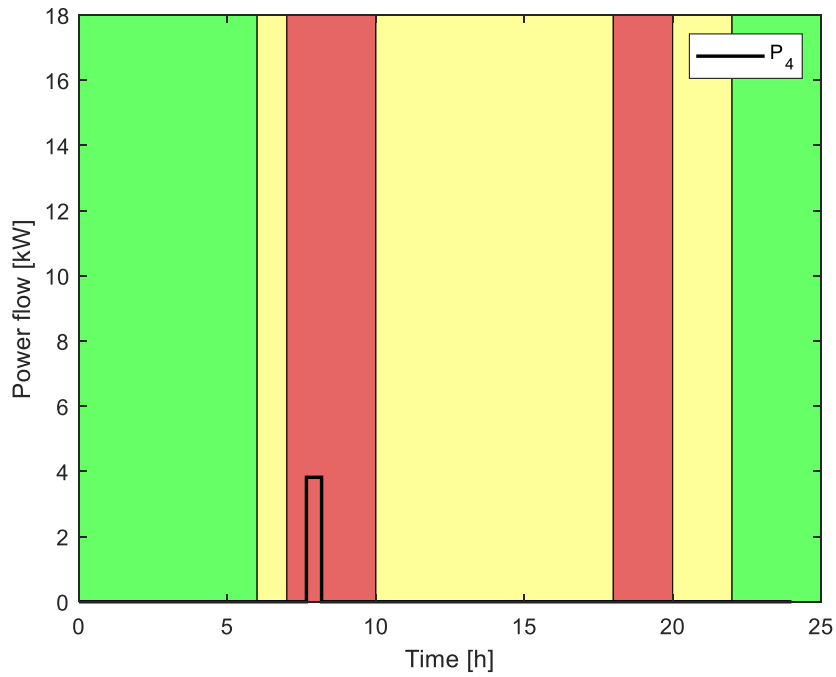


Figure 5.35 Optimal power flow from the BSS to the grid for area E

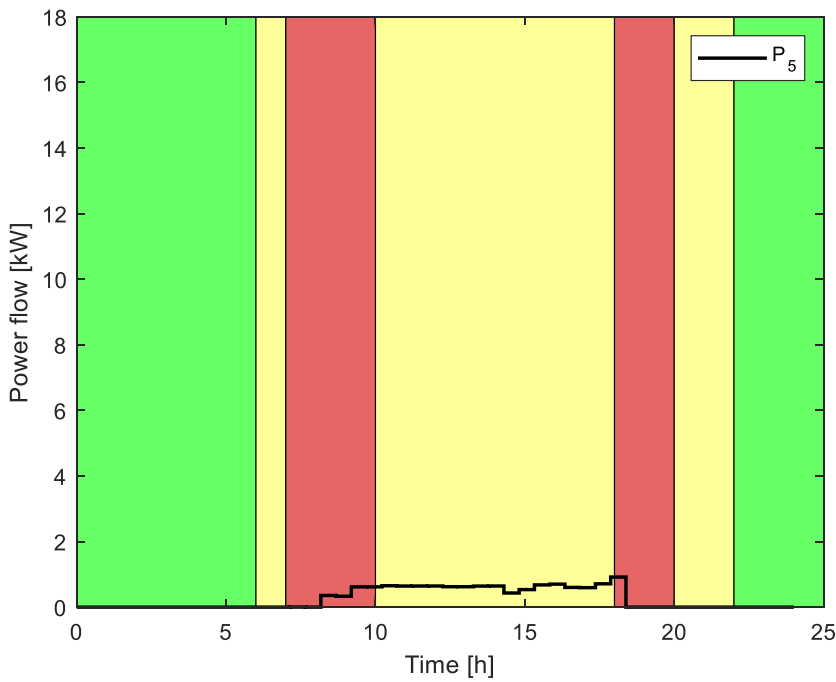


Figure 5.36 Optimal power flow from the PV to the BSS for area E

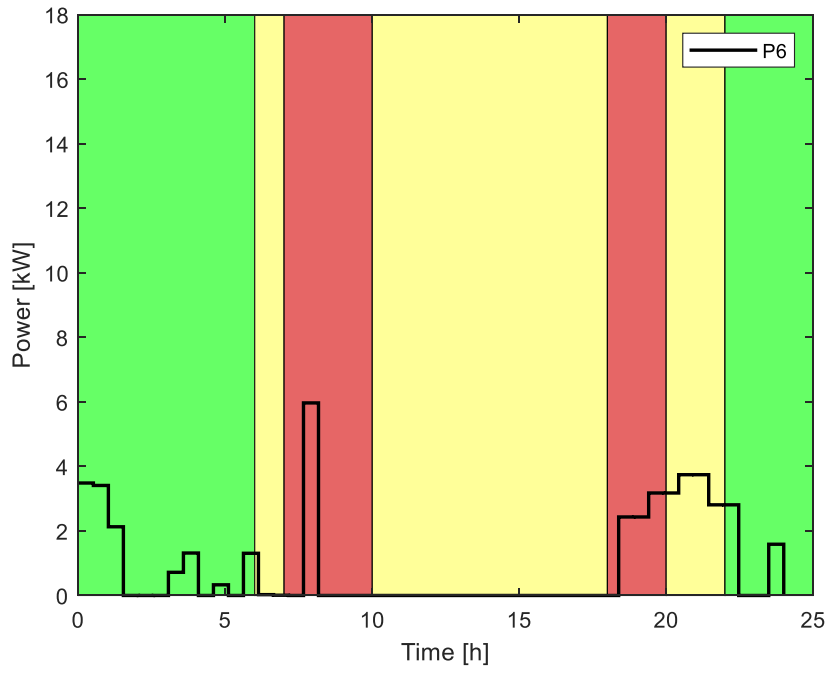


Figure 5.37 Optimal power flow from the BSS to the load for area E

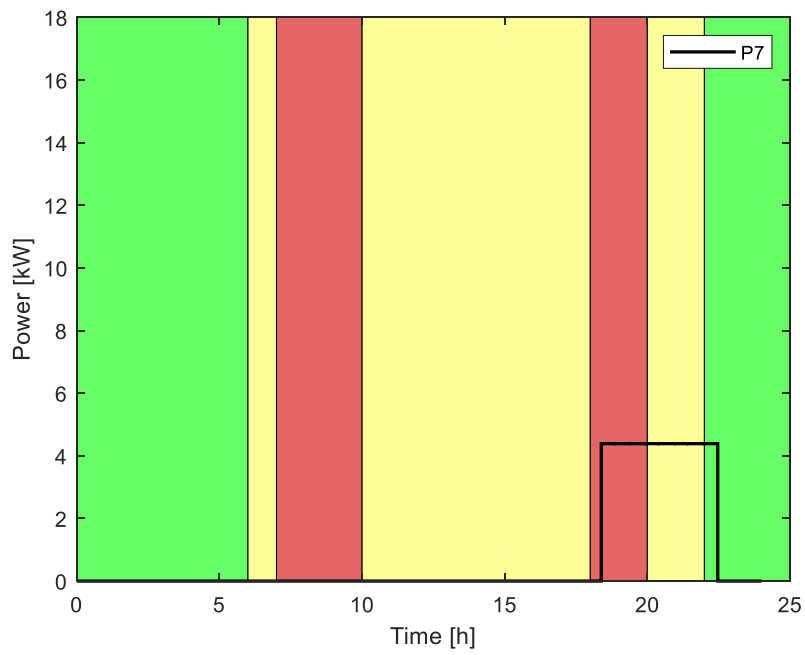


Figure 5.38 Optimal power flow from the DG to the load for area E

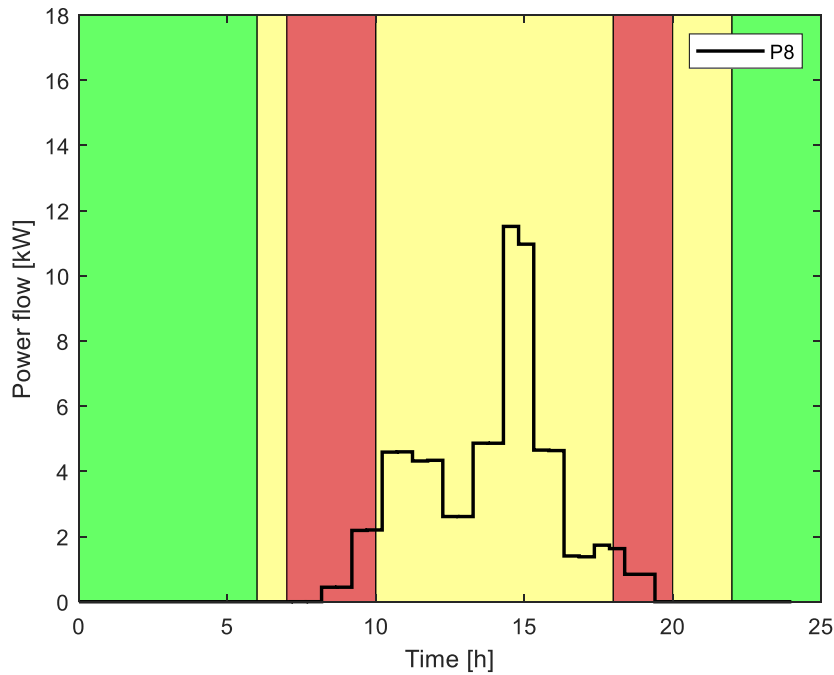


Figure 5.39 Optimal power flow from the PV to the load for area E

5.4.8 Daily economic analysis for Area E scheduled load shedding

An economic analysis has been conducted, to establish the possible energy savings of the proposed optimised energy system for Area E scheduled load shedding (18:00-22:00), for 31 July 2018, the maximum load demand day. The daily baseline and optimal costs for the optimal energy management of the proposed grid-connected hybrid PV-Battery-DG system for the building, in this scheduled load shedding area, are compared in Figure 5.40. From 00:00 to 10:00, the difference between the baseline cost and optimal cost in Figure 5.40, is minimal, as the optimised energy cost for the proposed hybrid system is less than the sole grid cost. From 10:00 to 24:00, the difference between the baseline cost and the optimal cost, increases continuously, as the optimised energy cost for the proposed hybrid system is significantly less than the sole grid cost. The overall daily baseline cost is \$25.0102, while the daily optimal cost is \$17.0850, and this represents daily savings of \$7.9252. The optimal operation of the proposed grid-connected hybrid PV-Battery-DG system for the building in this area, brings about the possible daily savings of 31.68%.

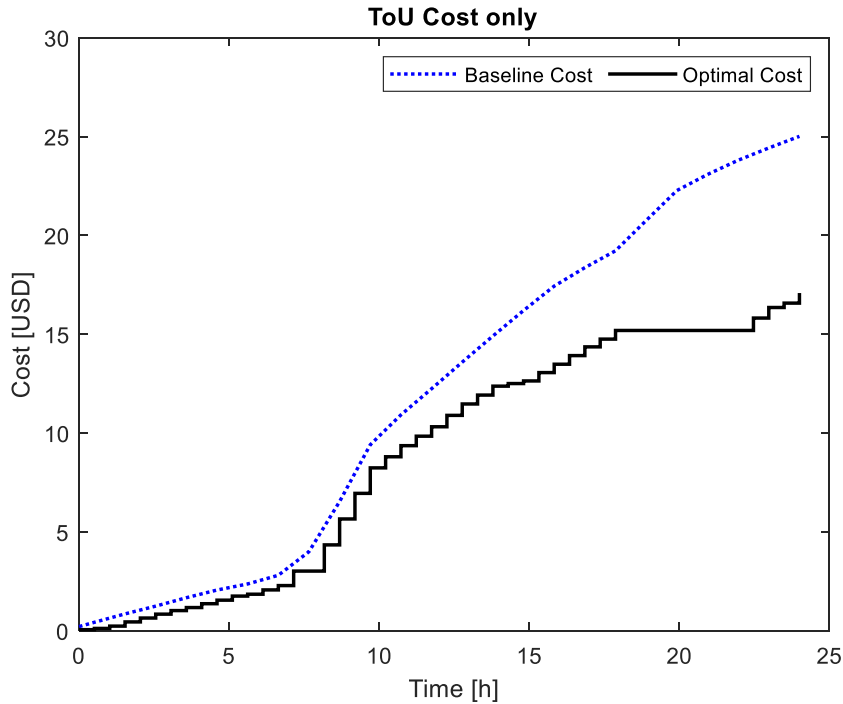


Figure 5.40 Area E (scheduled load shedding: 18:00-22:00) daily energy costs

5.4.9 Economic impact of scheduled load shedding on commercial consumers

To assess the impact of scheduled load shedding on commercial consumers on 31 July 2018, it is assumed that all consumers in areas A, B, C, D and E, have the same optimised grid-connected hybrid PV-Battery-DG systems, load profile and input data. It is further assumed that South African Stage 4 scheduled load shedding is implemented in areas B, C, D and E. Table 5.1 summarises the impact of scheduled load shedding on consumers' buildings in five areas.

Table 5.1 Impact of scheduled load shedding on consumers on 31 July 2018.

Area and schedule	Baseline cost (USD)	Optimal cost (USD)	Savings
A: None	25.0102	12.6264	49.51%
B: 00:00-04:00	25.0102	19.6008	21.63%
C: 06:00-10:00	25.0102	15.2696	38.95%
D: 12:00-16:00	25.0102	19.1884	23.28%
E: 18:00-22:00	25.0102	17.0850	31.69%

Table 5.1 shows that scheduled grid load shedding impacts negatively on Area B consumer (the savings' value is less than the no load shedding Area A by 27.88%), on Area C consumer (the savings' value is less than the no load shedding Area A by 10.66%), on Area D consumer (the savings' value is less than the no load shedding Area A by 26.23%) and on Area E consumer (the savings' value is less than the no load shedding Area A by 17.83%). The results show that scheduled load shedding impacts negatively on commercial consumers. The consumer in Area B load shedding schedule is most affected by a 27.88% loss in potential savings.

5.5 Conclusion

The objective of this Chapter is to assess the economic impact of scheduled grid load shedding on commercial consumers. The optimal operation of grid-tied hybrid energy system, under grid scheduled load shedding for a commercial building, has been studied in this Chapter. The study proposes a grid-connected hybrid PV-Battery-DG for a commercial building, to minimise the operational cost of the energy system under South African Stage 4 scheduled load shedding. Results indicate that the proposed grid-tied hybrid PV-Battery-DG, possesses the potential of mitigating the South African scheduled load shedding for a commercial consumer's building. They show that the optimal operation of the proposed grid-connected hybrid PV-Battery-DG system brings about the possible daily savings of 49.51% for Area A (no load shedding), 21.63% for Area B (load shedding schedule: 00:00-04:00), 38.95% for Area C (load shedding schedule: 06:00-10:00), 23.28% for Area D (load shedding schedule: 12:00-16:00) and 31.69% for Area E (load shedding schedule: 18:00-22:00), based on the data provided and the assumptions made. Although it is the same stage, the schedule of the daily load shedding will impact differently on the potential cost saving, on a daily basis. Daily scheduled grid load shedding impacts differently on commercial consumers; this is due to the available renewable resource, battery SOC, as well as the amount of DG energy used.

CHAPTER 6: CONCLUSIONS AND FUTURE RESEARCH

6.1 Conclusions

High consumption of electricity consumption in commercial buildings, is a global challenge faced by many countries in the world. The high consumption of purchased electricity from the utility, results in high electricity bills to commercial consumers. This situation requires that the supply and demand of electricity to a commercial building, to be matched in real time. This research aims to develop an optimal energy management model, which minimises the cost of the purchased electricity from the grid utility during the normal operating conditions, as well as during the scheduled load shedding. Conclusions on optimal sizing, simulation and optimal management of an on-site grid-tied PV-Battery-DG HRES are drawn in this chapter.

Chapter 3 provided the optimal sizing of the on-site grid-tied HRES using HOMER software. The HOMER model aims to optimally size the on-site grid-tied hybrid renewable energy system's components which meet the load demand of the commercial building with minimum NPC.

Chapter 4 outlined the formulated mathematical model for the HRES's optimal operation control under TOU. The aim of the model is to minimise the cost of electricity bought by the consumer from the grid under TOU, to minimise the cost of diesel required for running the DG as well as to maximise the potential surplus electricity generated by HRES, which may be sold to the grid. Solving Constraint Integer Programs (SCIP), which employs Interior Point Optimizer (IPOPT) and SoPlex algorithms was the selected optimisation solver and the reasons for the choice were stated. The results show that the electricity bought from the grid is reduced, the cost of running the DG is minimised and the optimal energy management of the hybrid system has potential daily savings.

In Chapter 5, the mathematical model for the HRES's optimal operation control under TOU and scheduled load shedding was formulated. The model aims to minimise the cost of operating the on-site grid-tied HRES under both TOU and South African

scheduled load shedding for a commercial building. The selection of the optimisation solver with the reasons for its choice were stated. The results indicate that the proposed grid-tied hybrid PV-Battery-DG has the potential of mitigating the South African scheduled load shedding for a commercial building.

In this research, the following conclusions are drawn using the formulated optimisation models which were verified through simulations:

- HOMER software may be used to optimally size an on-site grid-tied HRES's components, to meet the load demand of a commercial building with the minimum NPC.
- Optimal operation of on-site grid-tied HRES under TOU, reduces the cost of electricity bought from the grid, reduces the diesel cost required for running the DG as well as having the potential of daily savings for a commercial building. The reduced operation costs are achieved at the expense of the capital costs of HRES components as well as the diesel costs for running the DG.
- South African daily scheduled grid load shedding impacts differently on commercial consumers; this is due to the available renewable resource, battery SOC, as well as the amount of DG energy used.

6.2 Future Work

It is anticipated that in the future, Smart grid technologies may impact positively on commercial demand side management. Smart grid technologies consist of communication systems, monitoring systems, control devices and on-site HRESs. These technologies may enable a sustainable, efficient and secure electricity supply to a commercial building. Available communication technologies for commercial buildings, are Power Line Communication, Ethernet ZigBee, Wi-Fi and Wireless Mesh. These technologies enable a commercial consumer to communicate with the on-site HRES components, smart meters, monitoring systems, control devices and loads. Monitoring systems may enable commercial consumers, to monitor the status of on-site HRES components and loads, while control devices may enable the consumer to control the HRES components and loads.

Review the life cycle cost analysis of the proposed on-site grid-connected PV-Battery-DG HRES. This will include the impact of TOU on separate days, such as Saturdays and Sundays in different seasons, as well as the influence of variable load and resources within a season. Furthermore, the initial cost to calculate the cost of energy produced will be considered.

REFERENCES

- Abdulaal, A. and Asfour, S. (2016) “A linear optimization-based controller method for real-time load shifting in industrial and commercial buildings,” *Energy and Buildings*, 110, pp. 269–283. doi: 10.1016/j.enbuild.2015.10.046.
- Abushnaf, J. and Rassau, A. (2018) “Impact of energy management system on the sizing of a grid-connected PV/Battery system,” *Electricity Journal*, 31(2), pp. 58–66. doi: 10.1016/j.tej.2018.02.009.
- Aghaei, J. and Alizadeh, M.I. (2013) “Demand response in smart electricity grids equipped with renewable energy sources: A review,” *Renewable and Sustainable Energy Reviews*, pp. 64–72. doi: 10.1016/j.rser.2012.09.019.
- Aghajani, G.R., Shayanfar, H.A. and Shayeghi, H. (2017) “Demand side management in a smart micro-grid in the presence of renewable generation and demand response,” *Energy*, 126, pp. 622–637. doi: 10.1016/j.energy.2017.03.051.
- al Garni, H.Z., Awasthi, A. and Ramli, M.A.M. (2018) “Optimal design and analysis of grid-connected photovoltaic under different tracking systems using HOMER,” *Energy Conversion and Management*, 155, pp. 42–57. doi: 10.1016/j.enconman.2017.10.090.
- Albadi, M.H. and El-Saadany, E.F. (2008) “A summary of demand response in electricity markets,” *Electric Power Systems Research*, pp. 1989–1996. doi: 10.1016/j.epsr.2008.04.002.
- Allab, Y. *et al.* (2017) “Energy and comfort assessment in educational building: Case study in a French university campus,” *Energy and Buildings*, 143, pp. 202–219. doi: 10.1016/j.enbuild.2016.11.028.
- Alsayed, M. *et al.* (2013) “Multicriteria optimal sizing of photovoltaic-wind turbine grid connected systems,” *IEEE Transactions on Energy Conversion*, 28(2), pp. 370–379. doi:10.1109/TEC.2013.2245669.
- Ameen, A.M., Pasupuleti, J. and Khatib, T. (2015) “Simplified performance models of photovoltaic/diesel generator/battery system considering typical control strategies,” *Energy Conversion and Management*, 99, pp. 313–325. doi: 10.1016/j.enconman.2015.04.024.
- Ashok, S. (2007) “Optimised model for community-based hybrid energy system,” *Renewable Energy*, 32(7), pp. 1155–1164. doi: 10.1016/j.renene.2006.04.008.

- Askarzadeh, A. (2017) “Distribution generation by photovoltaic and diesel generator systems: Energy management and size optimization by a new approach for a stand-alone application,” *Energy*, 122, pp. 542–551. doi: 10.1016/j.energy.2017.01.105.
- Atzeni, I. *et al.* (2013) “Demand-side management via distributed energy generation and storage optimization,” *IEEE Transactions on Smart Grid*, 4(2), pp. 866–876. doi:10.1109/TSG.2012.2206060.
- Bajpai, P. and Dash, V. (2012) “Hybrid renewable energy systems for power generation in stand-alone applications: A review,” *Renewable and Sustainable Energy Reviews*, pp. 2926–2939. doi: 10.1016/j.rser.2012.02.009.
- Bakht, M.P. *et al.* (2021) “Stateflow-based energy management strategy for hybrid energy system to mitigate load shedding,” *Applied Sciences (Switzerland)*, 11(10). doi:10.3390/app11104601.
- Belfkira, R., Zhang, L. and Barakat, G. (2011) “Optimal sizing study of hybrid wind/PV/diesel power generation unit,” *Solar Energy*, 85(1), pp. 100–110. doi: 10.1016/j.solener.2010.10.018.
- Borowy, B.S. and Salameh, Z.M. (1996) *Methodology for Optimally Sizing the Combination of a Battery Bank and PV Array in a Wind/PV Hybrid System*, *IEEE Transactions on Energy Conversion*.
- Chung, M.H. and Rhee, E.K. (2014) “Potential opportunities for energy conservation in existing buildings on university campus: A field survey in Korea,” *Energy and Buildings*, 78, pp. 176–182. doi: 10.1016/j.enbuild.2014.04.018.
- Dagdougui, Y., Ouammi, A. and Benchrifa, R. (2020) “High Level Controller-Based Energy Management for a Smart Building Integrated Microgrid With Electric Vehicle,” *Frontiers in Energy Research*, 8. doi:10.3389/fenrg.2020.535535.
- dos Santos, L.T., Sechilariu, M. and Locment, F. (2016) “Optimized load shedding approach for grid-connected DC microgrid systems under realistic constraints,” *Buildings*, 6(4). doi:10.3390/buildings6040050.
- Dufo-López, R. and Bernal-Agustín, J.L. (2008) “Influence of mathematical models in design of PV-Diesel systems,” *Energy Conversion and Management*, 49(4), pp. 820–831. doi: 10.1016/j.enconman.2007.06.027.

- Eissa, M.M. (2011) “Demand side management program evaluation based on industrial and commercial field data,” *Energy Policy*, 39(10), pp. 5961–5969. doi: 10.1016/j.enpol.2011.06.057.
- Eltamaly, A.M. *et al.* (2021) “Iot-based hybrid renewable energy system for smart campus,” *Sustainability (Switzerland)*, 13(15). doi:10.3390/su13158555.
- Erdinc, O. and Uzunoglu, M. (2012) “Optimum design of hybrid renewable energy systems: Overview of different approaches,” *Renewable and Sustainable Energy Reviews*, pp. 1412–1425. doi: 10.1016/j.rser.2011.11.011.
- Gelazanskas, L. and Gamage, K.A.A. (2014) “Demand side management in smart grid: A review and proposals for future direction,” *Sustainable Cities and Society*, pp. 22–30. doi: 10.1016/j.scs.2013.11.001.
- Giglmayr, S. *et al.* (2015) “Utility-scale PV power and energy supply outlook for South Africa in 2015,” *Renewable Energy*, 83, pp. 779–785. doi: 10.1016/j.renene.2015.04.058.
- Güngör, V.C. *et al.* (2011) “Smart grid technologies: Communication technologies and standards,” *IEEE Transactions on Industrial Informatics*, 7(4), pp. 529–539. doi:10.1109/TII.2011.2166794.
- Hijjo, M., Felgner, F. and Frey, G., 2016. Energy management scheme for buildings subject to planned grid outages. *Journal of Engineering Research and Technology*, 3(3).
- Hohne, P.A., Kusakana, K. and Numbi, B.P., 2022. Energy cost minimization of a multifarious water heating system with energy recovery: A case of a healthcare institution. *Journal of Energy Storage*, 51, p.104451.
- Hohne, P.A., Kusakana, K. and Numbi, B.P., 2020. Model validation and economic dispatch of a dual axis pv tracking system connected to energy storage with grid connection: A case of a healthcare institution in South Africa. *Journal of Energy Storage*, 32, p.101986.
- Hohne, P.A., Kusakana, K. and Numbi, B.P., 2018, April. Operation cost and energy usage minimization of a hybrid solar/electrical water heating system. In *2018 international conference on the domestic use of energy (DUE)* (pp. 1-7). IEEE.
- Hohne, P.A., Kusakana, K. and Numbi, B.P., 2018. Operation cost minimisation of hybrid solar/electrical water heating systems: model development. *Advanced Science Letters*, 24(11), pp.8076-8080.

- Hohne, P.A., Kusakana, K. and Numbi, B.P., 2019. Optimal energy management and economic analysis of a grid-connected hybrid solar water heating system: A case of Bloemfontein, South Africa. *Sustainable Energy Technologies and Assessments*, 31, pp.273-291.
- Hohne, P.A., Kusakana, K. and Numbi, B.P., 2018. Scheduling and economic analysis of hybrid solar water heating system based on timer and optimal control. *Journal of Energy Storage*, 20, pp.16-29.
- Hohne, P.A., Kusakana, K. and Numbi, B.P., 2019. A review of water heating technologies: An application to the South African context. *Energy Reports*, 5, pp.1-19.
- Hohne, P.A., Kusakana, K. and Numbi, B.P., 2020. Model validation and economic dispatch of a dual axis pv tracking system connected to energy storage with grid connection: A case of a healthcare institution in South Africa. *Journal of Energy Storage*, 32, p.101986.
- Hohne, Percy Andrew, Kanzumba Kusakana, and Bubele P. Numbi. "Economic Power Dispatch for Energy Cost Reduction of a Hybrid Energy System Considering Maximum Demand Charges and Time-based Pricing in a Healthcare Institution." In *2020 6th IEEE International Energy Conference (ENERGYCon)*, pp. 395-400. IEEE.
- Hohne, P.A., Kusakana, K. and Numbi, B.P., 2020. Improving energy efficiency of thermal processes in healthcare institutions: A review on the latest sustainable energy management strategies. *Energies*, 13(3), p.569.
- Jin, X. *et al.* (2019) "Scheduling distributed energy resources and smart buildings of a microgrid via multi-time scale and model predictive control method," *IET Renewable Power Generation*, 13(6), pp. 816–833. doi:10.1049/iet-rpg.2018.5567.
- Katsigiannis, Y.A., Georgilakis, P.S. and Karapidakis, E.S. (2012) "Hybrid simulated annealing-tabu search method for optimal sizing of autonomous power systems with renewables," *IEEE Transactions on Sustainable Energy*, 3(3), pp. 330–338. doi:10.1109/TSTE.2012.2184840.
- Khare, V., Nema, S. and Baredar, P. (2016) "Solar-wind hybrid renewable energy system: A review," *Renewable and Sustainable Energy Reviews*. Elsevier Ltd, pp. 23–33. doi: 10.1016/j.rser.2015.12.223.

- Koutroulis, E. *et al.* (2006) “Methodology for optimal sizing of stand-alone photovoltaic/wind-generator systems using genetic algorithms,” *Solar Energy*, 80(9), pp. 1072–1088. doi: 10.1016/j.solener.2005.11.002.
- Kusakana, K. and Vermaak, H.J., 2012, April. Feasibility study of hydrokinetic power for energy access in rural South Africa. In *Proceedings of the LASTED Asian conference, power and energy systems* (pp. 433-438).
- Kusakana, K. and Vermaak, H.J., 2014. Hybrid diesel generator/renewable energy system performance modeling. *Renewable energy*, 67, pp.97-102.
- Kusakana, K., 2015. Optimal scheduled power flow for distributed photovoltaic/wind/diesel generators with battery storage system. *IET Renewable Power Generation*, 9(8), pp.916-924.
- Kusakana, K., 2017. Energy management of a grid-connected hydrokinetic system under Time of Use tariff. *Renewable Energy*, 101, pp.1325-1333.
- Kusakana, K., 2020. Optimal peer-to-peer energy management between grid-connected prosumers with battery storage and photovoltaic systems. *Journal of Energy Storage*, 32, p.101717.
- Kusakana, K., 2021. Optimal peer-to-peer energy sharing between grid-connected prosumers with different demand profiles and renewable energy sources. *IET Smart Grid*, 4(3), pp.270-283.
- Kuzlu, M., Pipattanasomporn, M. and Rahman, S. (2014) “Communication network requirements for major smart grid applications in HAN, NAN and WAN,” *Computer Networks*. Elsevier B.V., pp. 74–88. doi: 10.1016/j.comnet.2014.03.029.
- Lindberg, C.F. *et al.* (2014) “Potential and limitations for industrial demand side management,” in *Energy Procedia*. Elsevier Ltd, pp. 415–418. doi: 10.1016/j.egypro.2014.11.1138.
- Liu, P., Pistikopoulos, E.N. and Li, Z. (2010) “An energy systems engineering approach to the optimal design of energy systems in commercial buildings,” *Energy Policy*, 38(8), pp. 4224–4231. doi: 10.1016/j.enpol.2010.03.051.
- Mahmood, A. *et al.* (2014) “A new scheme for demand side management in future smart grid networks,” in *Procedia Computer Science*. Elsevier B.V., pp. 477–484. doi: 10.1016/j.procs.2014.05.450.

- Makhdoomi, S. and Askarzadeh, A. (2020) “Optimizing operation of a photovoltaic/diesel generator hybrid energy system with pumped hydro storage by a modified crow search algorithm,” *Journal of Energy Storage*, 27. doi: 10.1016/j.est.2019.101040.
- Mariaud, A. *et al.* (2017) “Integrated optimisation of photovoltaic and battery storage systems for UK commercial buildings,” *Applied Energy*, 199, pp. 466–478. doi: 10.1016/j.apenergy.2017.04.067.
- Mays, J. and Klabjan, D. (2017) “Optimization of time-varying electricity rates,” in *Energy Journal*. International Association for Energy Economics, pp. 67–91. doi: 10.5547/01956574.38.5.jmay.
- Mbungu, N.T., Naidoo, R.M. and Bansal, R.C. (2017) “Real-time Electricity Pricing: TOU-MPC Based Energy Management for Commercial Buildings,” in *Energy Procedia*. Elsevier Ltd, pp. 3419–3424. doi: 10.1016/j.egypro.2017.03.781.
- Meyabadi, A.F. and Deihimi, M.H. (2017) “A review of demand-side management: Reconsidering theoretical framework,” *Renewable and Sustainable Energy Reviews*. Elsevier Ltd, pp. 367–379. doi: 10.1016/j.rser.2017.05.207.
- Mohammed, Y.S., Mustafa, M.W. and Bashir, N. (2014) “Hybrid renewable energy systems for off-grid electric power: Review of substantial issues,” *Renewable and Sustainable Energy Reviews*. Elsevier Ltd, pp. 527–539. doi: 10.1016/j.rser.2014.04.022.
- Moji, L.P., Kusakana, K. and Numbi, B.P. (2020) “Sizing and Operation Control of a Grid-Interactive Photovoltaic-Battery-Diesel System for Commercial Buildings,” in *6th IEEE International Energy Conference, ENERGYCon 2020*. Institute of Electrical and Electronics Engineers Inc., pp. 401–406. doi:10.1109/ENERGYCon48941.2020.9236449.
- Mondol, J.D., Yohanis, Y.G. and Norton, B. (2009) “Optimising the economic viability of grid-connected photovoltaic systems,” *Applied Energy*, 86(7–8), pp. 985–999. doi: 10.1016/j.apenergy.2008.10.001.
- Ndwali, P.K., Njiri, J.G. and Wanjiru, E.M. (2020) “Optimal Operation Control of Microgrid Connected Photovoltaic-Diesel Generator Backup System Under Time of Use Tariff,” *Journal of Control, Automation and Electrical Systems*, 31(4), pp. 1001–1014. doi:10.1007/s40313-020-00585-w.

- Numbi, B.P. and Malinga, S.J. (2017) “Optimal energy cost and economic analysis of a residential grid-interactive solar PV system- case of eThekweni municipality in South Africa,” *Applied Energy*, 186, pp. 28–45. doi: 10.1016/j.apenergy.2016.10.048.
- Olatomiwa, L. (2016) “Optimal configuration assessments of hybrid renewable power supply for rural healthcare facilities,” *Energy Reports*, 2, pp. 141–146. doi: 10.1016/j.egy.2016.06.001.
- Pérez-Lombard, L., Ortiz, J. and Pout, C. (2008) “A review on buildings energy consumption information,” *Energy and Buildings*, 40(3), pp. 394–398. doi: 10.1016/j.enbuild.2007.03.007.
- Setiawan, M.A. *et al.* (2015) “ZigBee-Based Communication System for Data Transfer Within Future Microgrids,” *IEEE Transactions on Smart Grid*, 6(5), pp. 2343–2355. doi:10.1109/TSG.2015.2402678.
- Shaahid, S.M. and Elhadidy, M.A. (2007) “Technical and economic assessment of grid-independent hybrid photovoltaic-diesel-battery power systems for commercial loads in desert environments,” *Renewable and Sustainable Energy Reviews*, pp. 1794–1810. doi: 10.1016/j.rser.2006.03.001.
- Shaukat, N. *et al.* (2018) “A survey on consumers empowerment, communication technologies, and renewable generation penetration within Smart Grid,” *Renewable and Sustainable Energy Reviews*. Elsevier Ltd, pp. 1453–1475. doi: 10.1016/j.rser.2017.05.208.
- Siano, P. (2014) “Demand response and smart grids - A survey,” *Renewable and Sustainable Energy Reviews*. Elsevier Ltd, pp. 461–478. doi: 10.1016/j.rser.2013.10.022.
- Sichilalu, S.M. and Xia, X. (2015) “Optimal energy control of grid tied PV-diesel-battery hybrid system powering heat pump water heater,” *Solar Energy*, 115, pp. 243–254. doi: 10.1016/j.solener.2015.02.028.
- Siecker, J., Kusakana, K. and Numbi, B.P., 2017. A review of solar photovoltaic systems cooling technologies. *Renewable and Sustainable Energy Reviews*, 79, pp.192-203.
- Tazvinga, H., Xia, X. and Zhang, J. (2013) “Minimum cost solution of photovoltaic-diesel-battery hybrid power systems for remote consumers,” *Solar Energy*, 96, pp. 292–299. doi: 10.1016/j.solener.2013.07.030.

- Tazvinga, H., Zhu, B. and Xia, X. (2015) “Optimal power flow management for distributed energy resources with batteries,” *Energy Conversion and Management*, 102, pp. 104–110. doi: 10.1016/j.enconman.2015.01.015.
- Ullah, K. *et al.* (2020) “An optimal energy optimization strategy for smart grid integrated with renewable energy sources and demand response programs,” *Energies*, 13(21). doi:10.3390/en13215718.
- Upadhyay, S. and Sharma, M.P. (2014) “A review on configurations, control and sizing methodologies of hybrid energy systems,” *Renewable and Sustainable Energy Reviews*. Elsevier Ltd, pp. 47–63. doi: 10.1016/j.rser.2014.05.057.
- Vadabhat, V. and Banerjee, R. (2014) “Modeling of demand side management options for commercial sector in Maharashtra,” in *Energy Procedia*. Elsevier Ltd, pp. 541–551. doi: 10.1016/j.egypro.2014.07.108.
- Wang, Y. and Li, L. (2016) “Critical peak electricity pricing for sustainable manufacturing: Modeling and case studies,” *Applied Energy*, 175, pp. 40–53. doi: 10.1016/j.apenergy.2016.04.100.
- Warren, P. (2014) “A review of demand-side management policy in the UK,” *Renewable and Sustainable Energy Reviews*, pp. 941–951. doi: 10.1016/j.rser.2013.09.009.
- Wu, Z. and Xia, X. (2015) “Optimal switching renewable energy system for demand side management,” *Solar Energy*, 114, pp. 278–288. doi: 10.1016/j.solener.2015.02.001.
- Wu, Z., Tazvinga, H. and Xia, X. (2015) “Demand side management of photovoltaic-battery hybrid system,” *Applied Energy*, 148, pp. 294–304. doi: 10.1016/j.apenergy.2015.03.109.